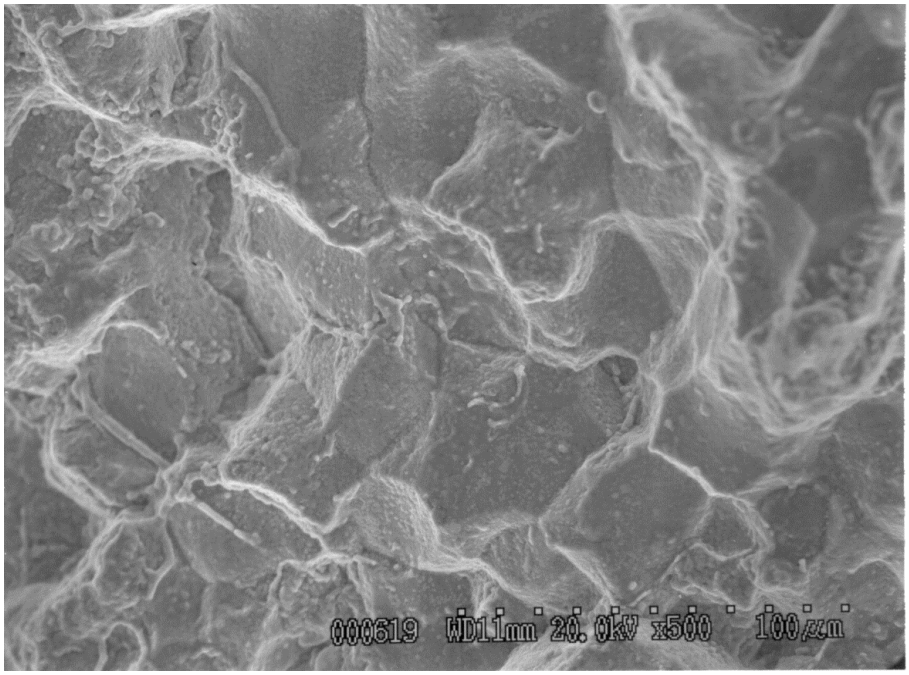

Fig. 187. Scanning electron microscope fractograph of SID 14875 "B4" Area "E".

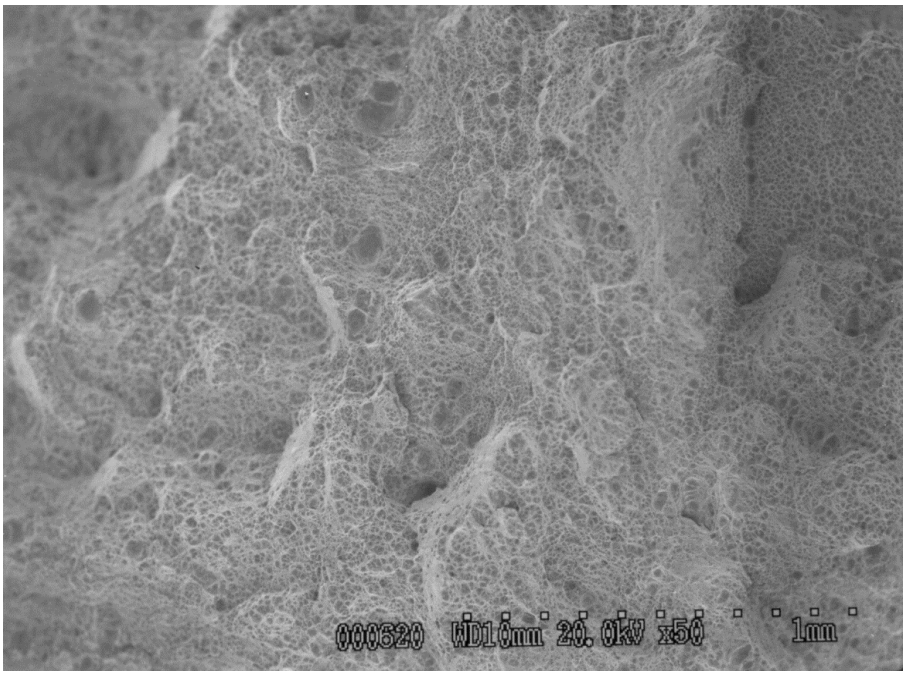

Fig. 188. Scanning electron microscope fractograph of SID 14875 "B4" Area "F".

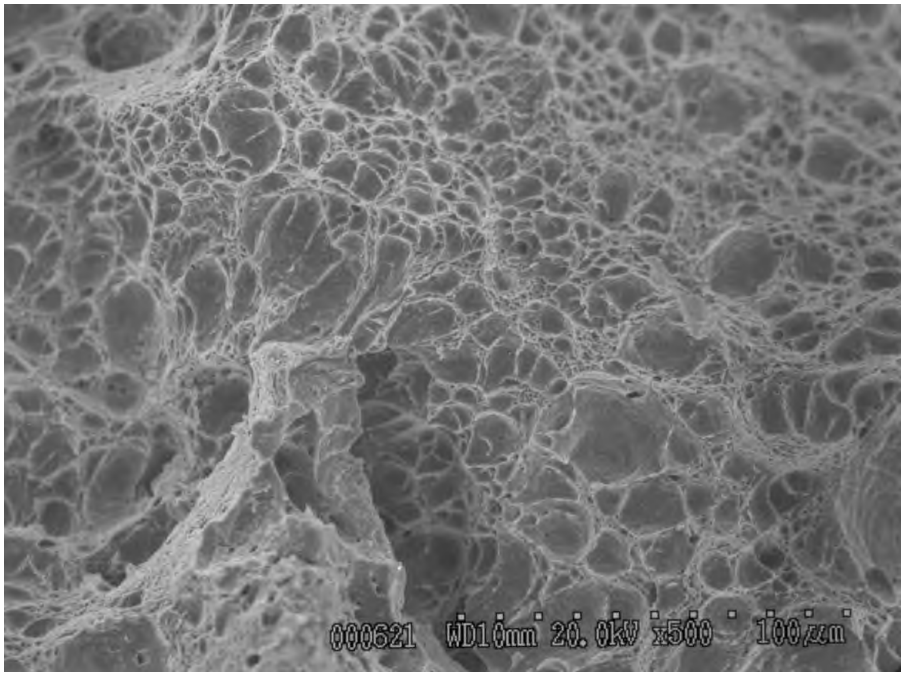

Fig. 189 Scanning electron microscope fractograph of SID 14875 "B4" Area "F".

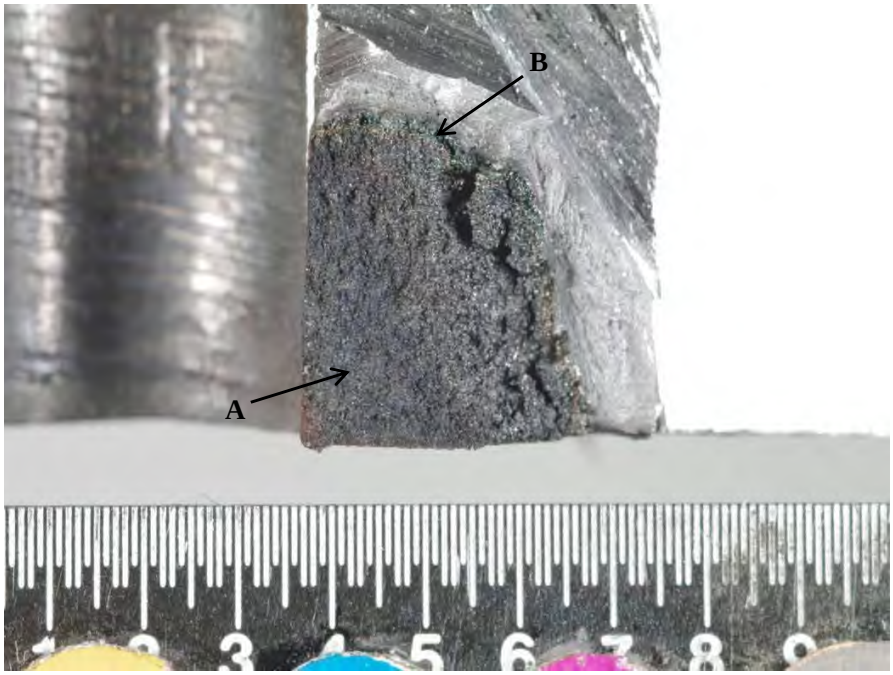

Fig. 190. Photograph of fracture through crack at pin hole in SID 14875 subsegment "C4b" showing areas examined by scanning electron microscope.

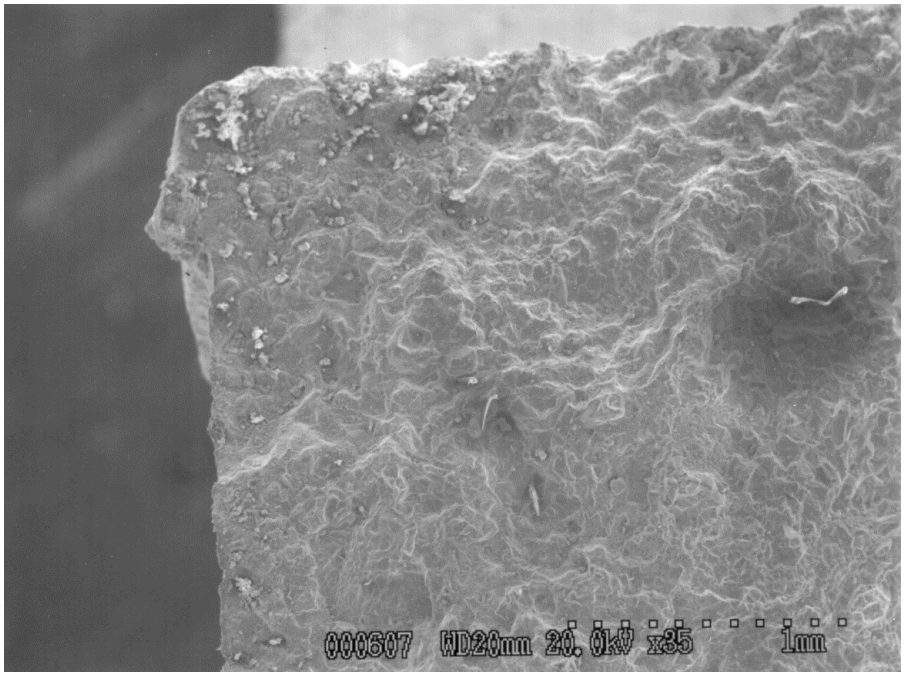

Fig. 191. Scanning electron microscope fractograph of SID 14875 "C4b" Area "A" shown in Fig. 190.

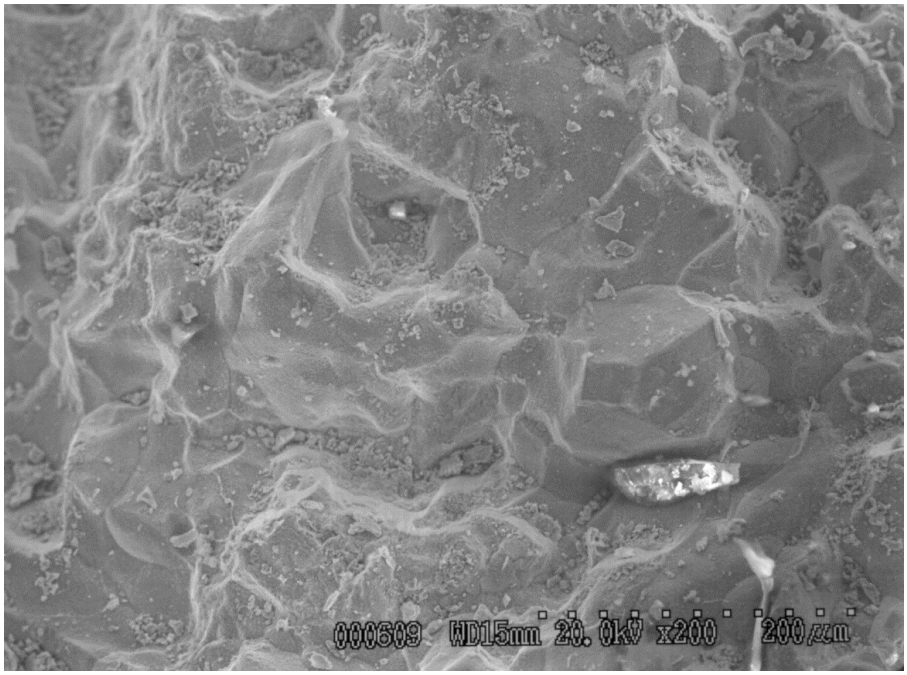

Fig 192. Scanning electron microscope fractograph of SID 14875 "C4b" Area "A".

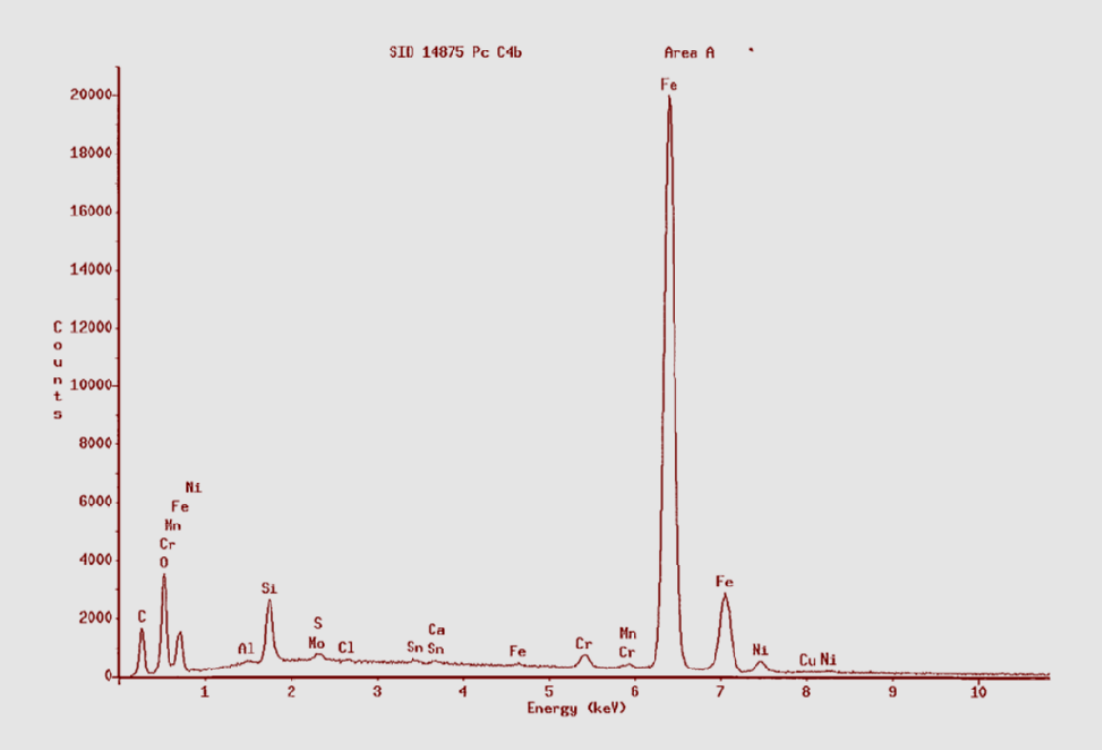

Fig. 193. X-Ray Energy Dispersive Spectrograph of SID 14875 "C4b" Area "A".

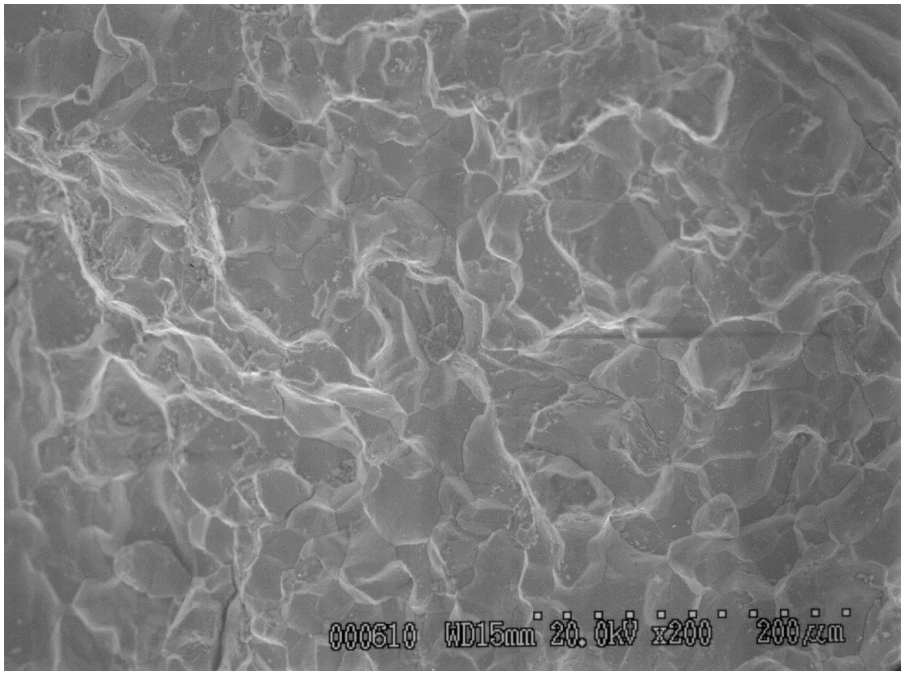

Fig. 194. Scanning electron microscope fractograph of SID 14875 "C4b " Area "B" shown in Fig. 190.

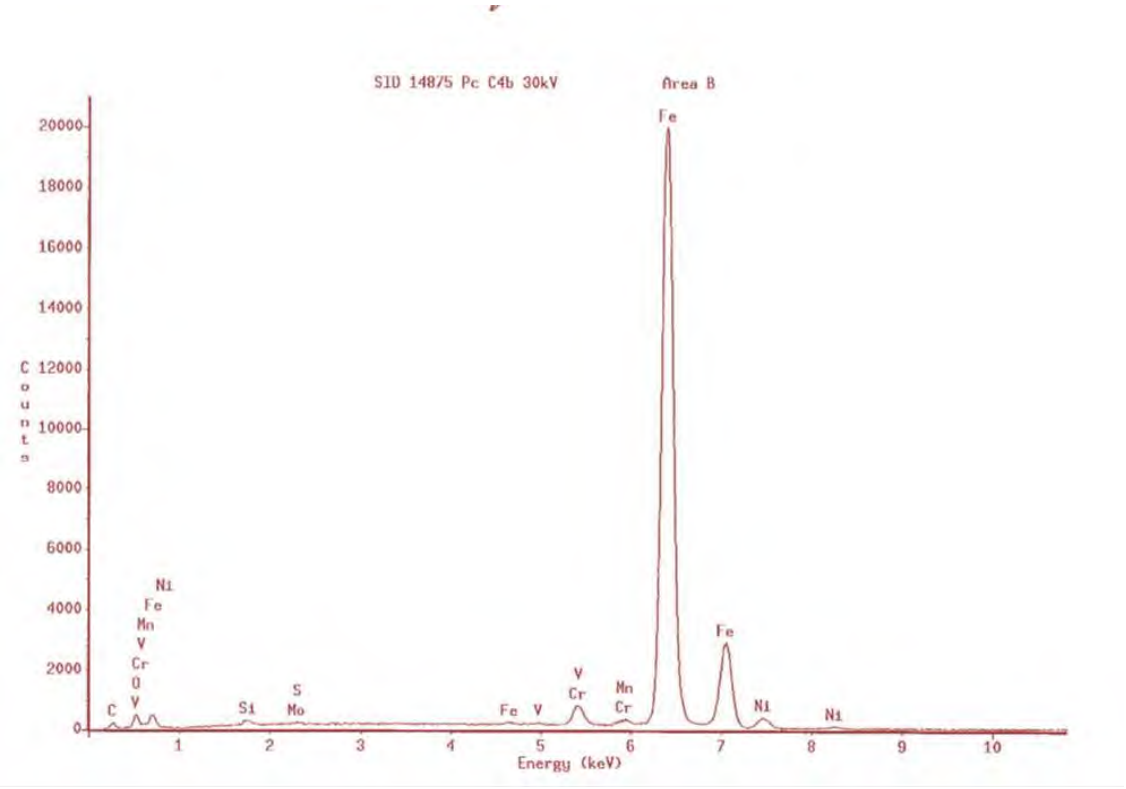

Fig. 195. X-Ray Energy Dispersive Spectrograph of SID 14875 "C4b" Area "B".

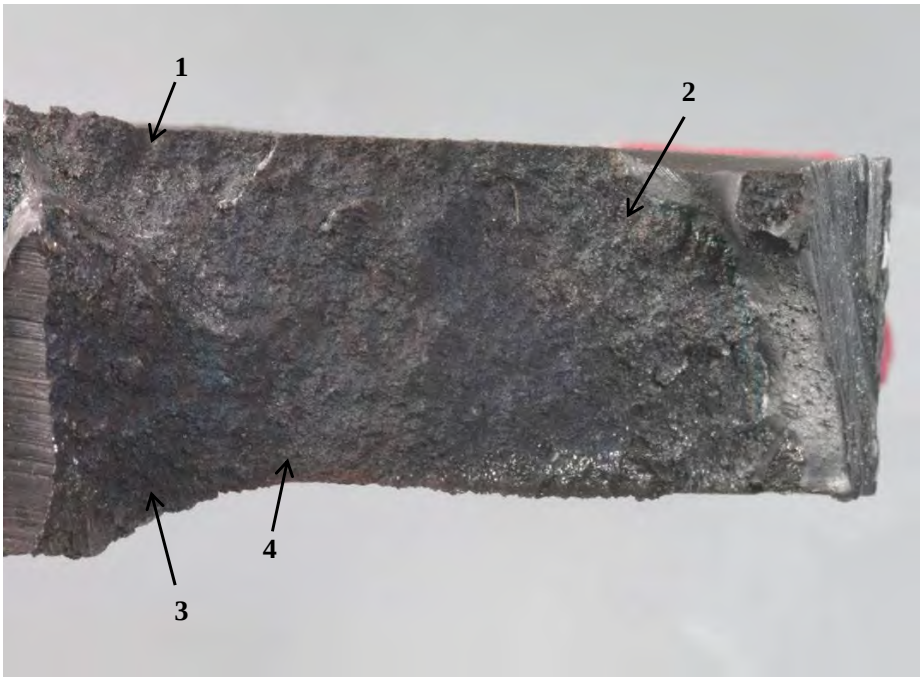

Fig. 196. Close-up photograph of fracture through crack in SID 14875 subsegment "C4d" prior to cleaning, showing areas examined by scanning electron microscopy.

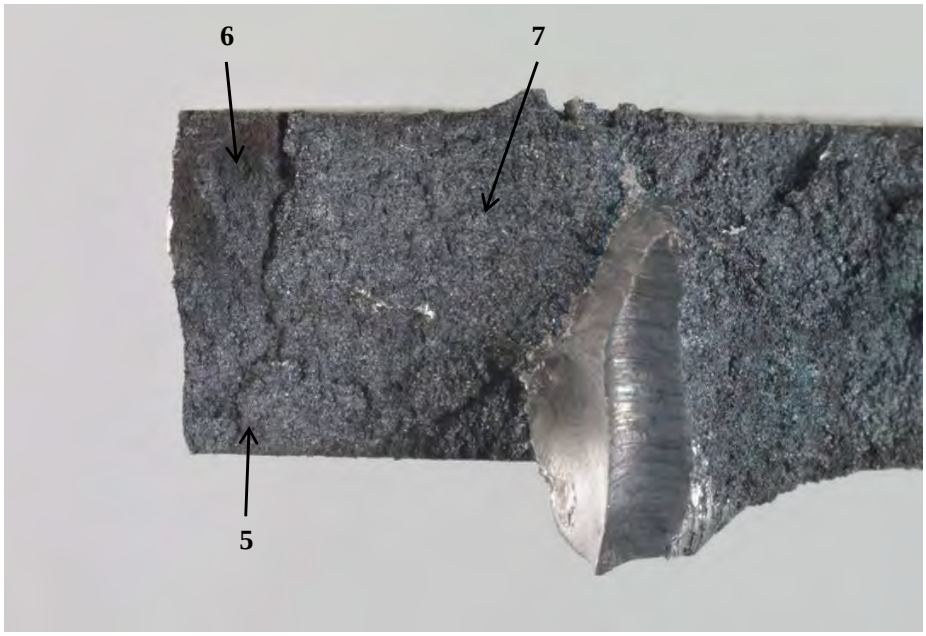

Fig. 197. Photograph of fracture through crack in SID 14875 subsegment "C4d", prior to cleaning, showing areas examined by Scanning electron microscopy.

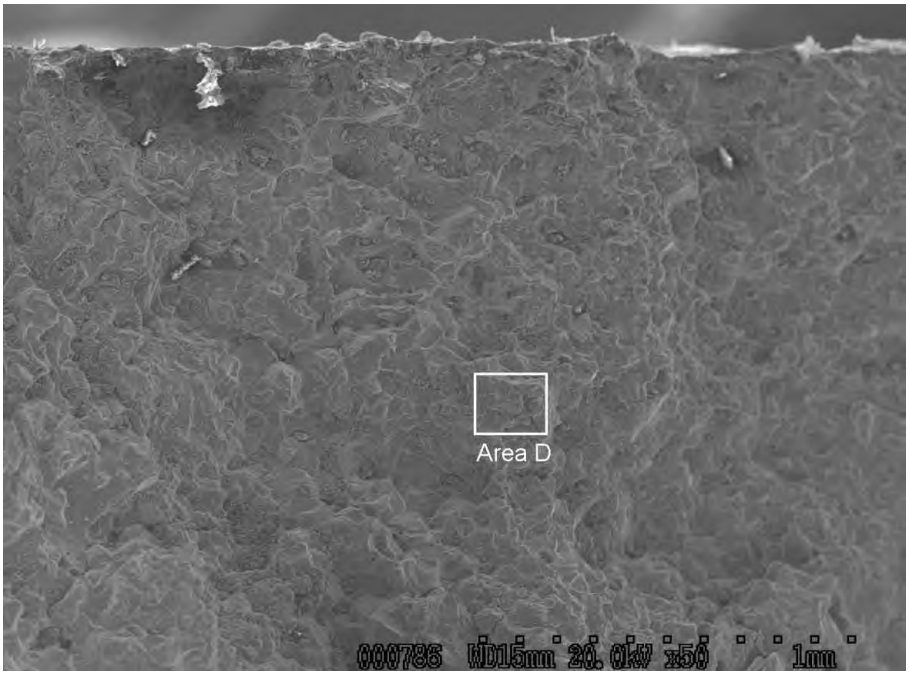

Fig 198. Scanning electron fractograph of crack surface from SID 14875 subsegment "C4d" Area "1" showing EDS area "D".

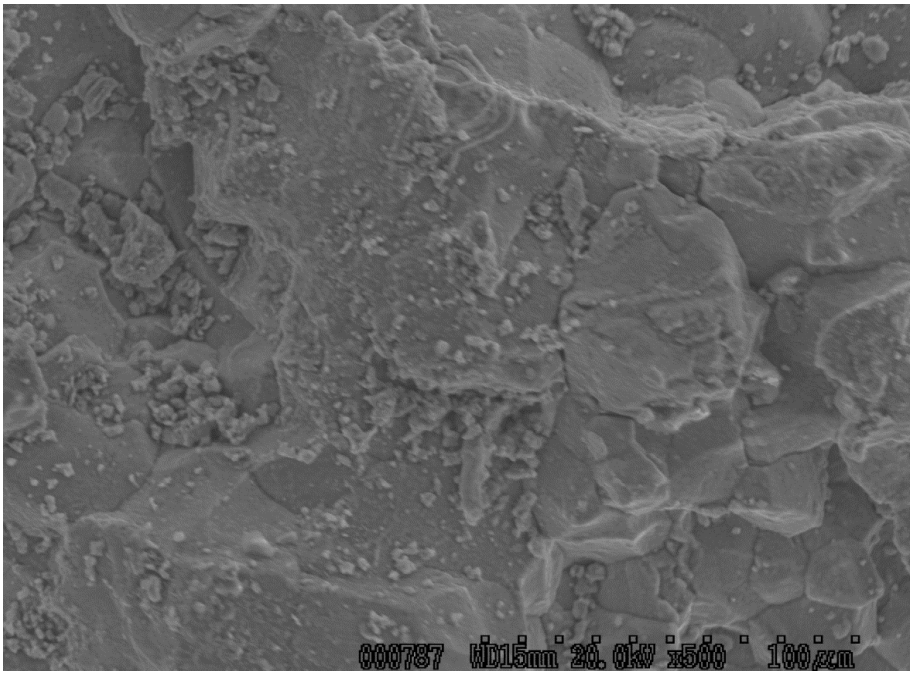

Fig 199. Scanning electron fractograph of crack surface from SID 14875 subsegment "C4d" Area "1".

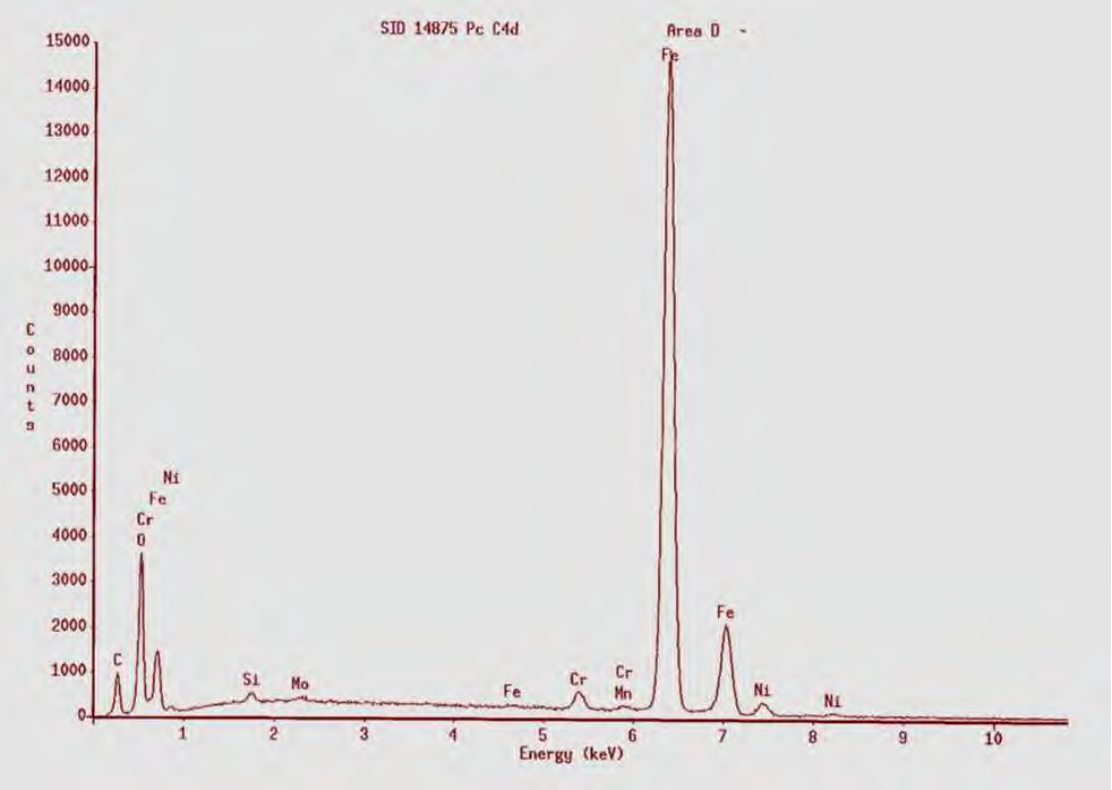

Fig. 200. X-Ray Energy Dispersive Spectrograph of SID 14875 "C4d" Area "1"at area D shown in Fig. 198 .

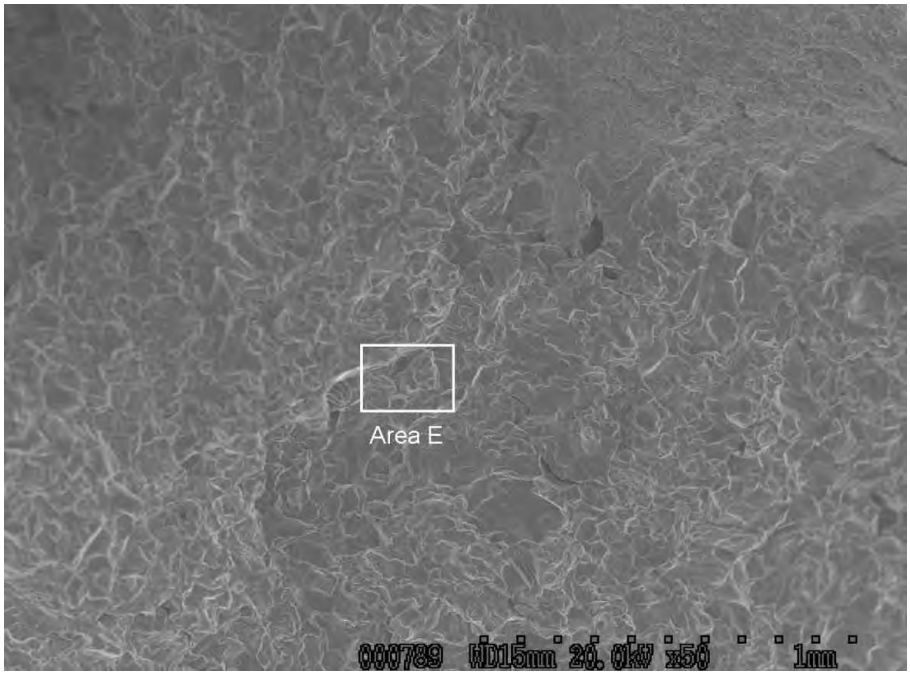

Fig. 201. Scanning electron fractograph of crack surface from SID 14875 subsegment "C4d" Area "2" showing EDS area "E".

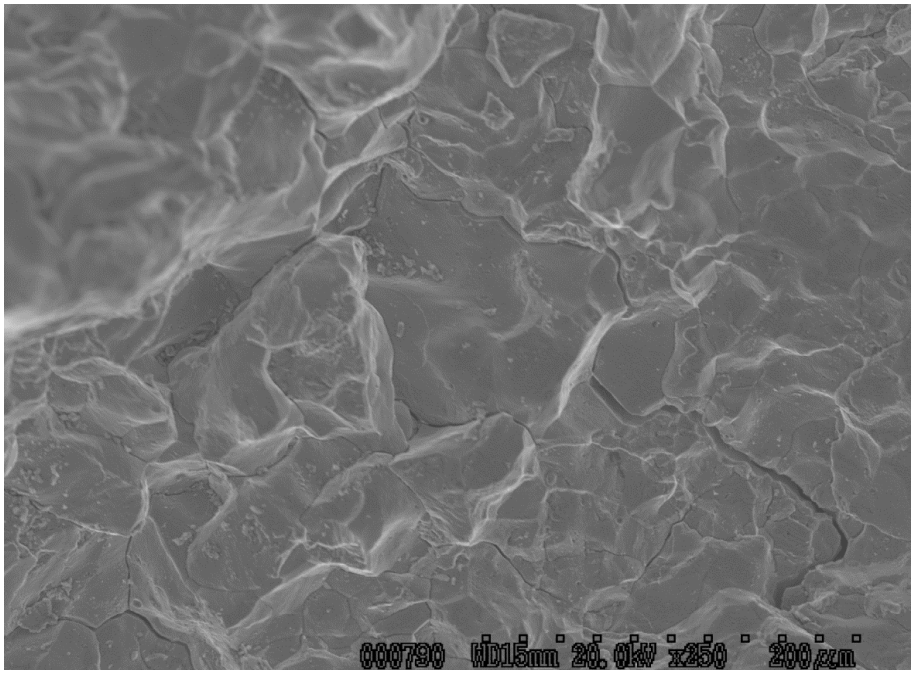

Fig 202. Scanning electron fractograph of crack surface from SID 14875 subsegment "C4d" Area "2".

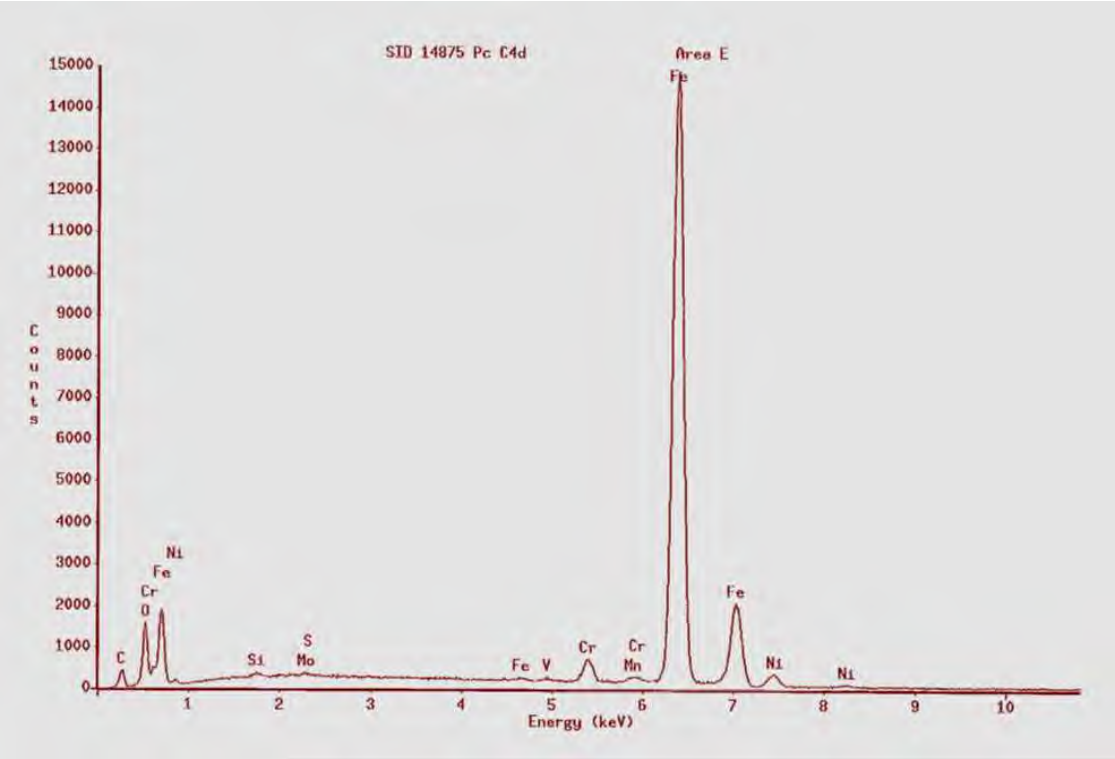

Fig. 203. X-Ray Energy Dispersive Spectrograph of SID 14875 "C4d" Area "2" at Area "E" shown in Fig. 201.

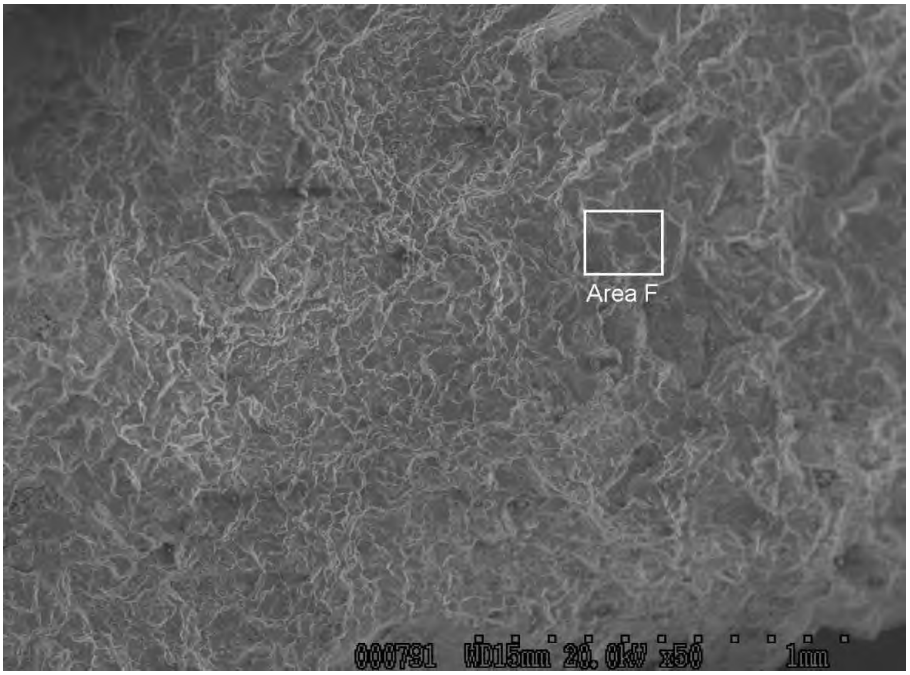

Fig. 204. Scanning electron fractograph of crack surface from SID 14875 subsegment "C4d" Area "3" showing EDS area "F".

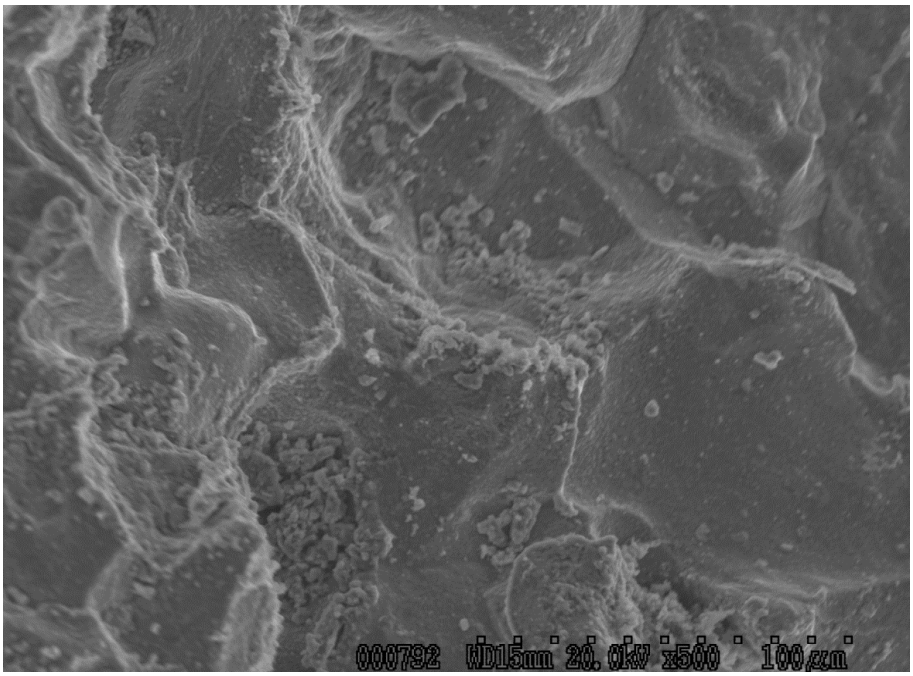

Fig. 205. Scanning electron fractograph of crack surface from SID 14875 subsegment "C4d" Area "3".

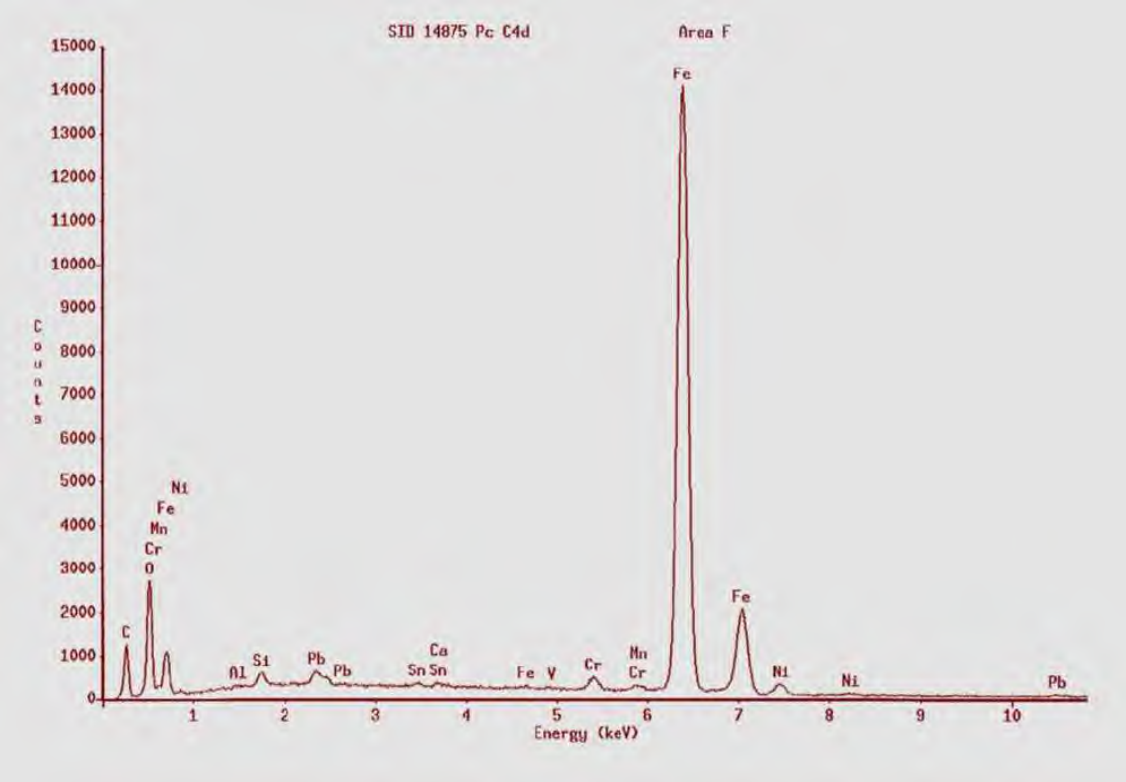

Fig. 206 X-Ray Energy Dispersive Spectrograph of SID 14875 "C4d" Area "3" at area "F" shown in Fig. 204.

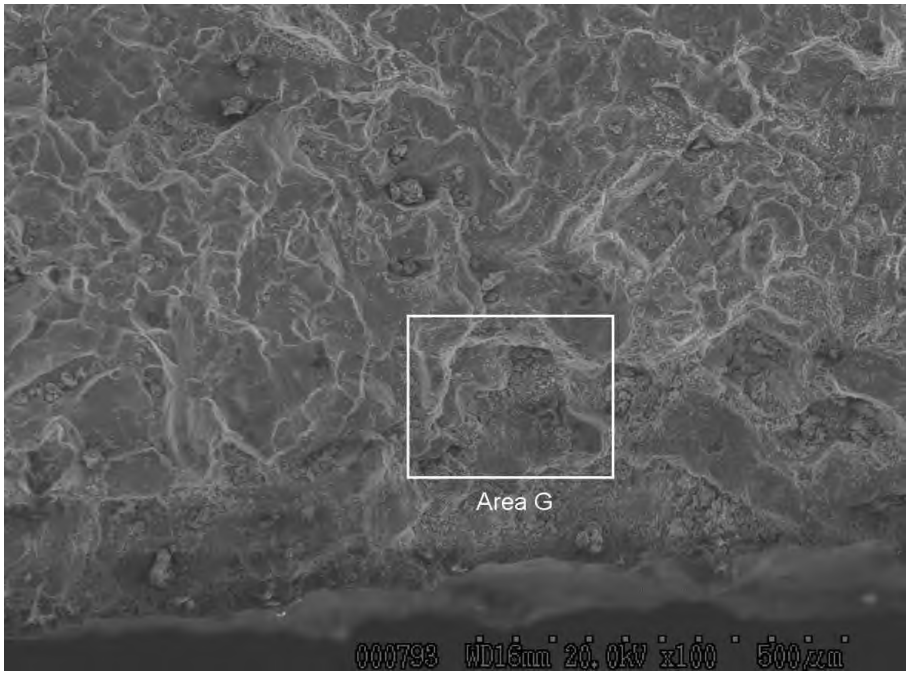

Fig. 207. Scanning electron fractograph of crack surface from SID 14875 subsegment "C4d" Area "4" showing EDS area "G".

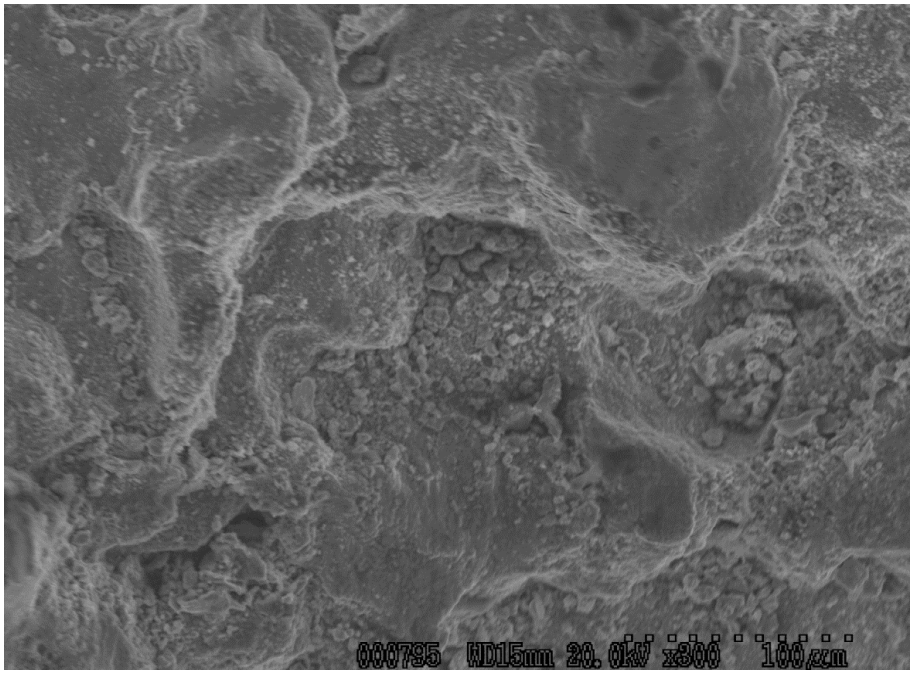

Fig. 208. Scanning electron fractograph of crack surface from SID 14875 subsegment "C4d" Area "4".

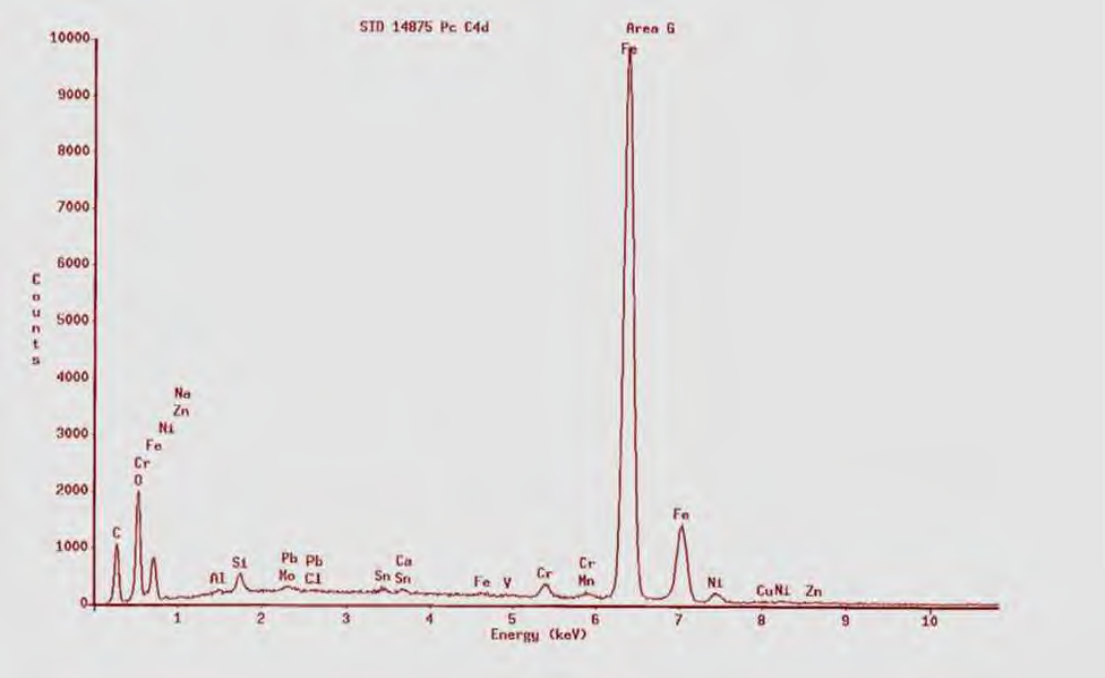

Fig. 209. X-Ray Energy Dispersive Spectrograph of SID 14875 "C4d" Area "4" at area "F" shown in Fig. 207.

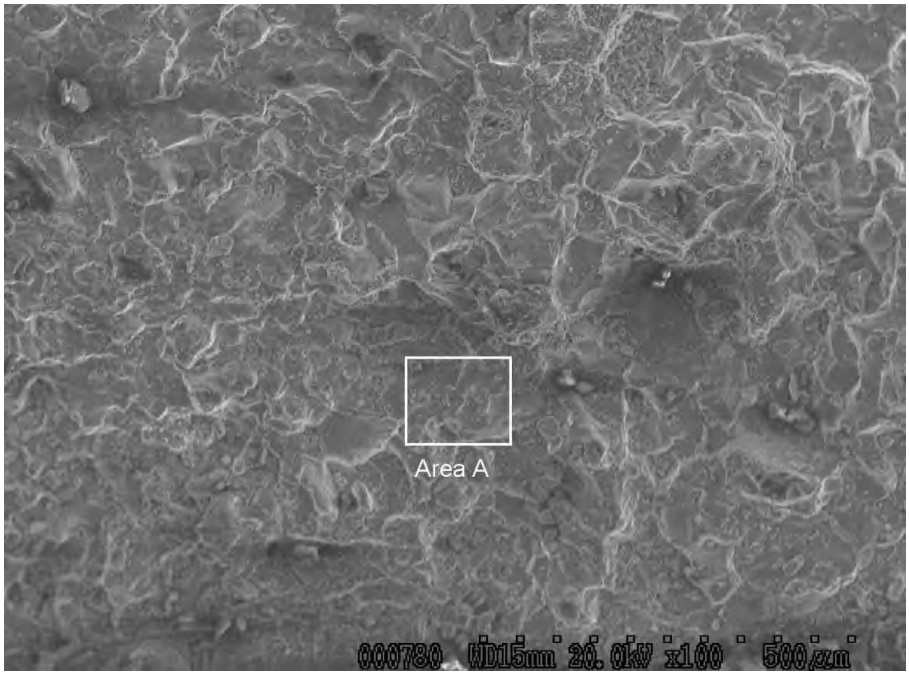

Fig. 210. Scanning electron fractograph of crack surface from SID 14875 subsegment "C4d" Area "5" showing EDS area "A".

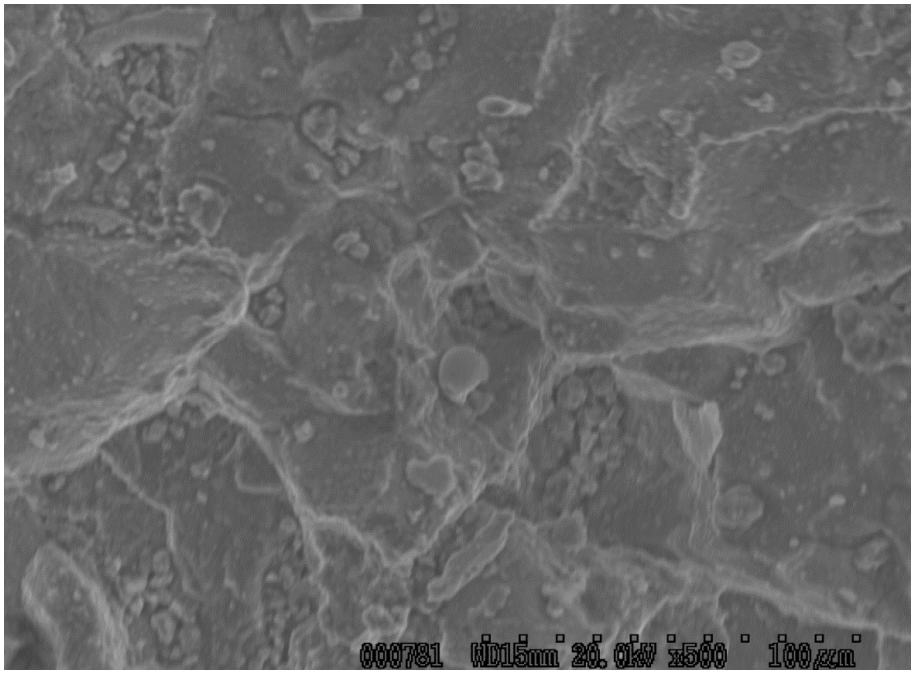

Fig. 211. Scanning electron fractograph of crack surface from SID 14875 subsegment "C4d" Area "5".

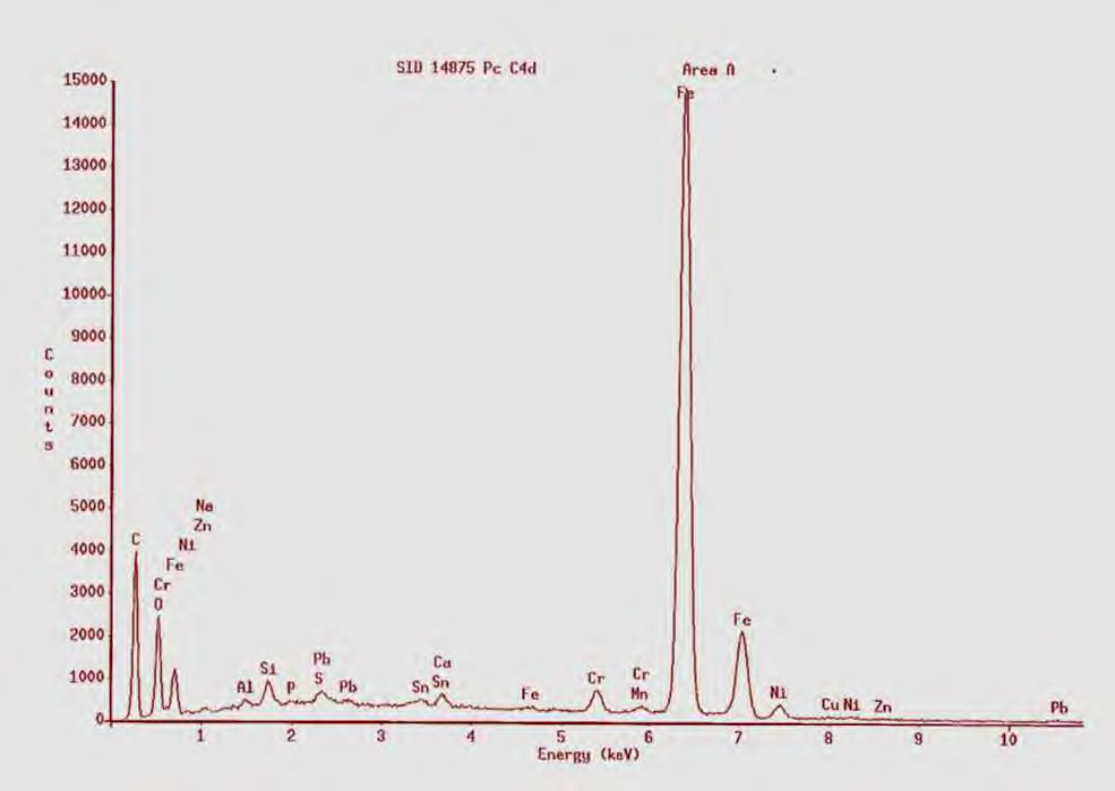

Fig. 212. X-Ray Energy Dispersive Spectrograph of SID 14875 "C4d" Area "5" at area "A" shown in Fig. 210.

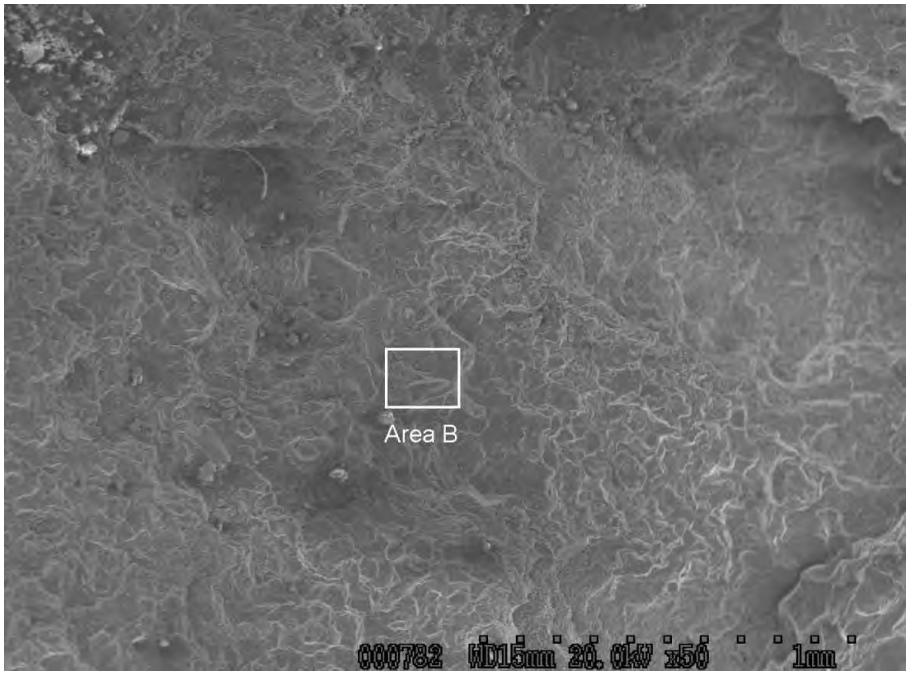

Fig. 213. Scanning electron fractograph of crack surface from SID 14875 subsegment "C4d" Area "6" showing EDS area "B".

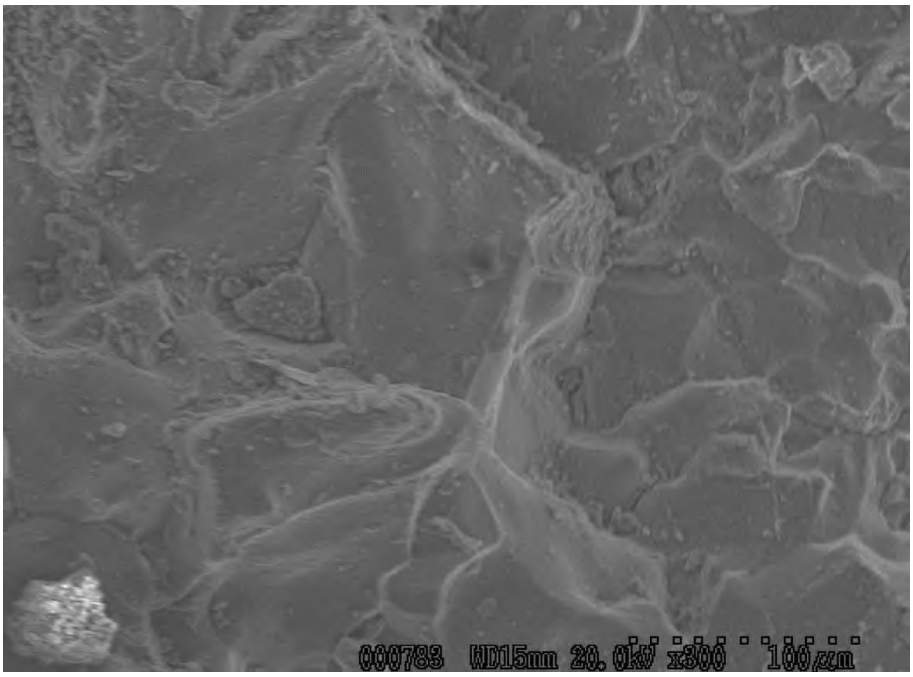

Fig. 214. Scanning electron fractograph of crack surface from SID 14875 subsegment "C4d" Area "6".

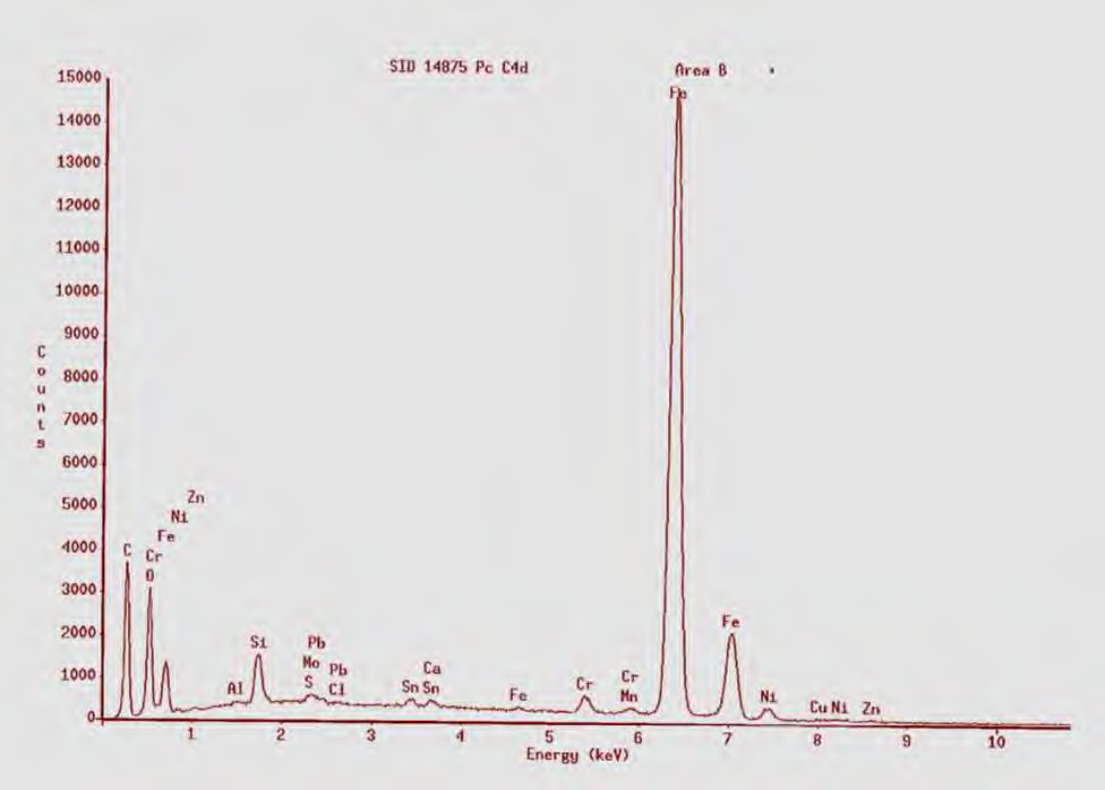

Fig. 215. X-Ray Energy Dispersive Spectrograph of SID 14875 "C4d" Area "6" at area "B" shown in Fig. 213.

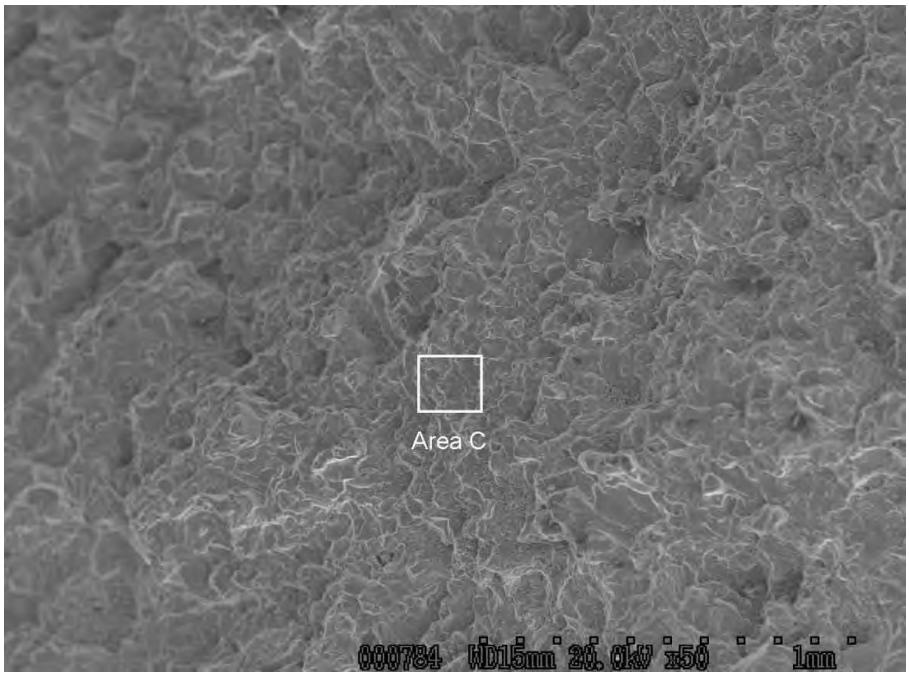

Fig 216. Scanning electron fractograph of crack surface from SID 14875 subsegment "C4d" Area "7" showing EDS area "C".

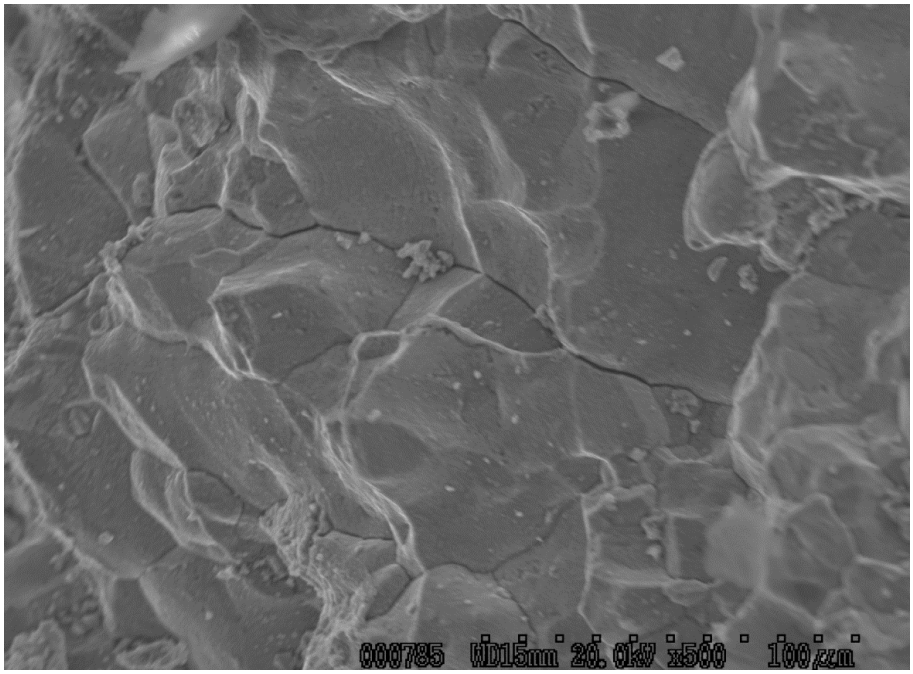

Fig. 217. Scanning electron fractograph of crack surface from SID 14875 subsegment "C4d" Area "7".

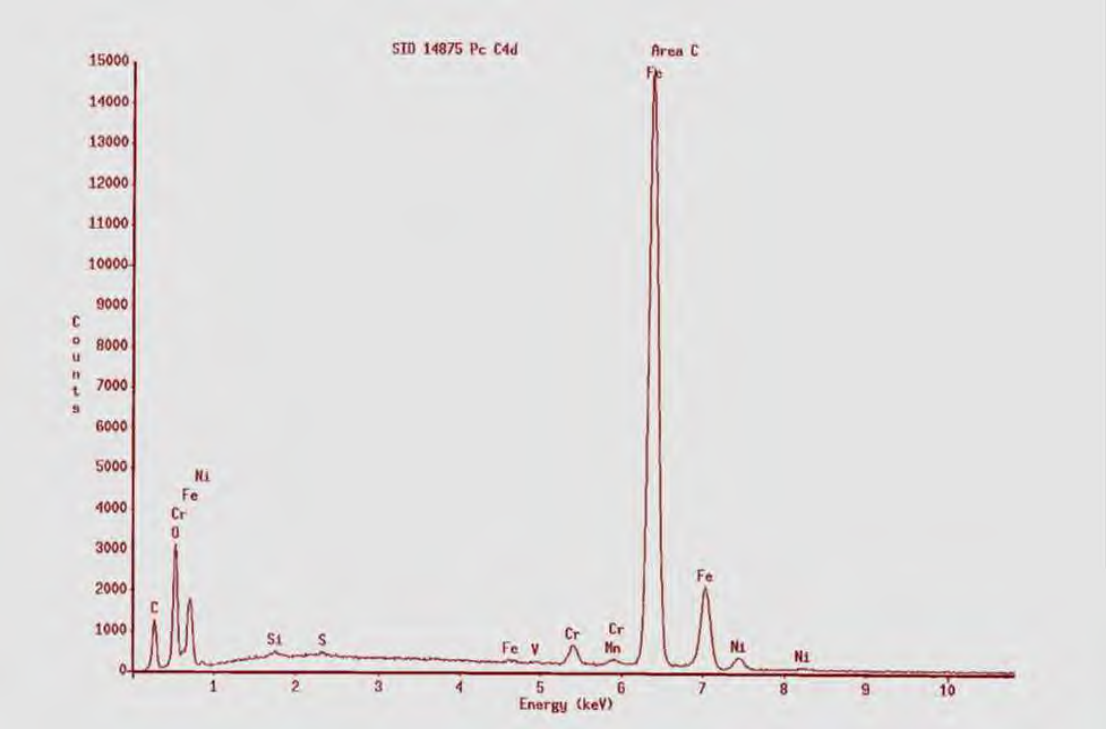

Fig. 218. X-Ray Energy Dispersive Spectrograph of SID 14875 "C4d" Area "7"at area "C" shown in Fig. 216.

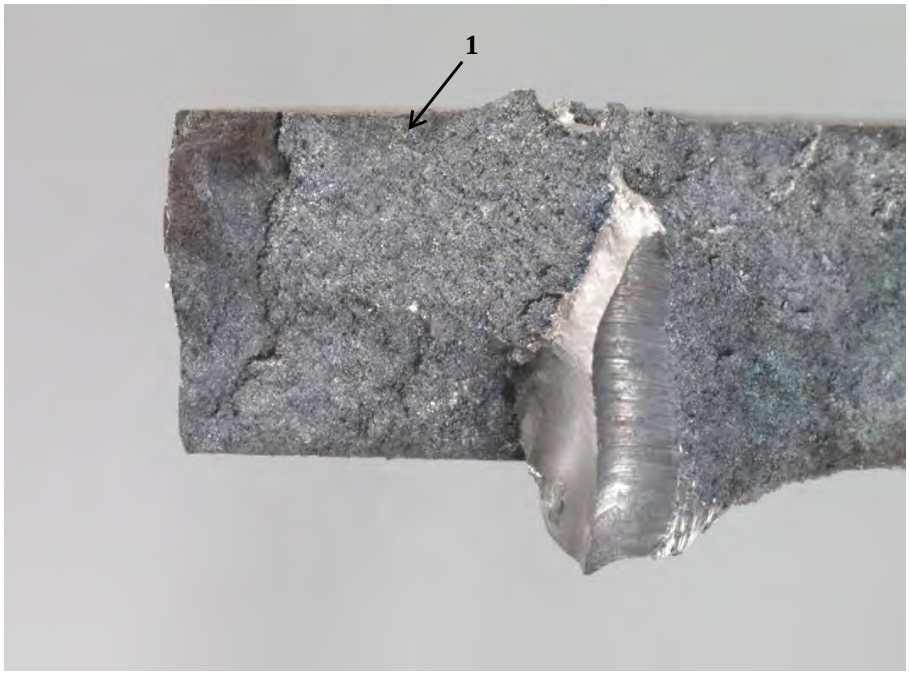

Fig. 219. Photograph of SID 14875 "C4d" fracture, after cleaning, showing areas examined by Scanning Electron Microscopy.

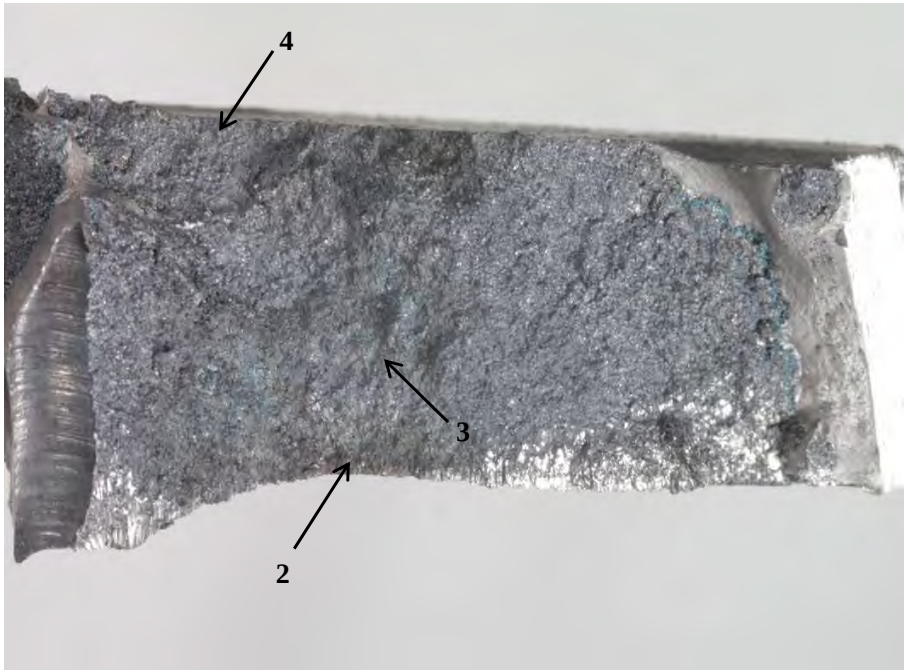

Fig. 220. Photograph of SID 14875 "C4d" fracture, after cleaning, showing areas examined by Scanning Electron Microscopy.

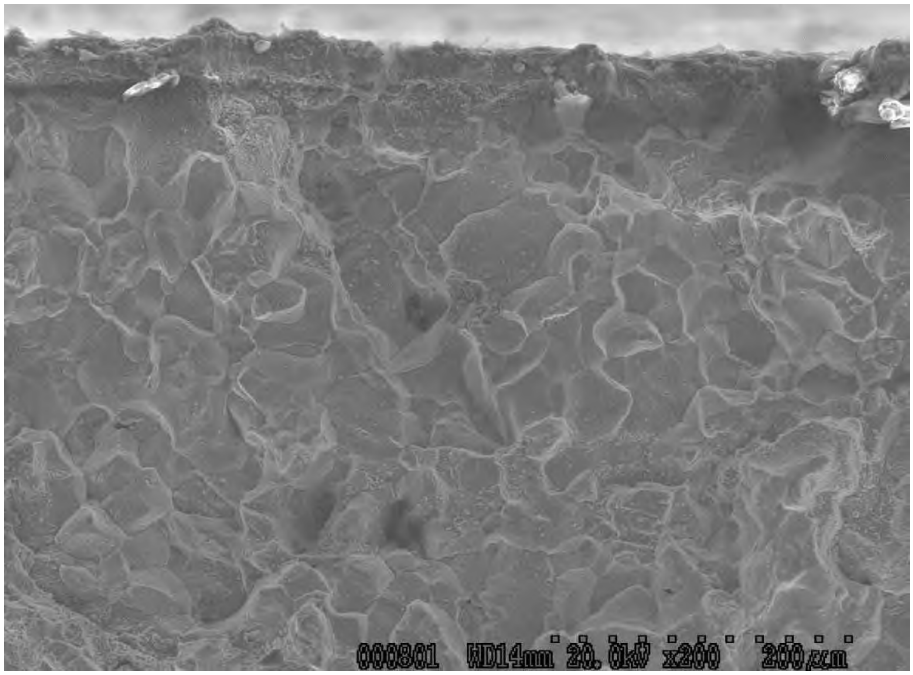

Fig. 221. Scanning electron fractograph of crack surface from SID 14875 subsegment "C4d" Area "1".

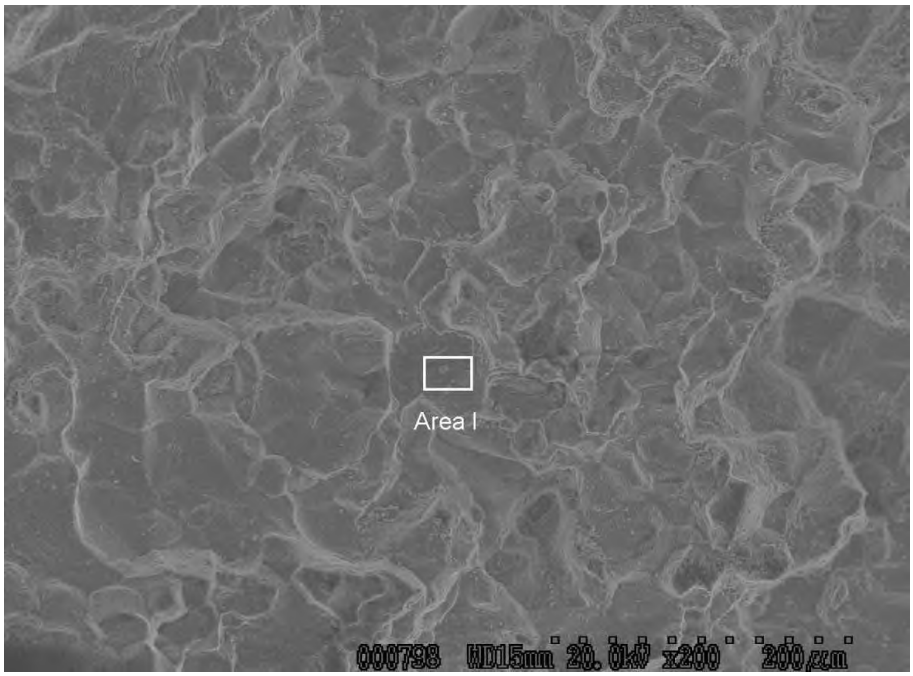

Fig. 222. Scanning electron fractograph of crack surface from SID 14875 subsegment "C4d" Area "2" showing EDS area "I".

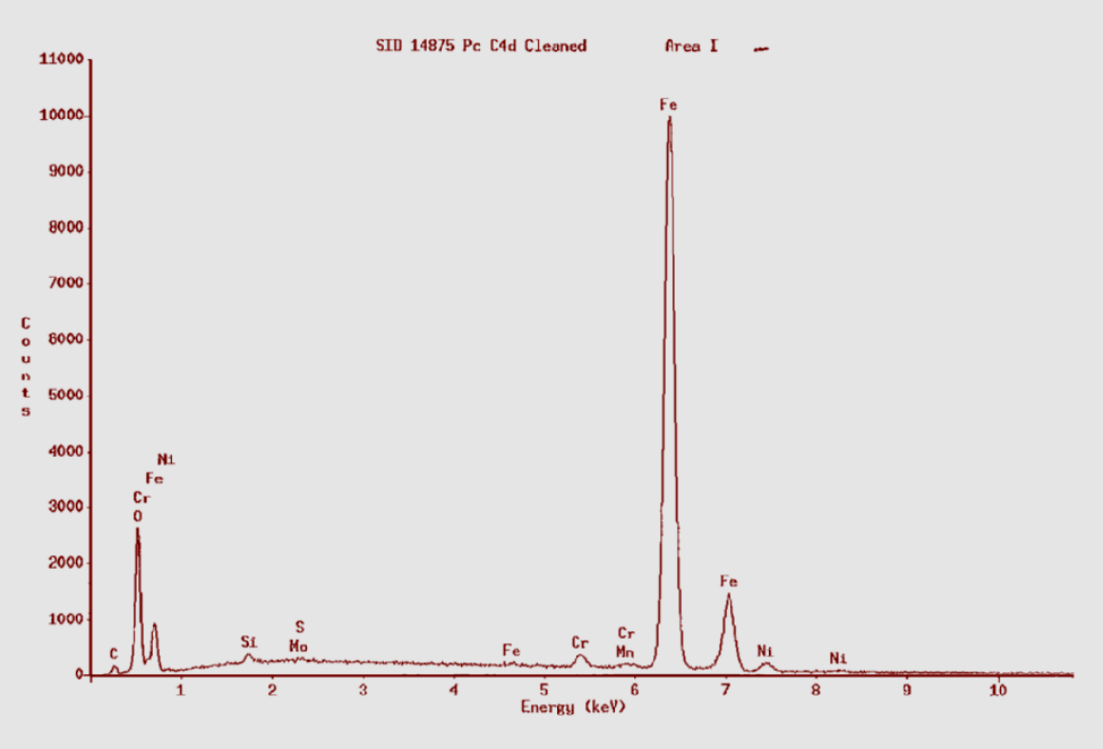

Fig. 223. X-Ray Energy Dispersive Spectrograph of SID 14875 "C4d" Area "2"at area "I" shown in Fig. 222.

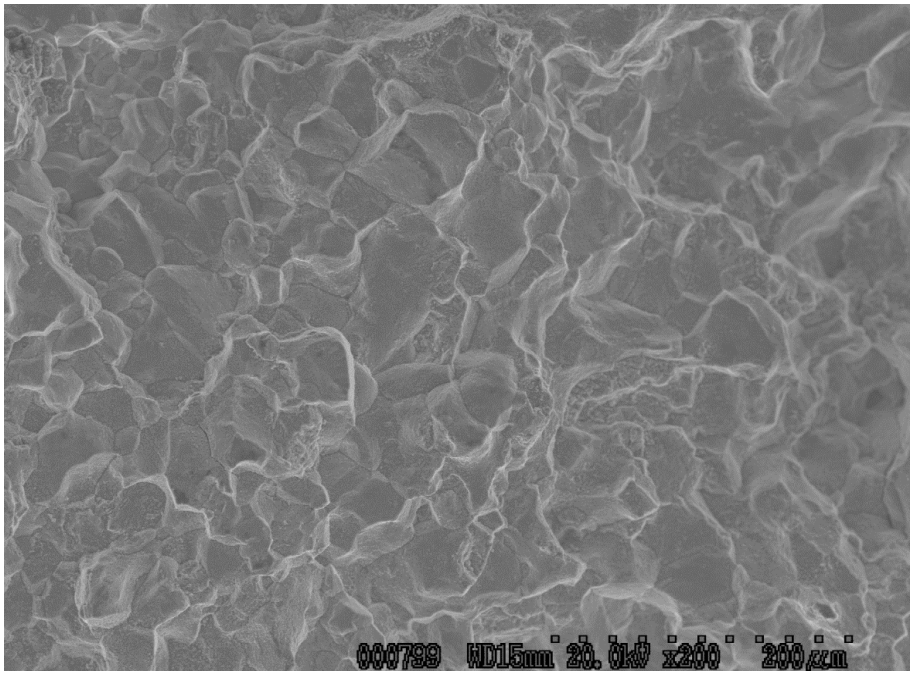

Fig. 224. Scanning electron fractograph of crack surface from SID 14875 subsegment "C4d" Area "3".

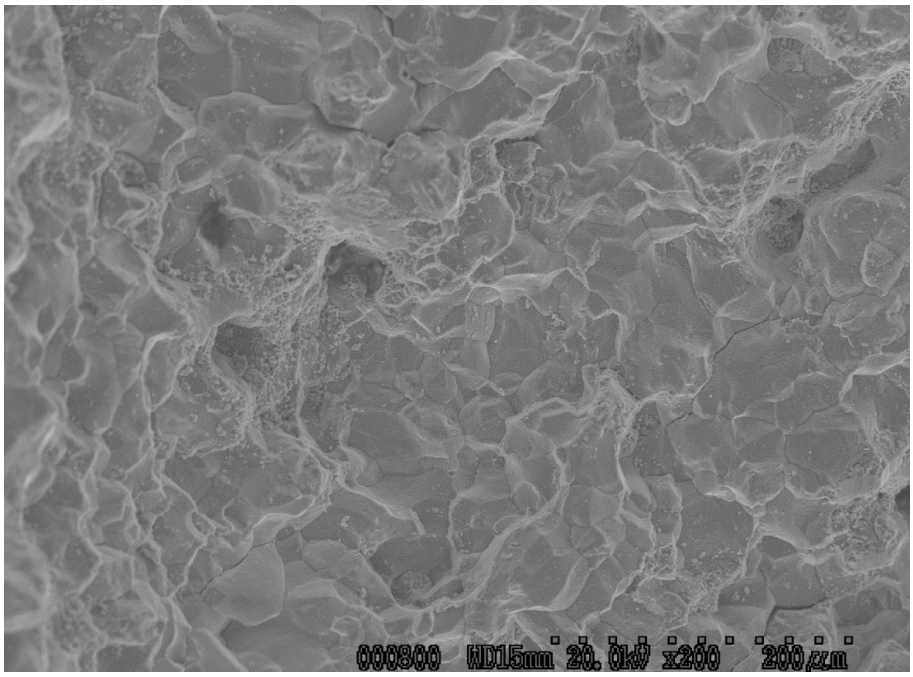

Fig. 225. Scanning electron fractograph of crack surface from SID 14875 subsegment "C4d" Area "4".

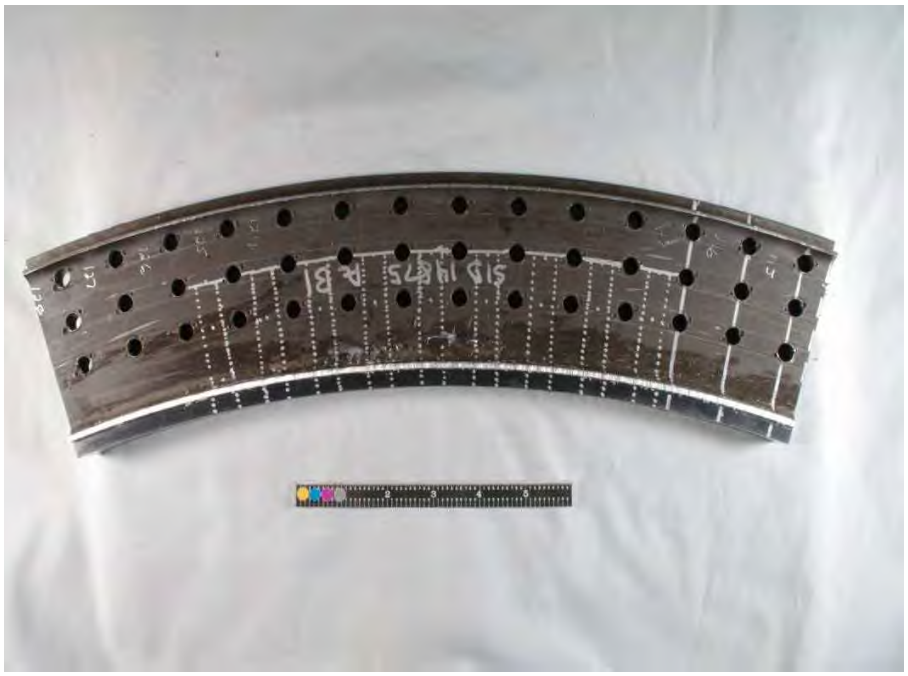

Fig. 226. SID 14875 subsegment "B1" showing layout of mechanical test coupons.

Fig. 227. Mechanical test coupons removed from SID 14875 subsegment "B1".

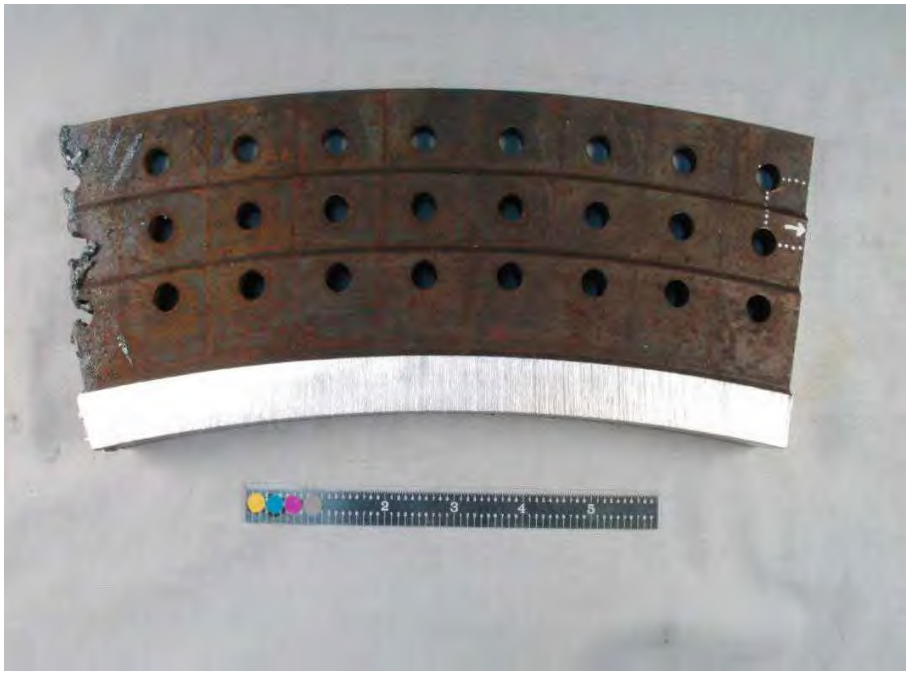

Fig. 228. SID 18475 "D2" finger pinned blade attachment showing location of met sample L349101. Arrow indicates mounting direction.

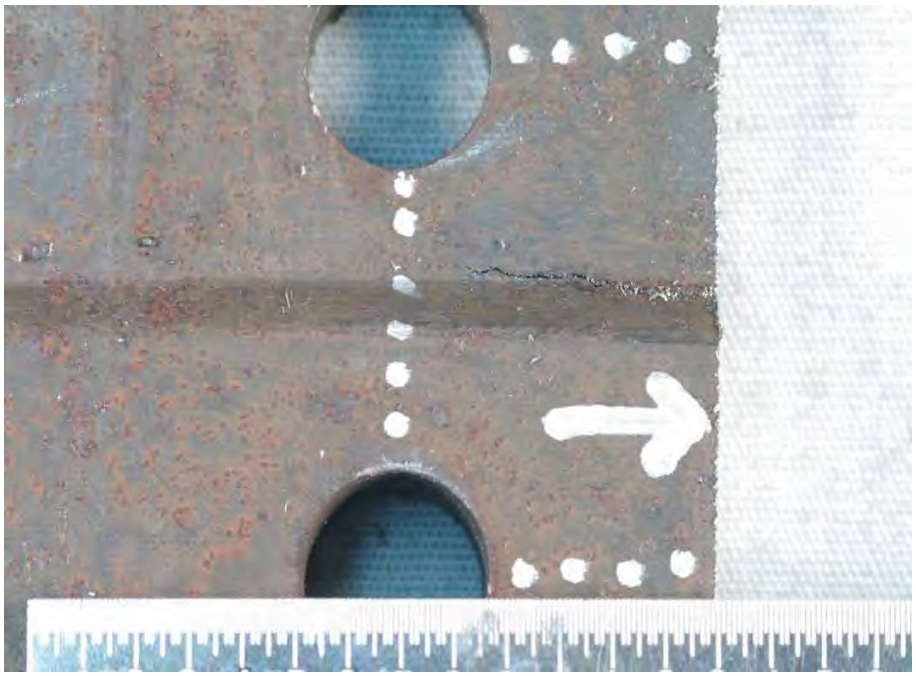

Fig. 229. Close-up of met sample L349101 shown in Fig. 228.

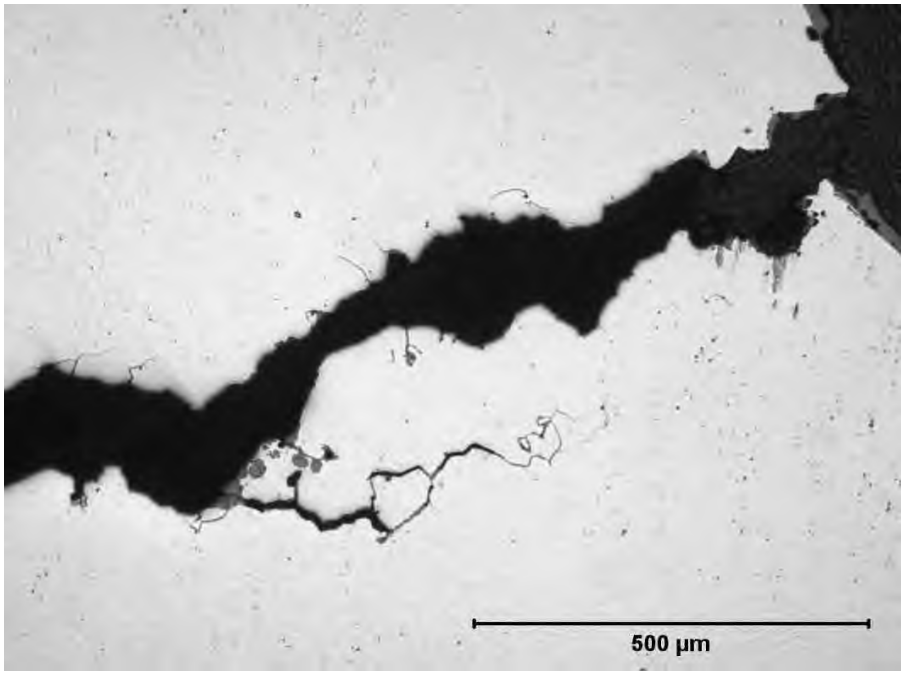

Fig. 230. Photomicrograph of met section L349101.

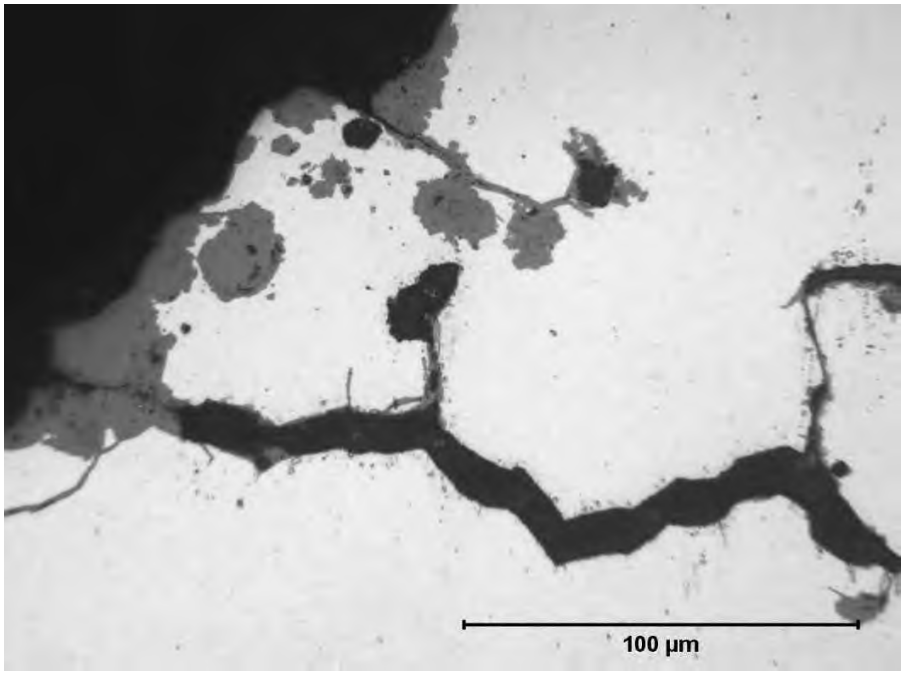

Fig 231. Photomicrograph of met section L349101.

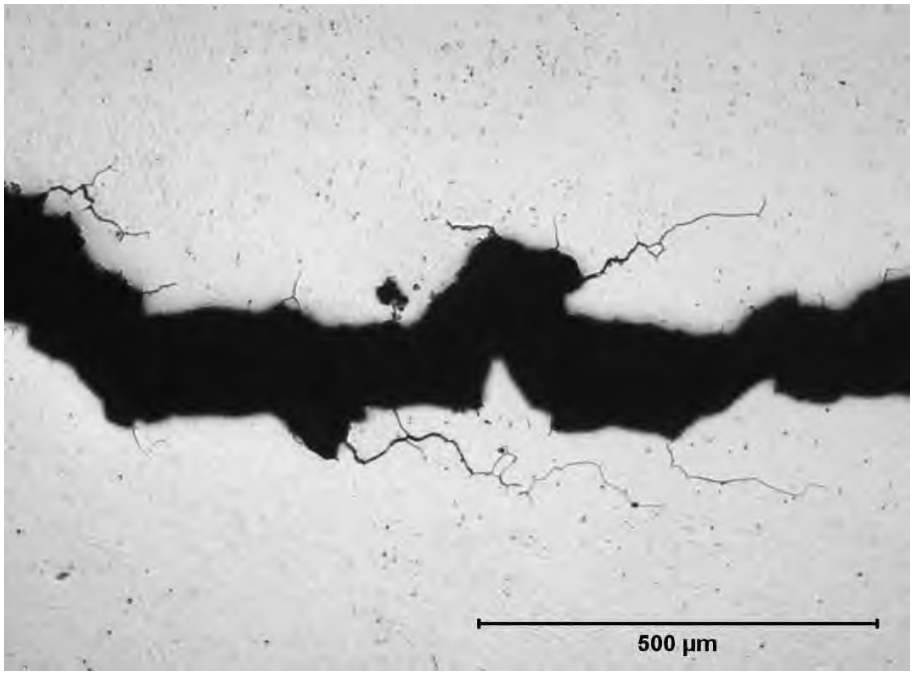

Fig. 232. Photomicrograph of met section L349101.

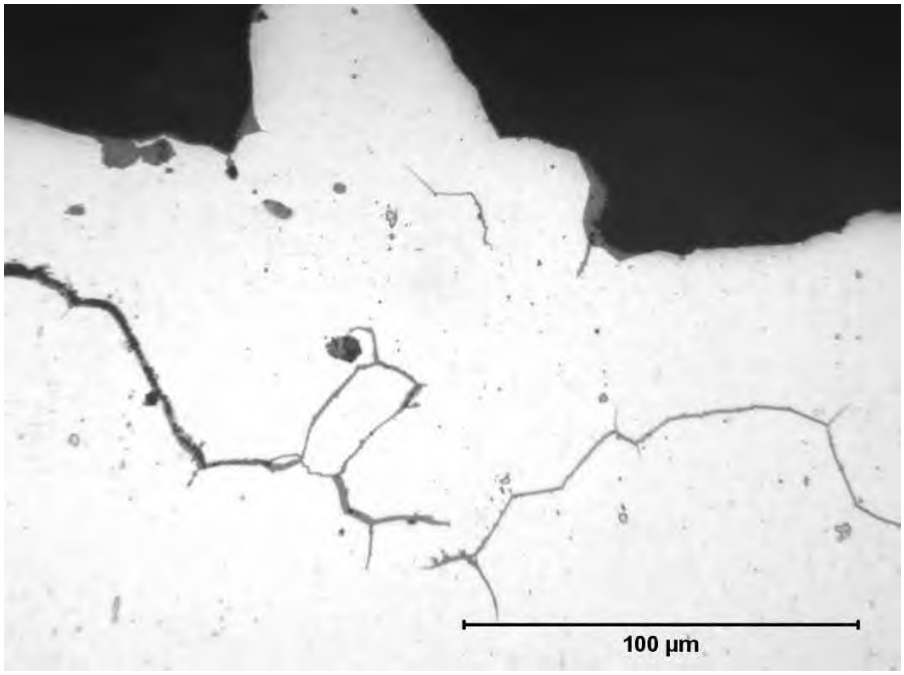

Fig. 233. Photomicrograph of met section L349101.

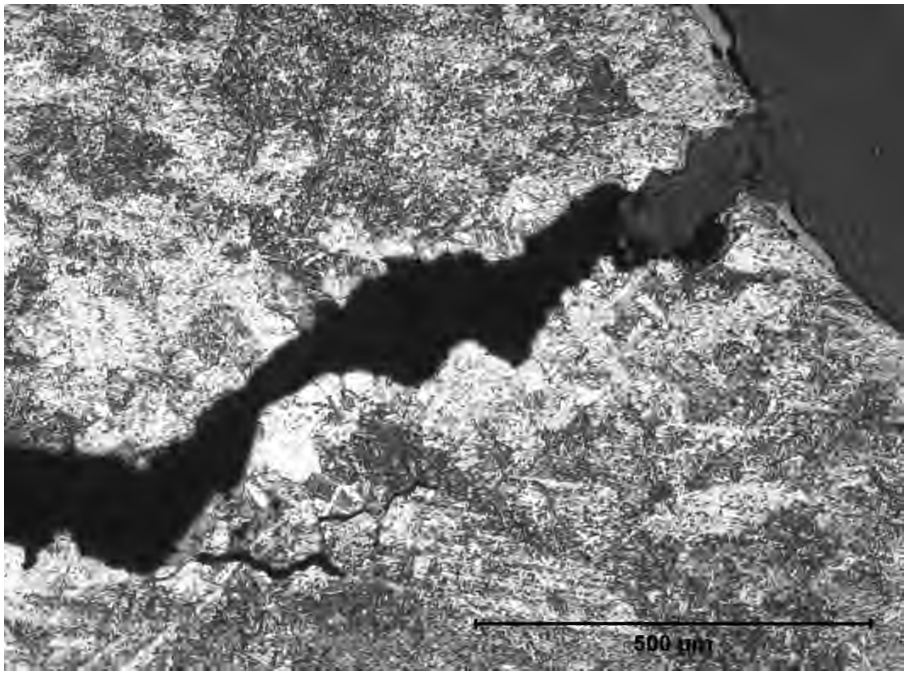

Fig. 234. Photomicrograph of met section L349101.

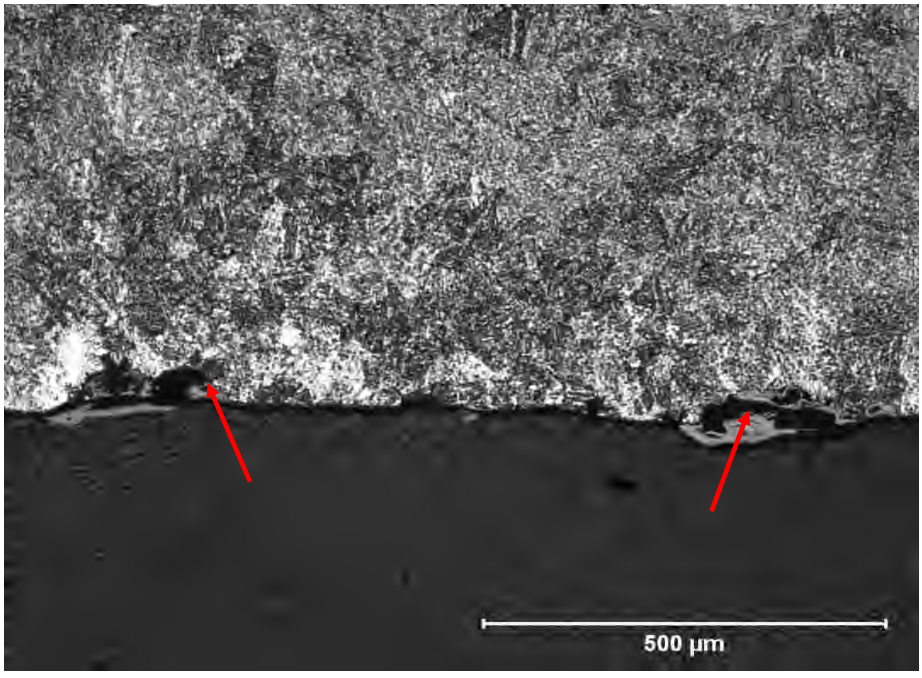

Fig. 235. Photomicrograph of met section L349101. Corrosion pits denoted by arrows.

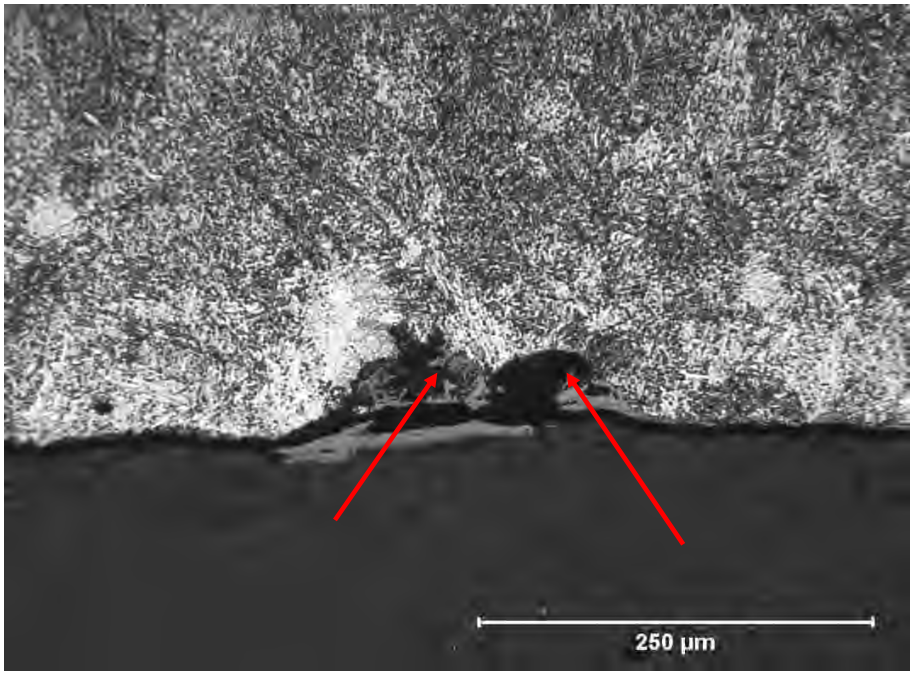

Fig. 236. Photomicrograph of met section L349101. Corrosion pits denoted by arrows.

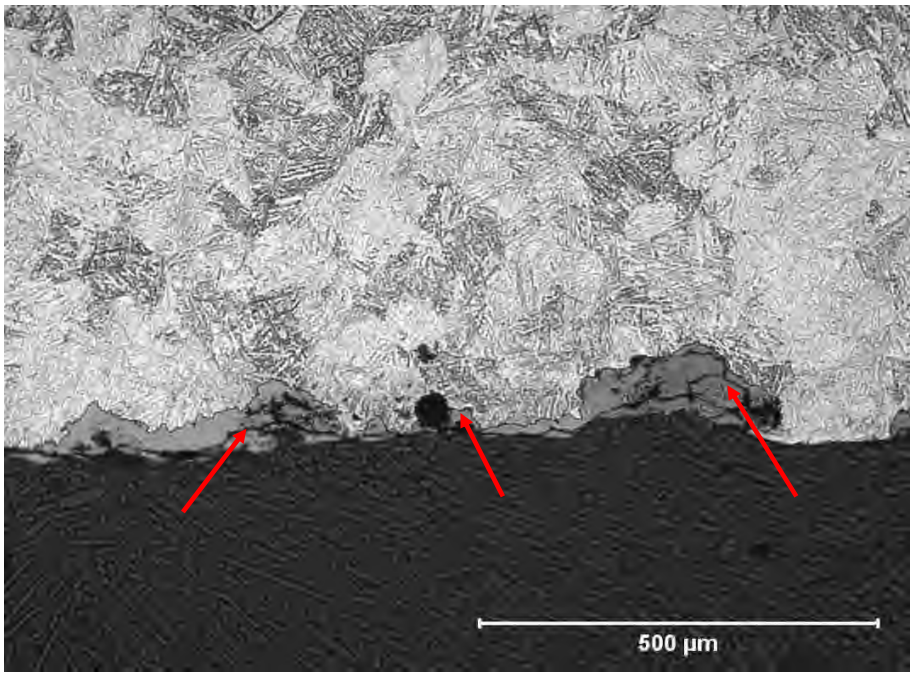

Fig. 237. Photomicrograph of met section L349101. Corrosion pits denoted by arrows.

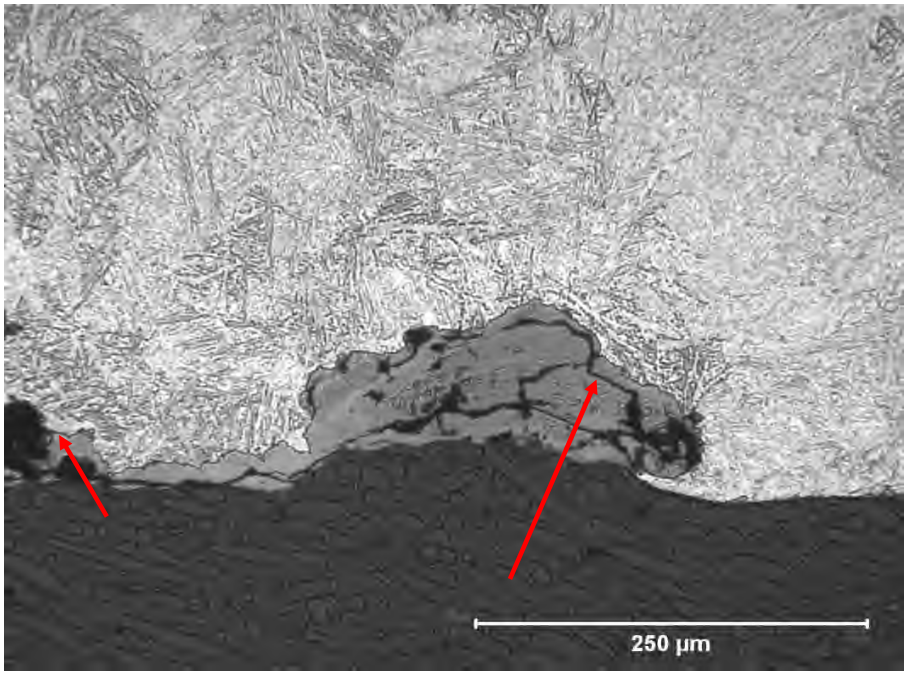

Fig. 238. Photomicrograph of met section L349101. Corrosion pits denoted by arrows.

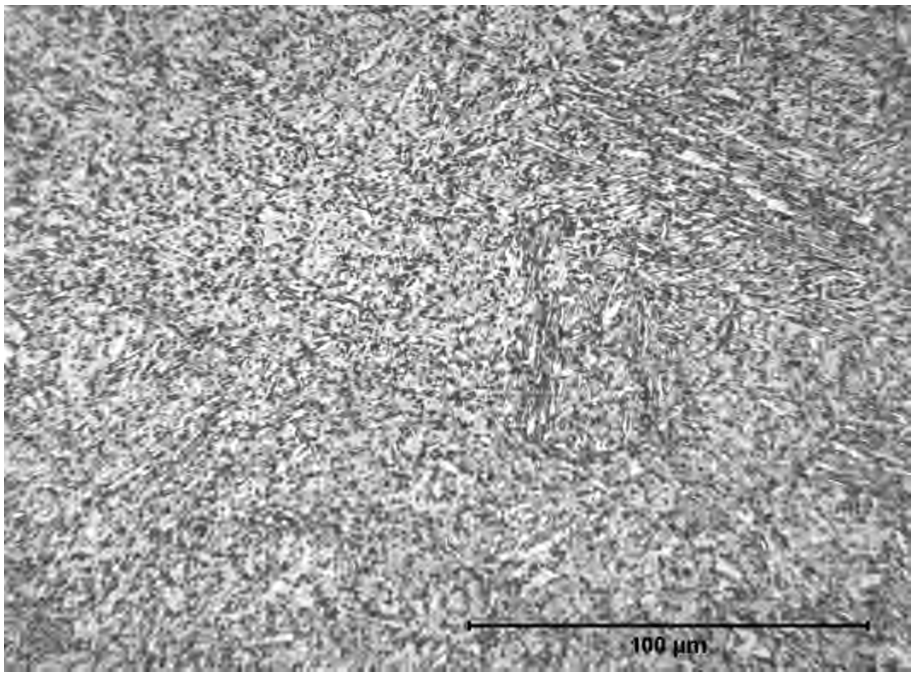

Fig. 239. Photomicrograph of met section L349101.

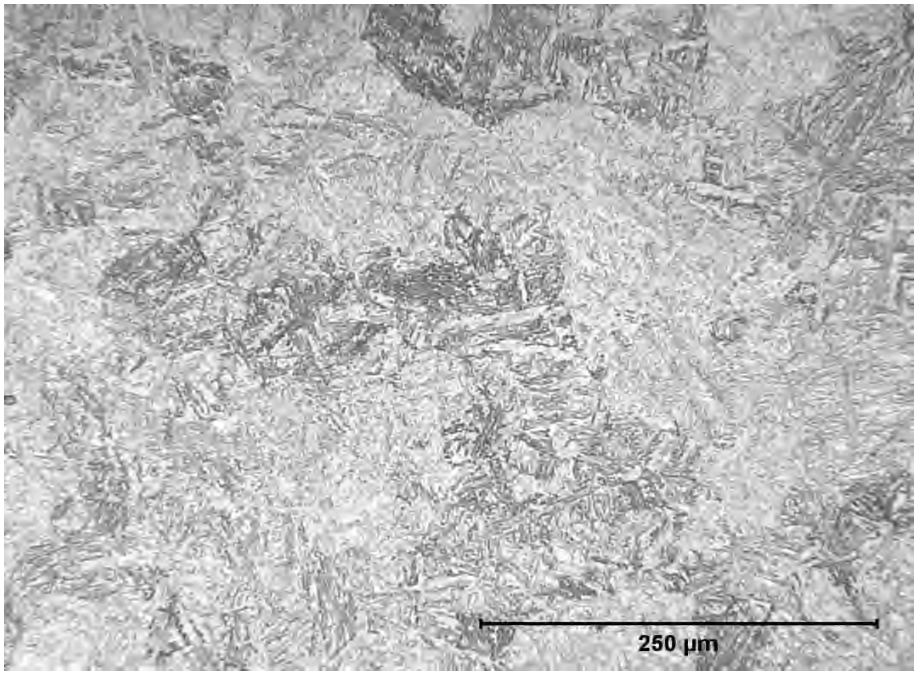

Fig. 240. Photomicrograph of met section L349101.

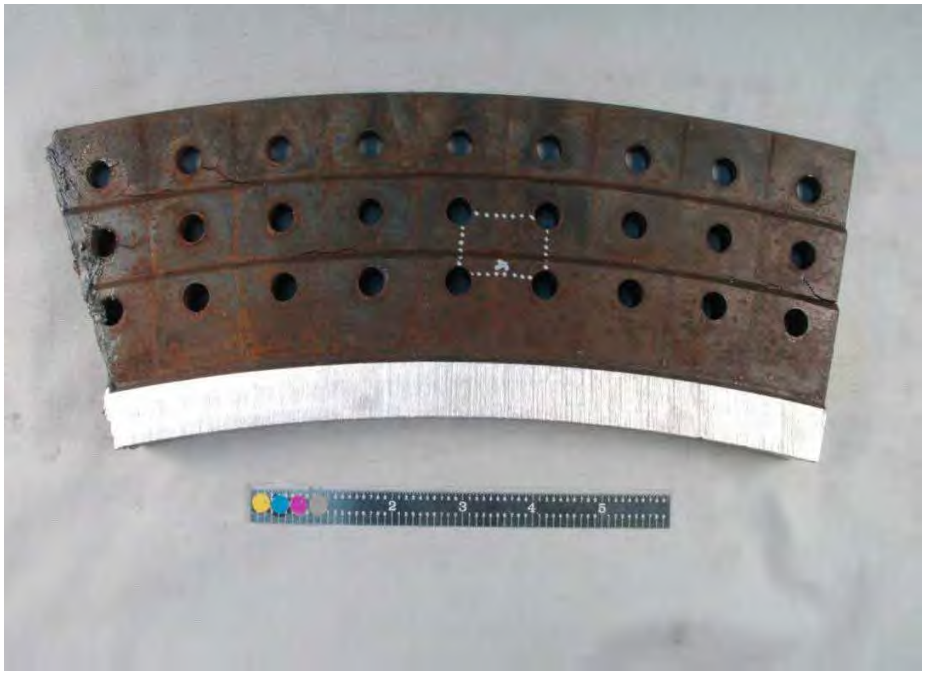

Fig. 241. SID 18475 "D3" finger pinned blade attachment showing location of met Sample L349102.

Fig. 242. Close-up of met sample L349102.

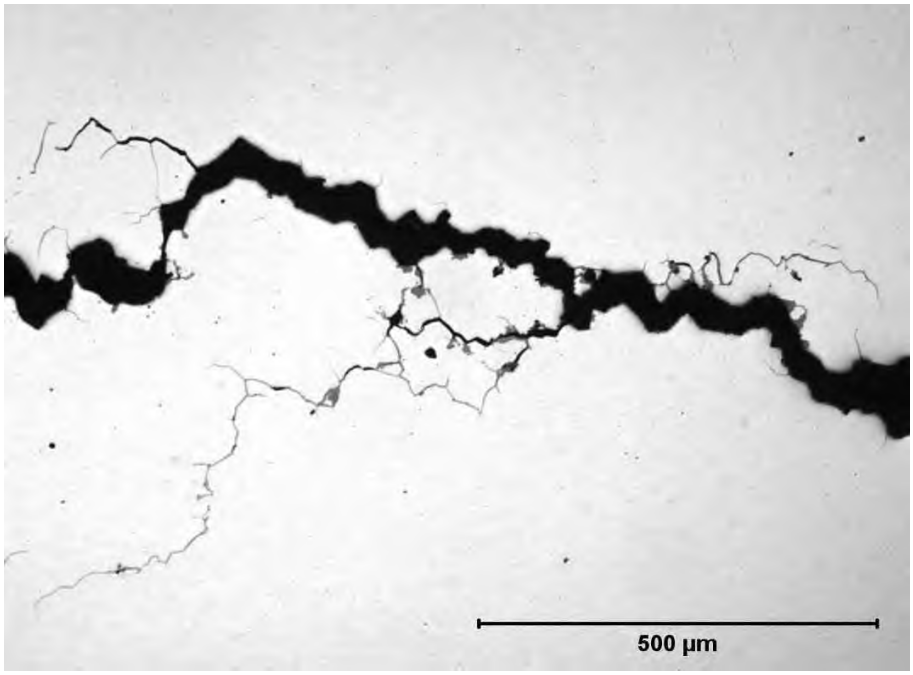

Fig. 243. Photomicrograph of met sample L349102.

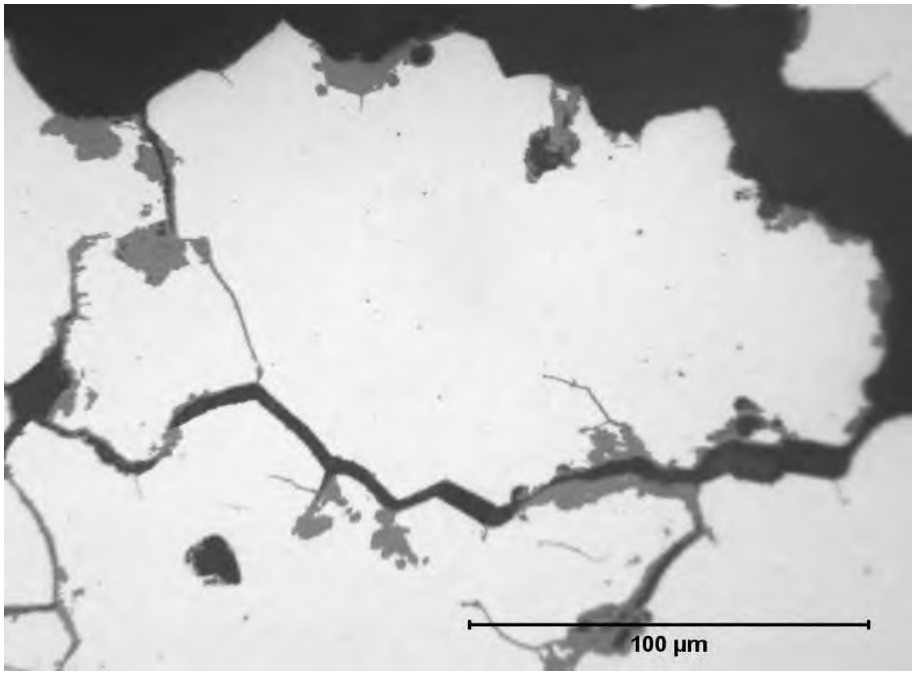

Fig. 244. Photomicrograph of met sample L349102.

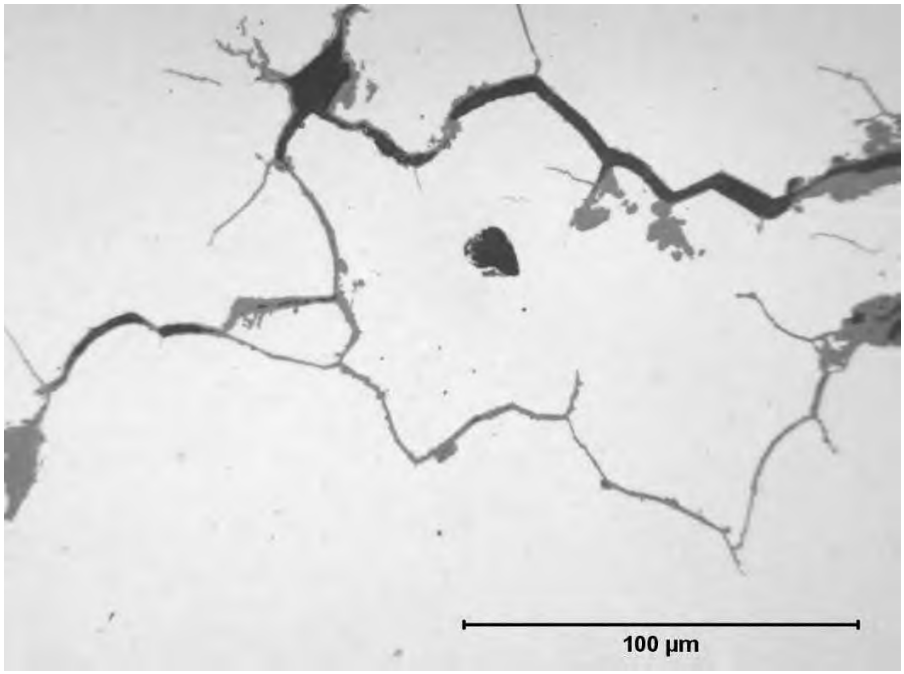

Fig. 245. Photomicrograph of met sample L349102.

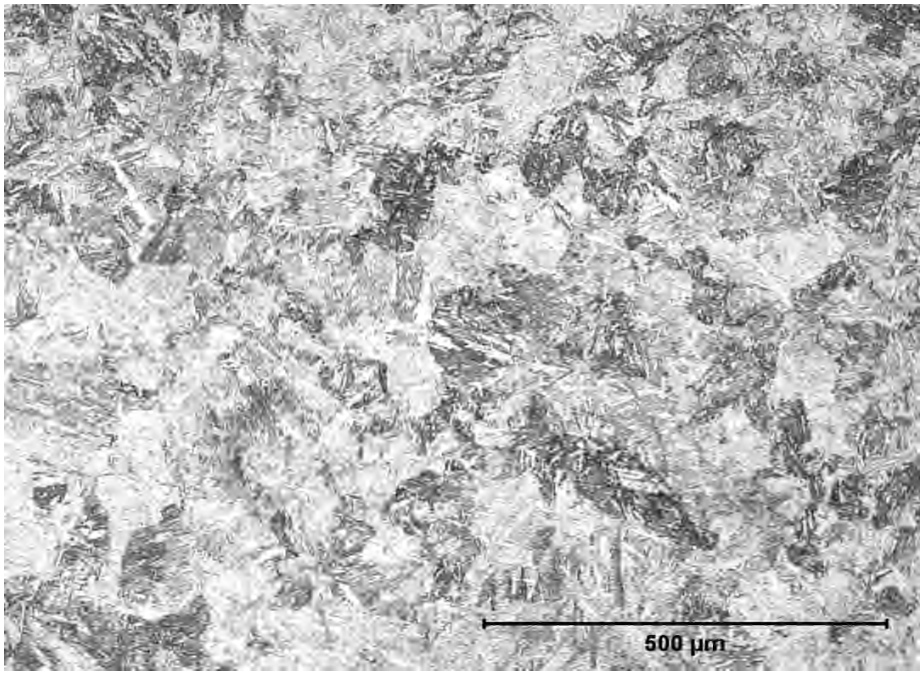

Fig. 246. Photomicrograph of met sample L349102.

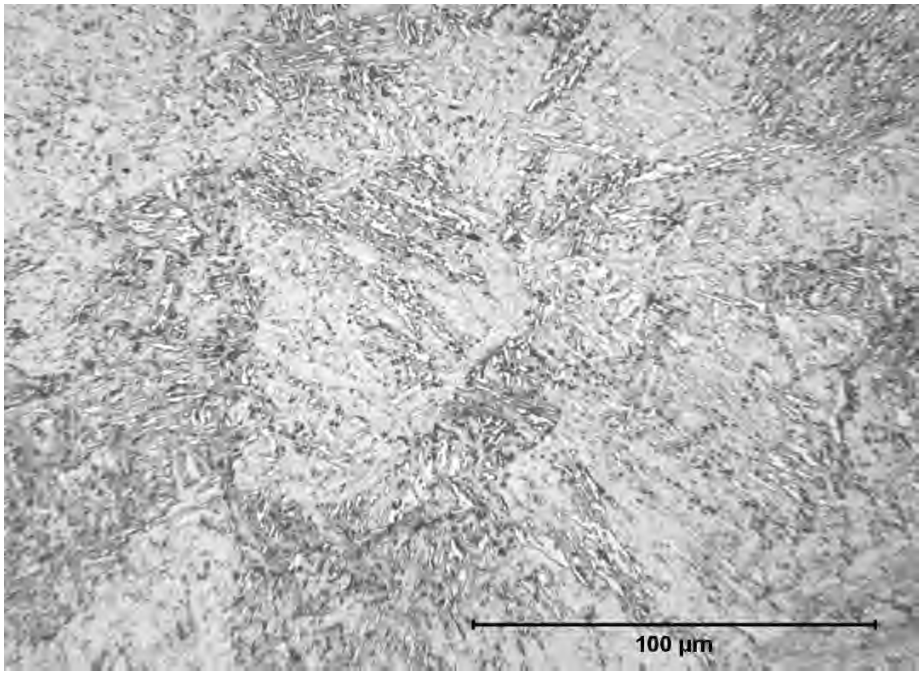

Fig. 247. Photomicrograph of met sample L349102.

Fig. 248. SID 18475 "D5" finger pinned blade attachment showing location of met Samples L349103 and L349104.

Fig. 249. Close-up of met samples L349103 sand L349104.

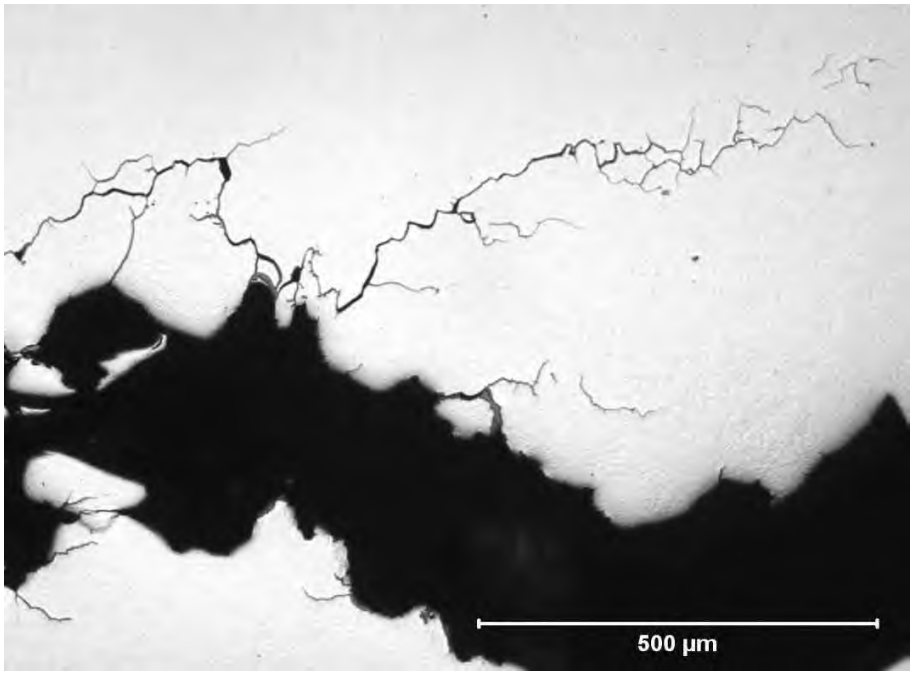

Fig. 250. Photomicrograph of met sample L349103.

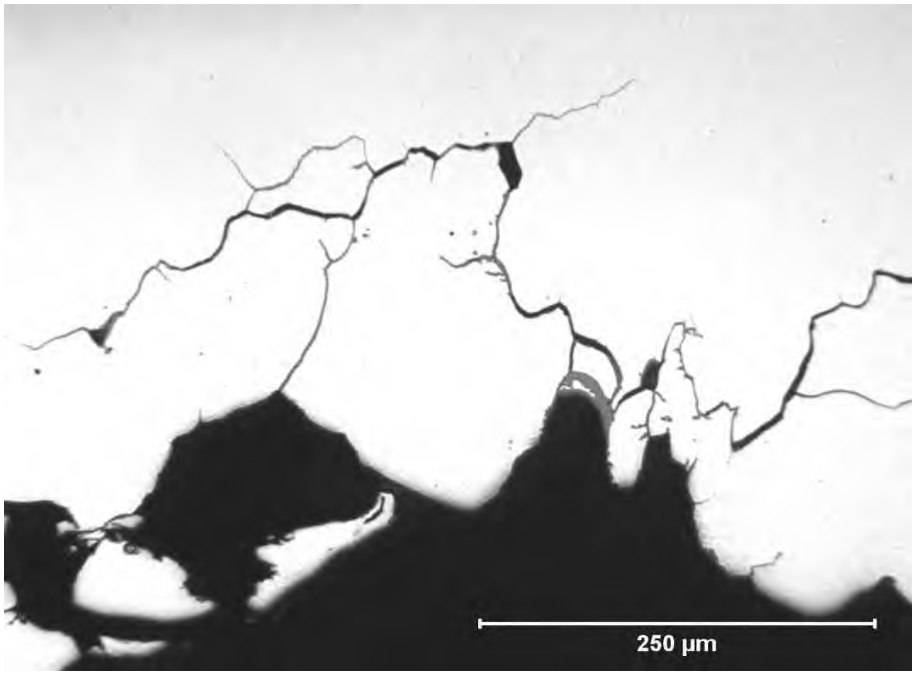

Fig. 251. Photomicrograph of met sample L349103.

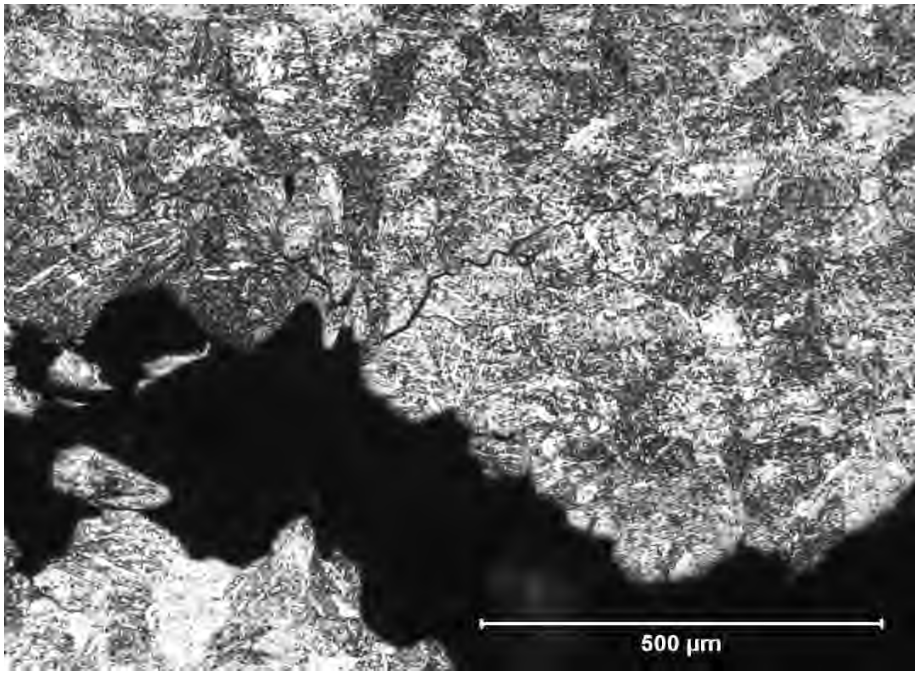

Fig. 252. Photomicrograph of met sample L349103.

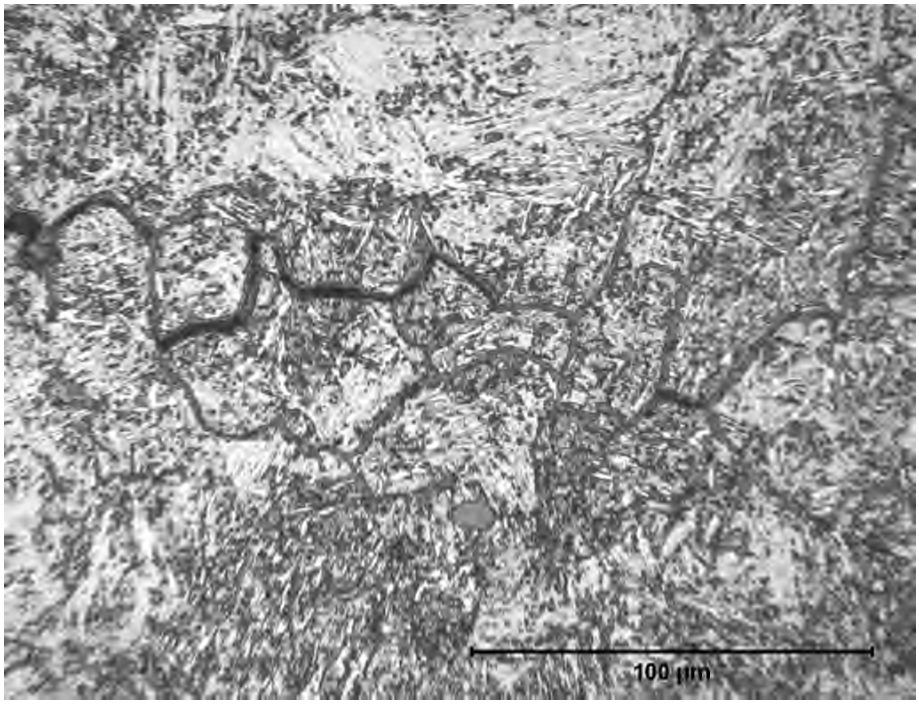

Fig. 253. Photomicrograph of met sample L349103.

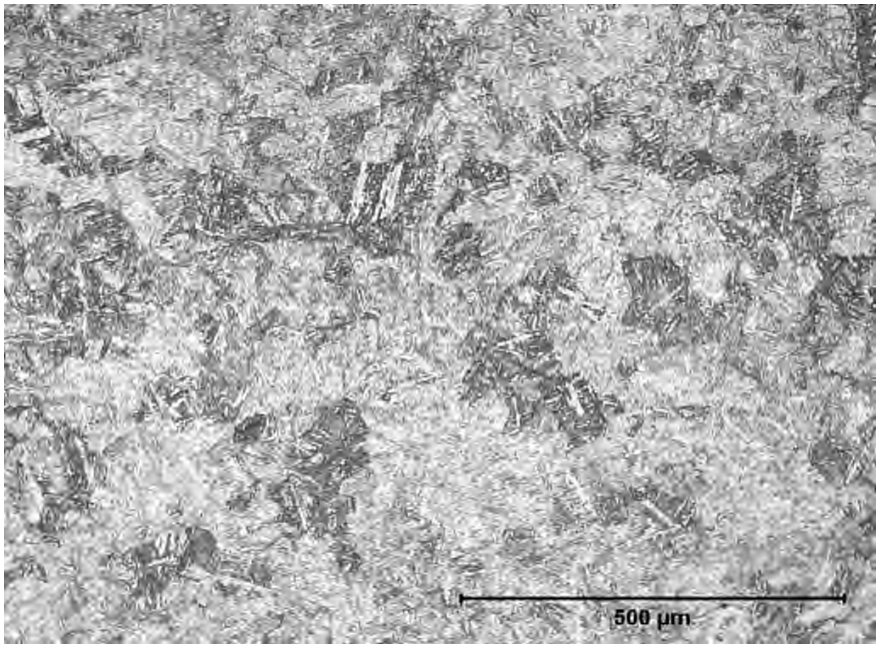

Fig. 254. Photomicrograph of met sample L349103.

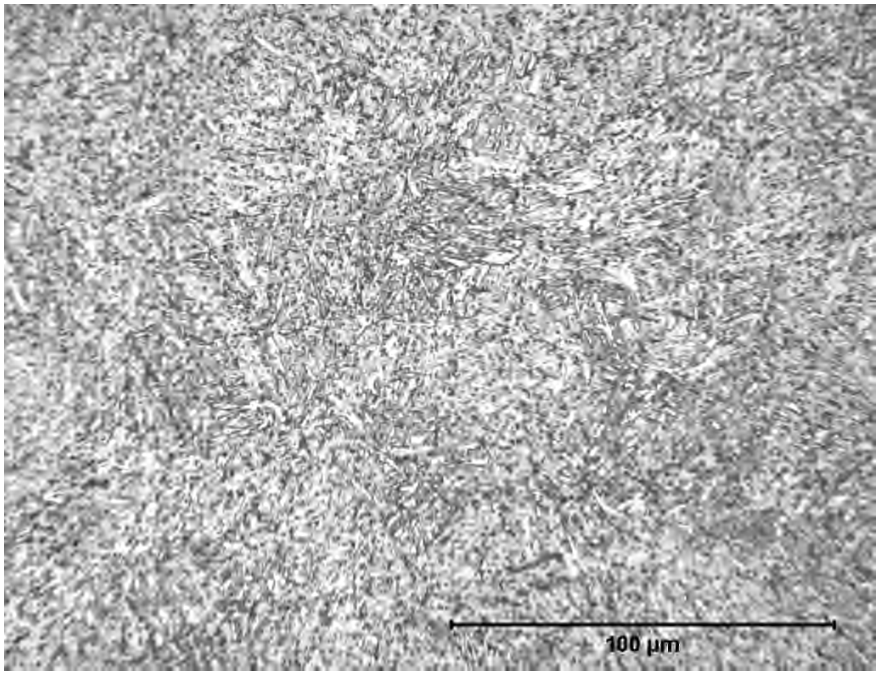

Fig. 255. Photomicrograph of met sample L349103.

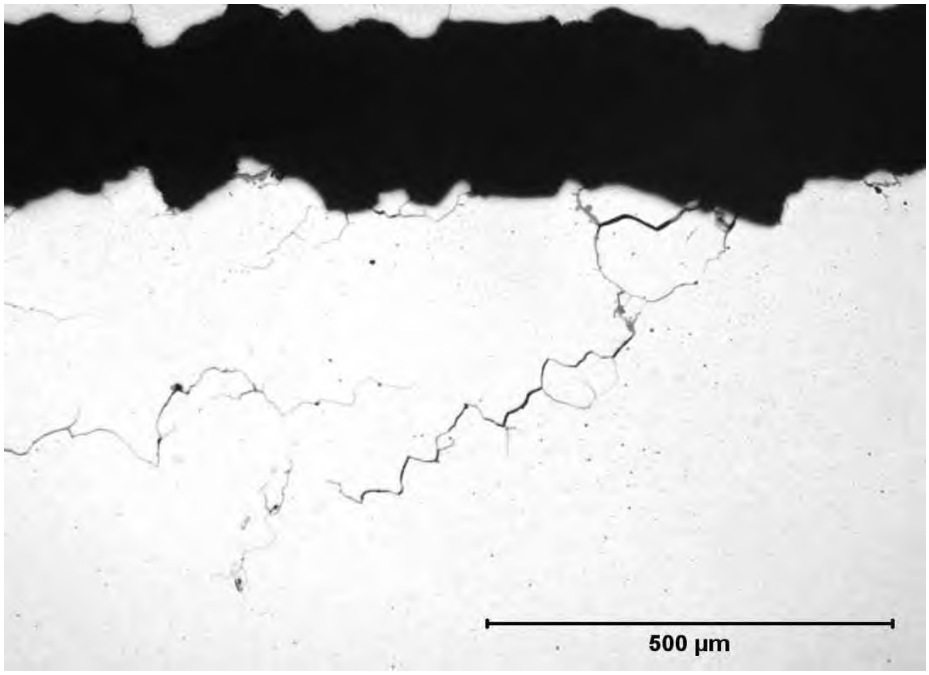

Fig. 256. Photomicrograph of met sample L349104.

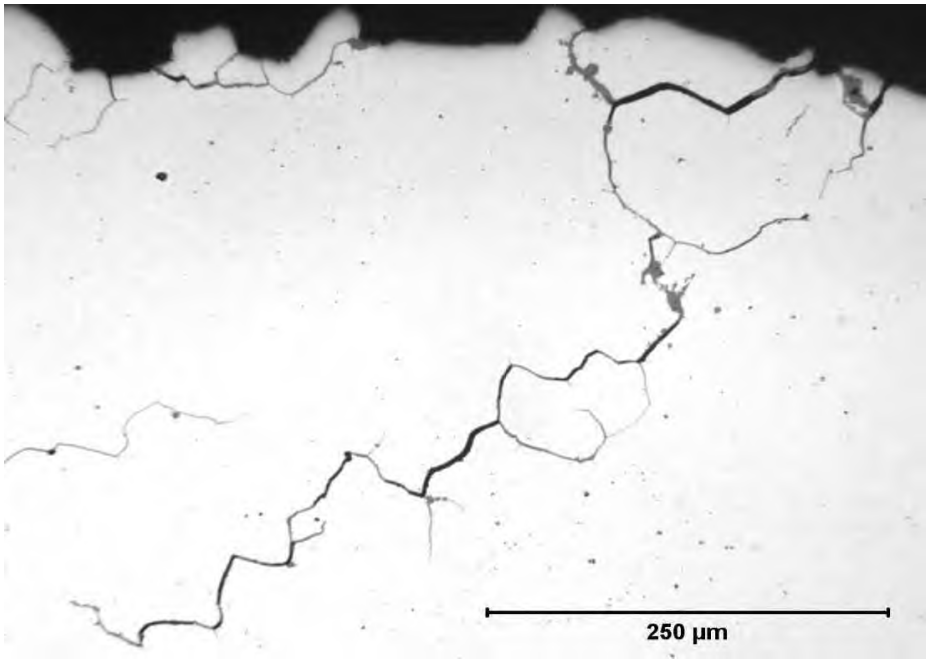

Fig. 257. Photomicrograph of met sample L349104.

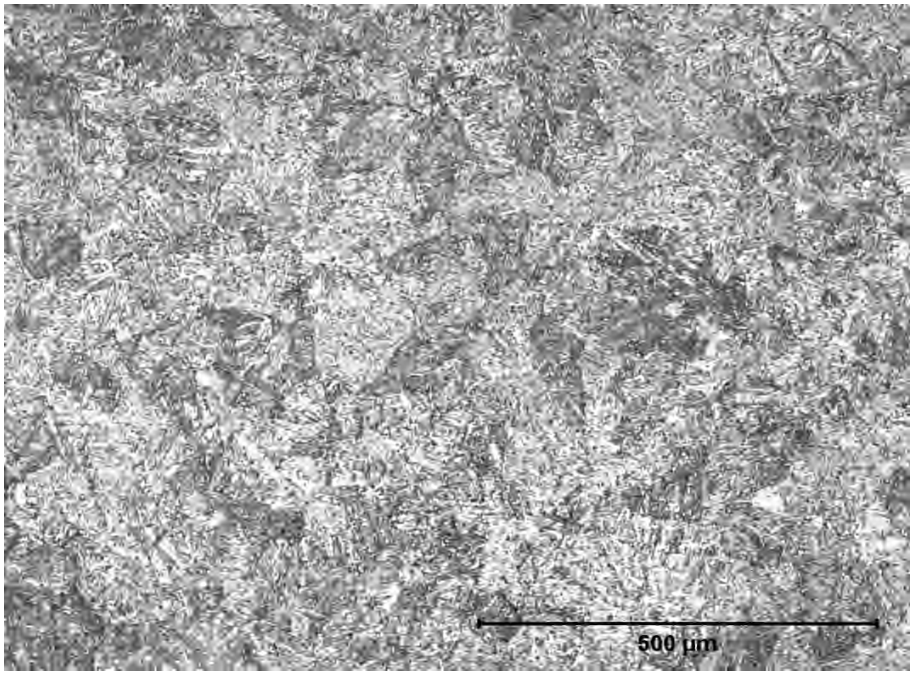

Fig. 258. Photomicrograph of met sample L349104.

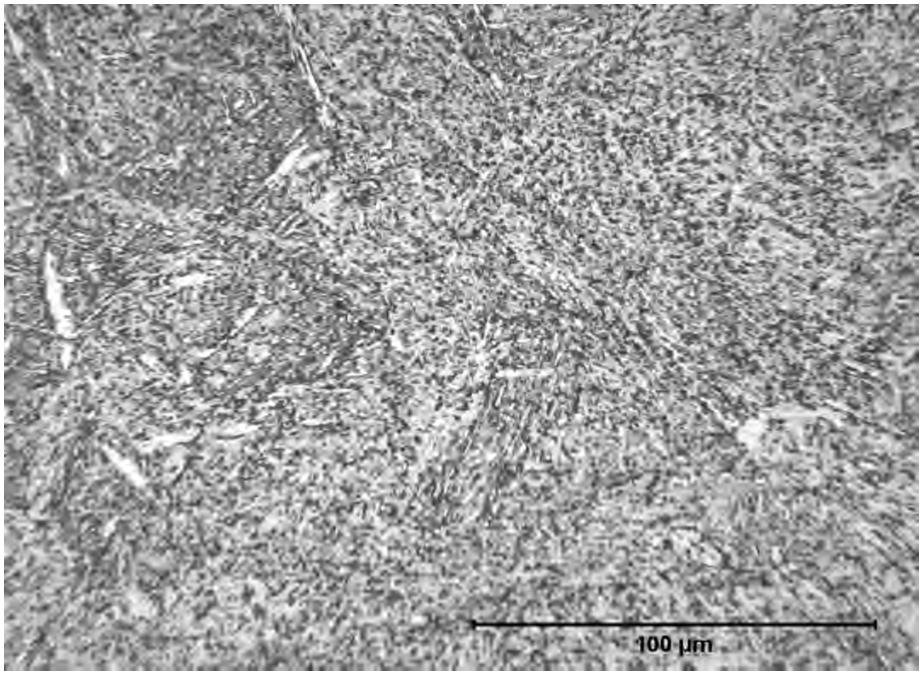

Fig. 259. Photomicrograph of met sample L349104.

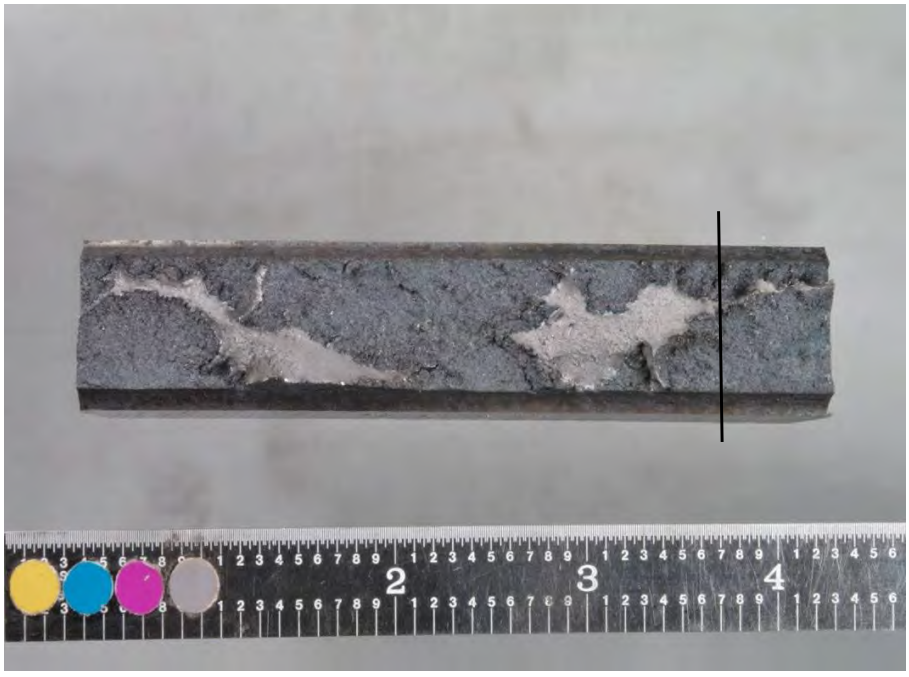

Fig. 260. SID 18475 "B4" finger pinned blade attachment showing location of met Sample L349105.

Fig. 261. SID 18475 "B4" finger pinned blade attachment showing location of met Sample L349105.

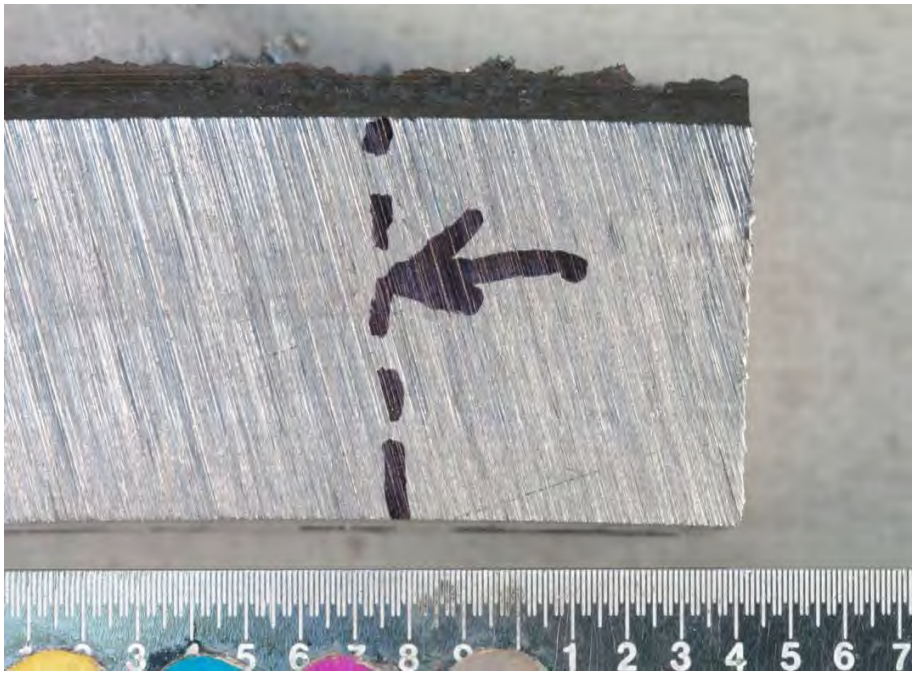

Fig. 262. Close-up of met sample L349105.

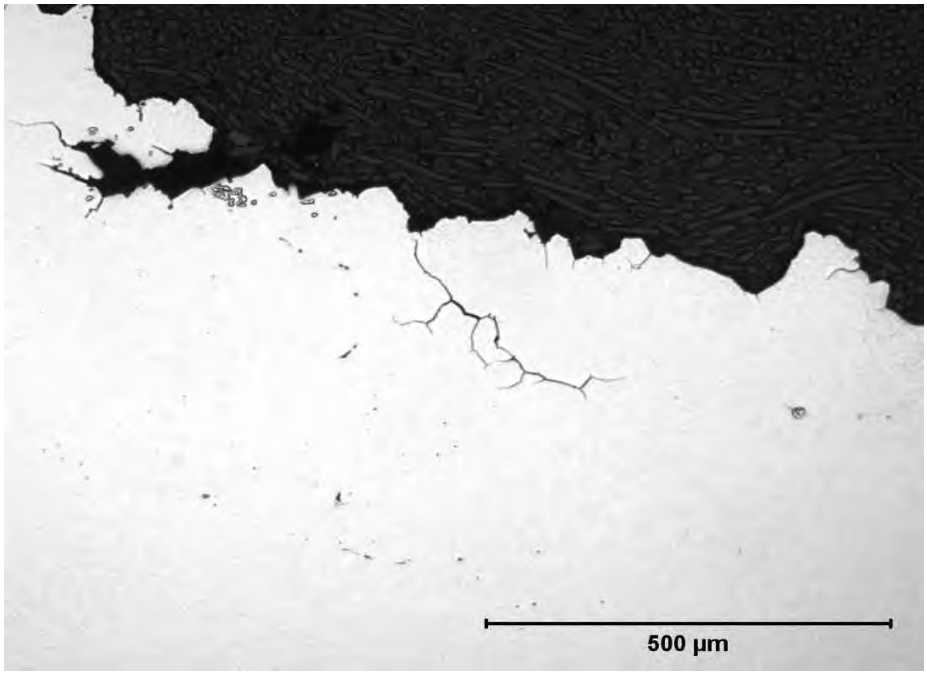

Fig. 263. Photomicrograph of met sample L349105.

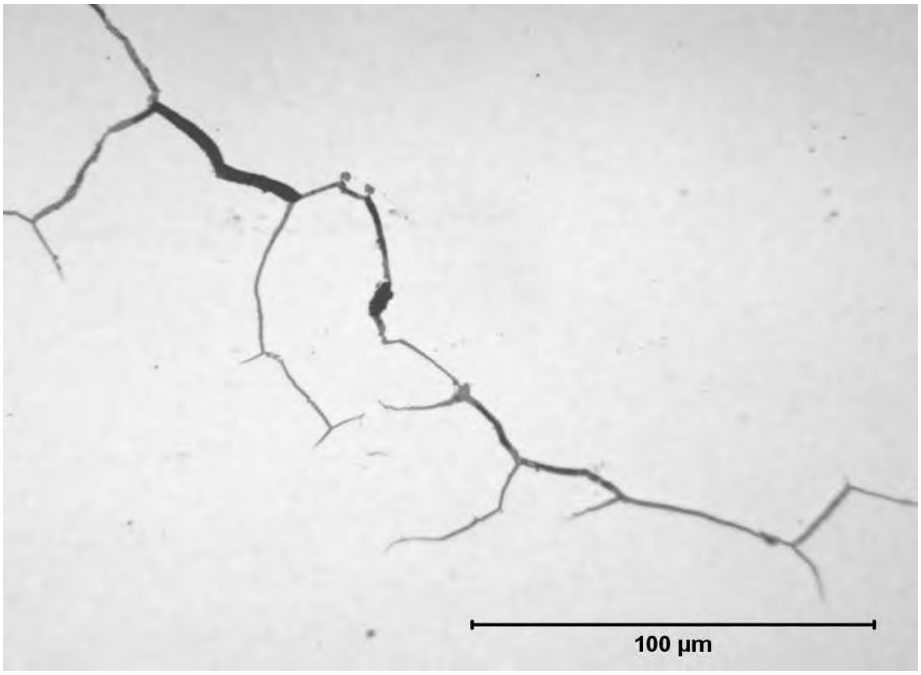

Fig. 264. Photomicrograph of met sample L349105.

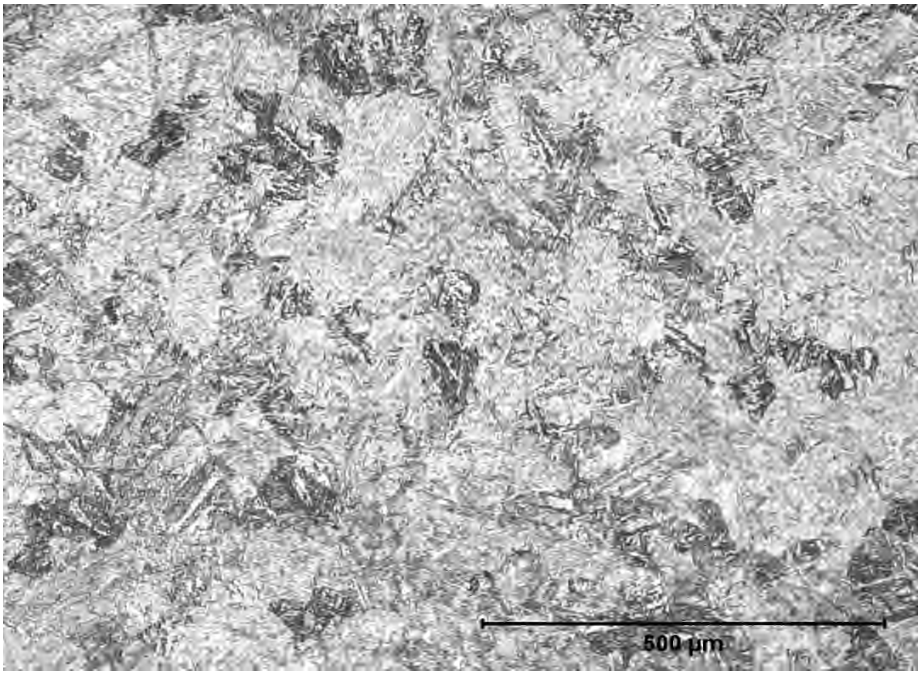

Fig. 265. Photomicrograph of met sample L349105.

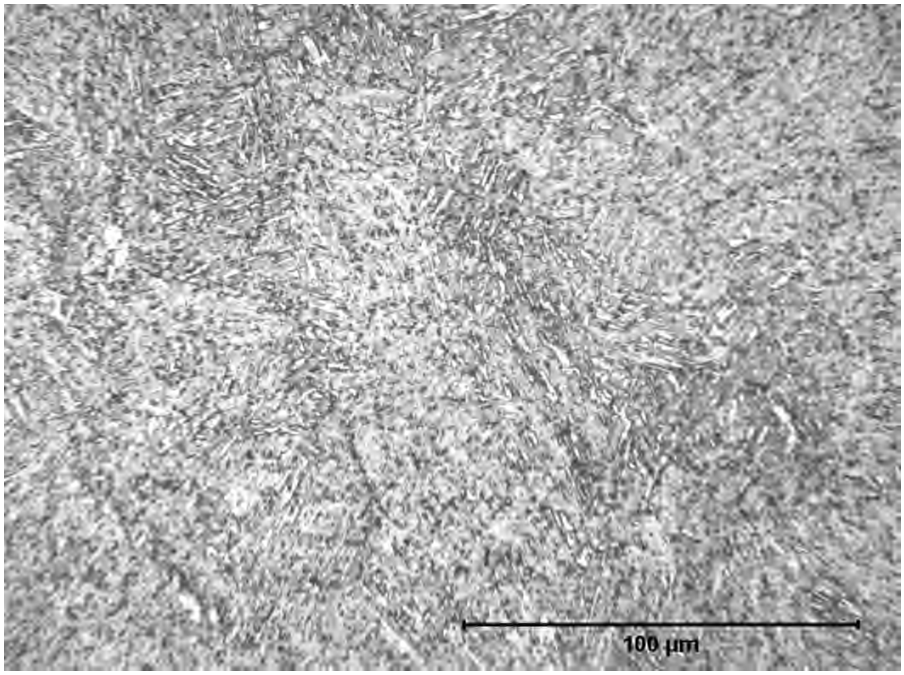

Fig. 266. Photomicrograph of met sample L349105.

Fig. 267. SID 18474 "A4" finger pinned blade attachment showing location of met Sample L349106.

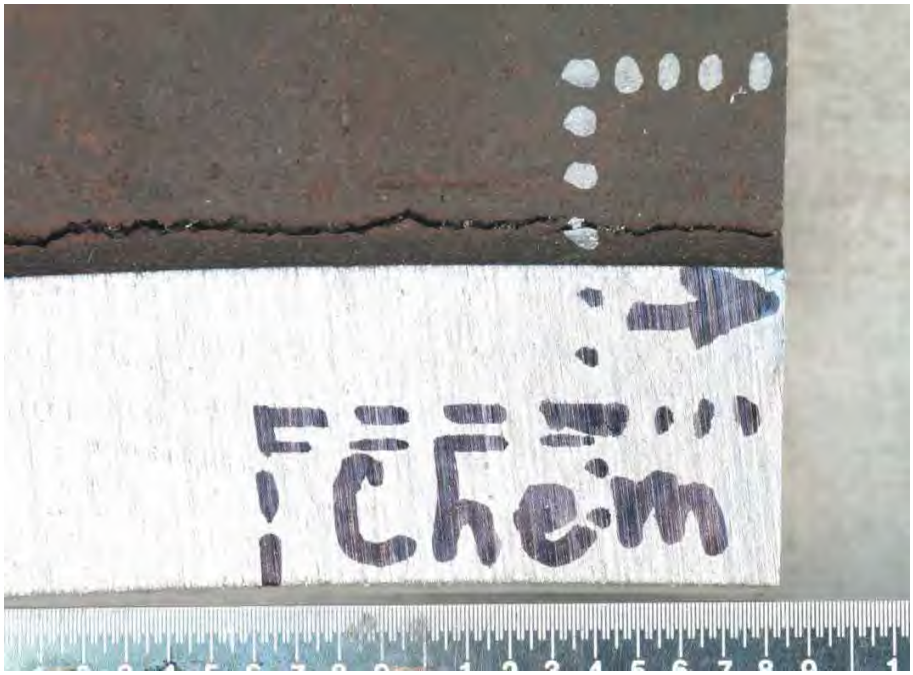

Fig. 268. Close-up of met sample L349106.

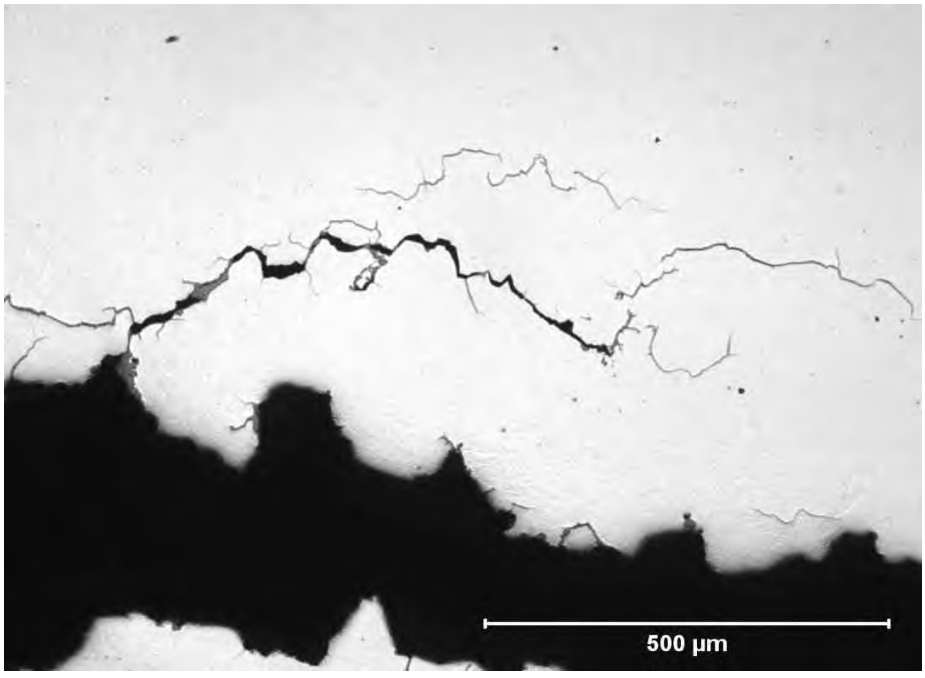

Fig. 269. Photomicrograph of met sample L349106.

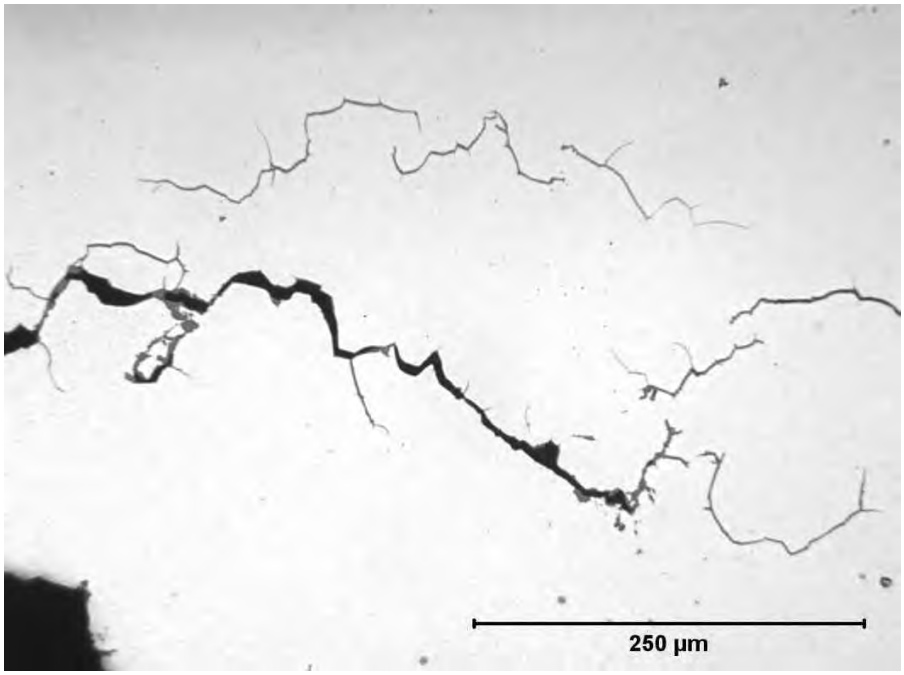

Fig. 270. Photomicrograph of met sample L349106.

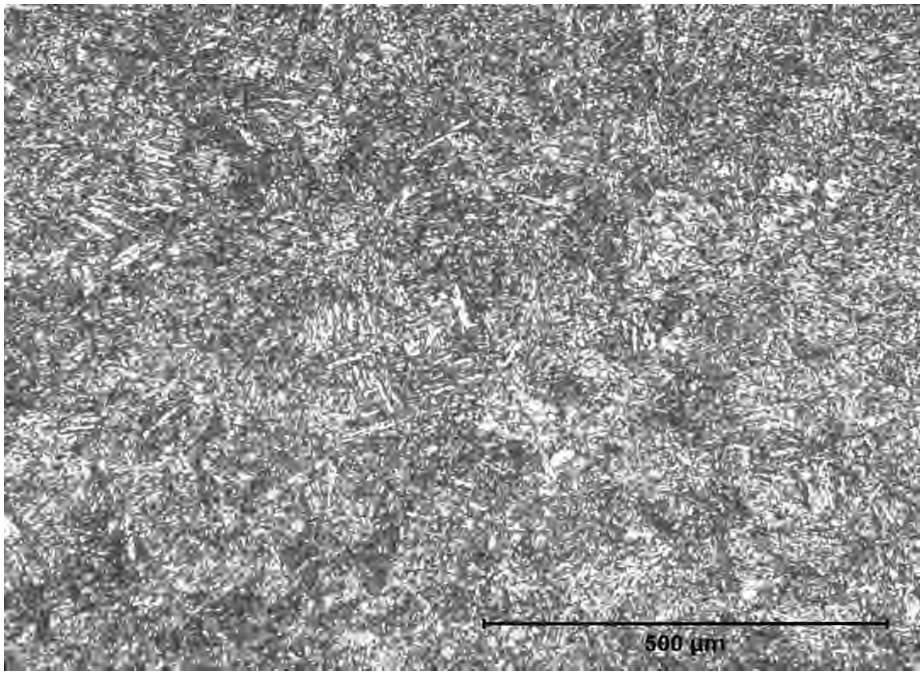

Fig. 271. Photomicrograph of met sample L349106.

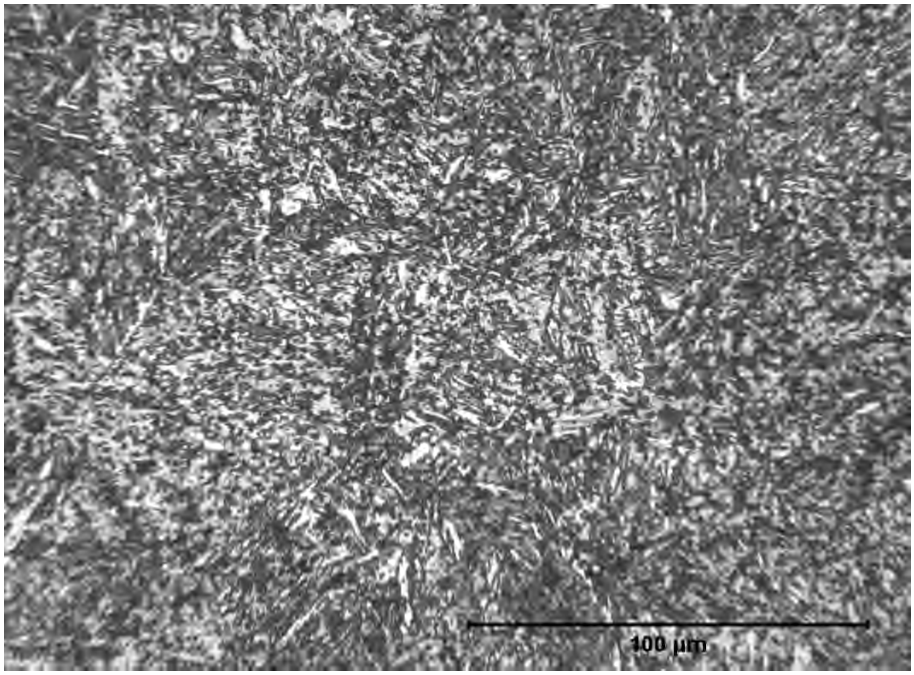

Fig. 272. Photomicrograph of met sample L349106.

Fig. 273. Photograph of low pressure turbine "B" turbine end L-1 blades recovered at the plant site and received for forensic examination.

Fig. 274 . Photograph of low pressure turbine "B" turbine end L-1 blades recovered at the plant site and received for forensic examination.

Fig. 275. Photograph of low pressure turbine "B" turbine end L-1 blades recovered at the plant site and received for forensic examination.

Fig. 276. Photograph of low pressure turbine "B" turbine end L-1 blade recovered at the plant site and received for forensic examination.

Fig. 277. Photograph of low pressure turbine "B" turbine end L-1 blade removed at the GE Repair Facility in Chicago, IL and received for forensic examination.

Fig. 278. Photograph of low pressure turbine "B" turbine end L-1 blade which had fractured through the airfoil.

Fig. 279. Photograph of low pressure turbine "B" turbine end L-1 blade which had fractured through the airfoil.

Fig. 280. Photograph of low pressure turbine "B" turbine end L-1 blade which had fractured through the airfoil.

Fig. 281. Photograph of low pressure turbine "B" turbine end L-1 blade which fractured transversely through airfoil just above root platform.

Fig. 282. Close-up photograph of blade airfoil fracture shown in Fig. 281.

Fig. 283. Close-up photograph of blade airfoil fracture shown in Fig. 281.

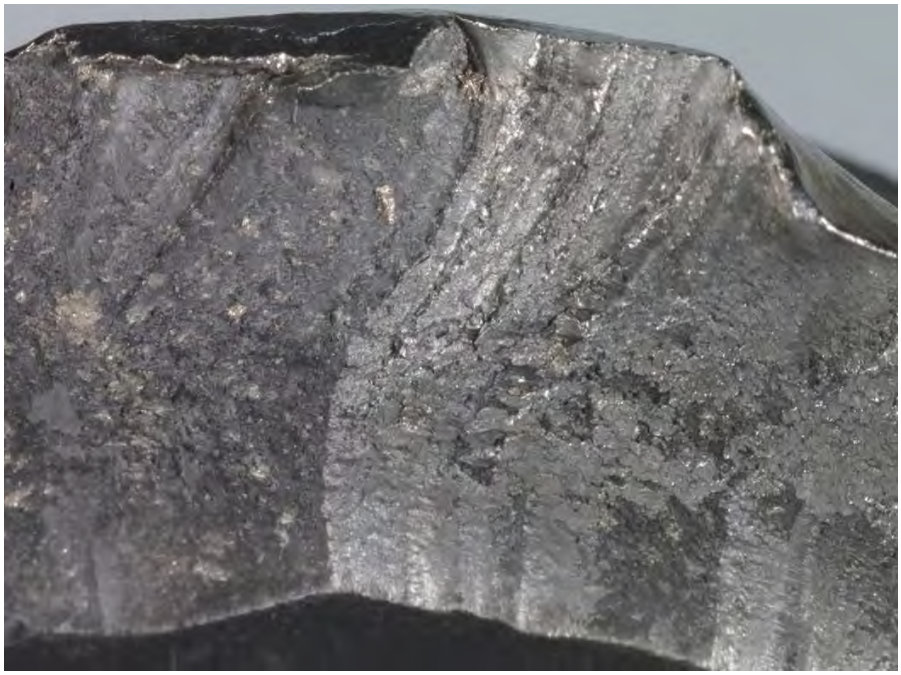

Fig. 284 Close-up photograph of blade airfoil fracture surface shown in Fig. 283.

Fig. 285. Close-up photograph of blade airfoil fracture surface shown in Fig. 283.

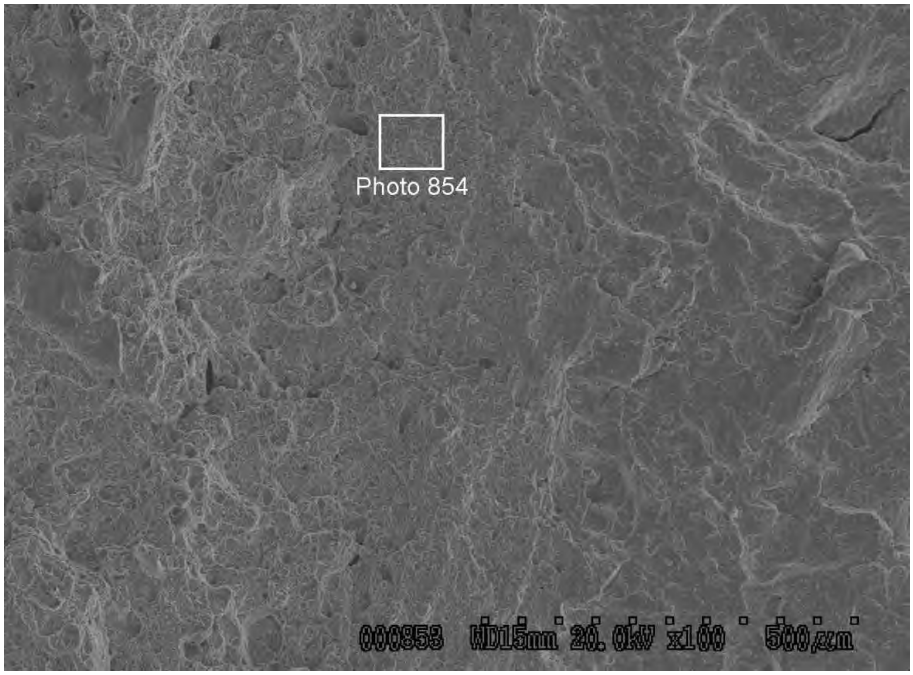

Fig. 286. Scanning electron microscope fractograph of blade airfoil fracture surface at Area "853" shown in Fig. 283.

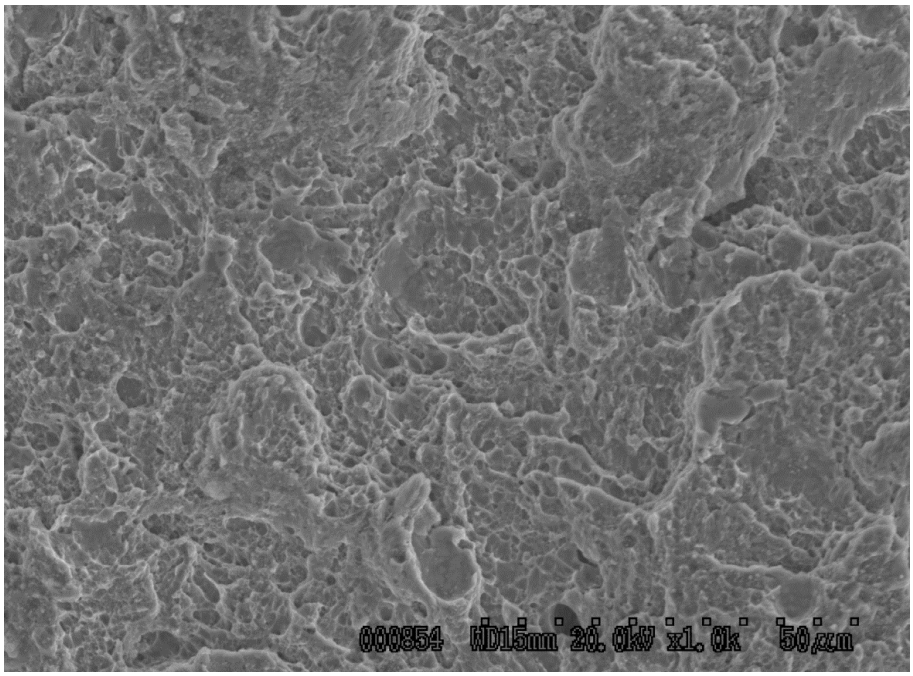

Fig. 287. Scanning electron microscope fractograph of blade airfoil fracture surface at Area "854" shown in Fig. 286.

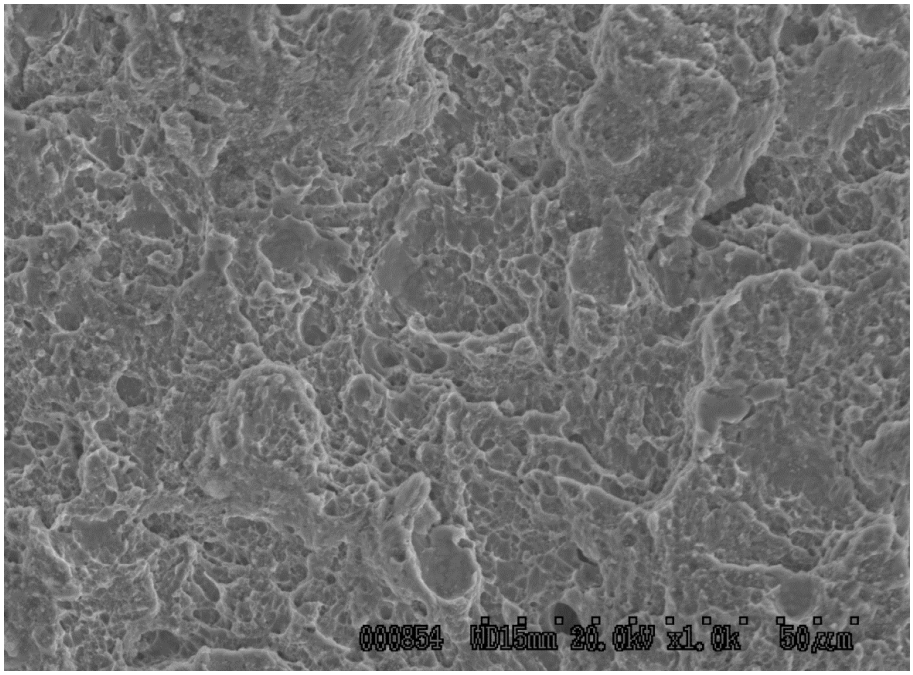

Fig. 288 Scanning electron microscope fractograph of blade airfoil fracture surface at Area "855" shown in Fig. 283.

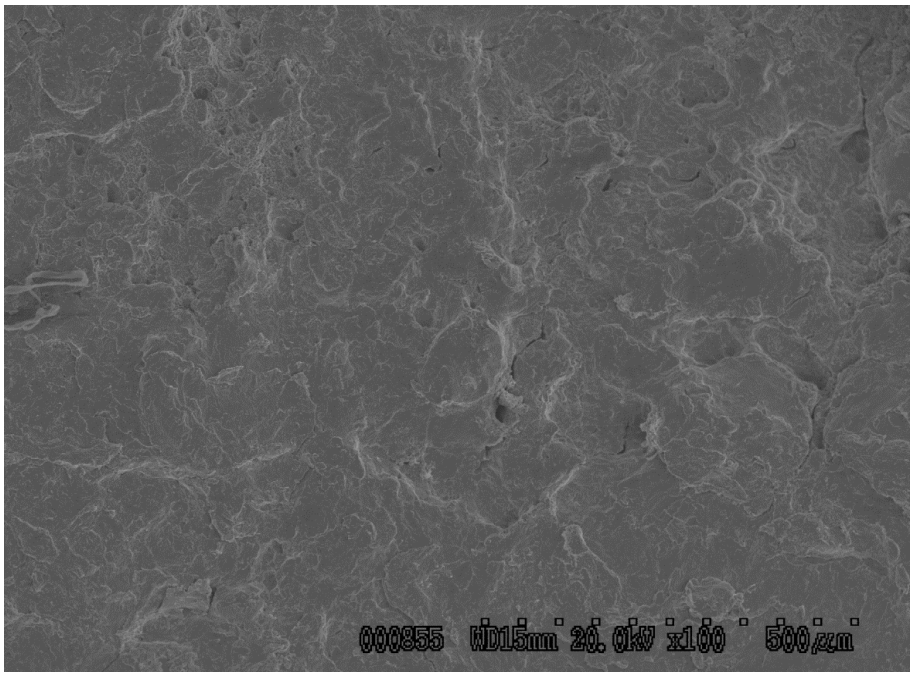

Fig. 289 Scanning electron microscope fractograph of blade airfoil fracture surface at Area "856" shown in Fig. 283.

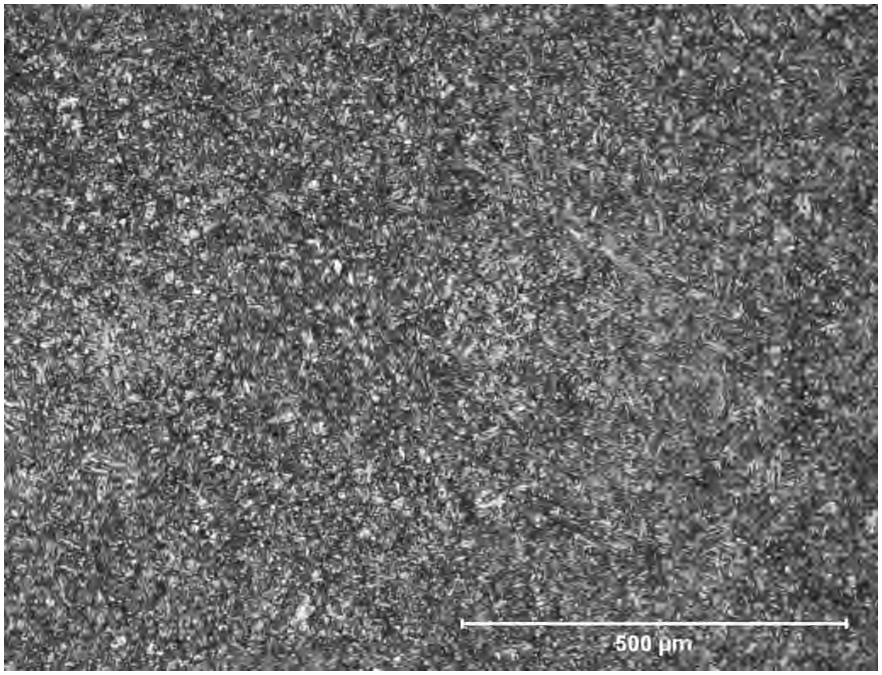

Fig. 290. Photomicrograph of planar section through a finger pinned blade attachment from a low pressure turbine "B" turbine end L-1 blade, SID 14914, Pc "A3".

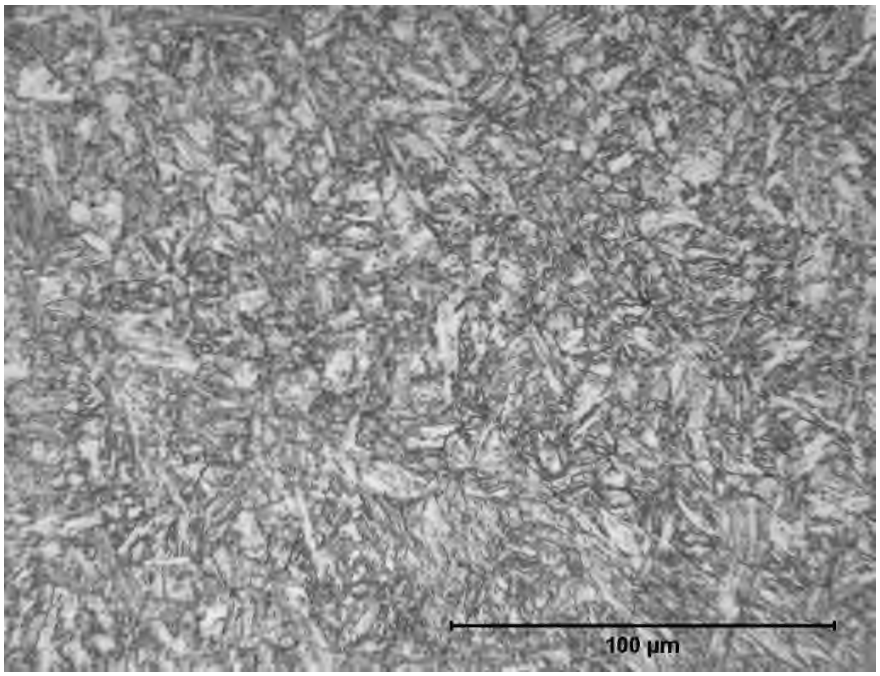

Fig. 291 Photomicrograph of planar section through a finger pinned blade attachment from a low pressure turbine "B" turbine end L-1 blade, SID 14914, Pc "A3".

Fig. 292. Photograph of low pressure turbine "B" turbine end L-1 blade and pins received for forensic examination.

Fig. 293. Photograph of low pressure turbine "B" turbine end L-1 blade and pins received for forensic examination.

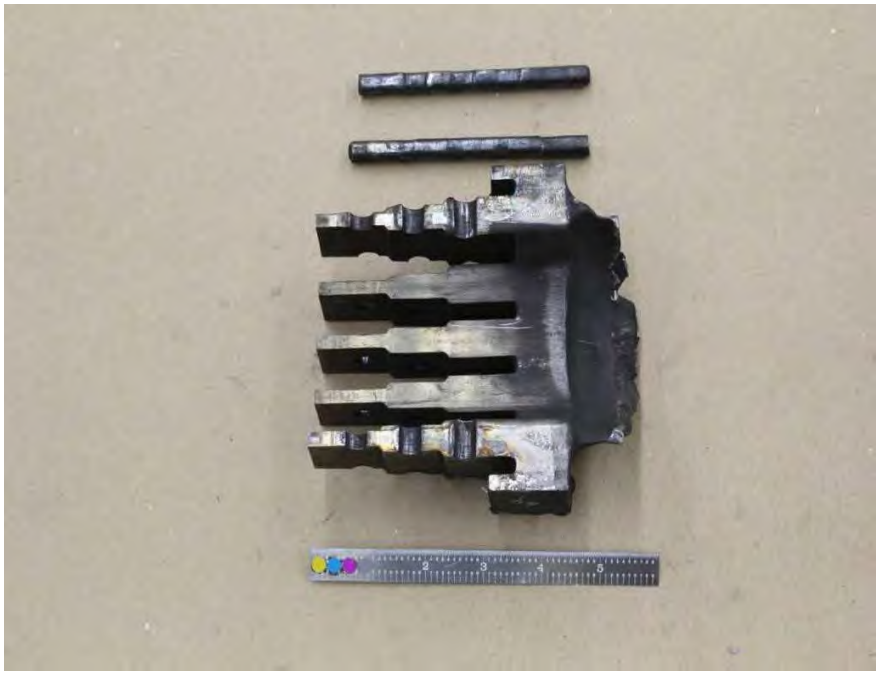

Fig. 294. Photograph of low pressure turbine "B" turbine end L-1 blade and pins received for forensic examination.

Fig. 295. Photograph of blade pin SID 14936 Pc "B" showing extent of yielding.

Fig. 296. Photograph of blade pin SID 14936 Pc "C" showing extent of yielding.

Fig 297. Photograph of blade pin SID 14936 Pc "B" showing extent of yielding.

Fig. 298. Photograph of blade pin SID 14936 Pc "C" showing extent of yielding.

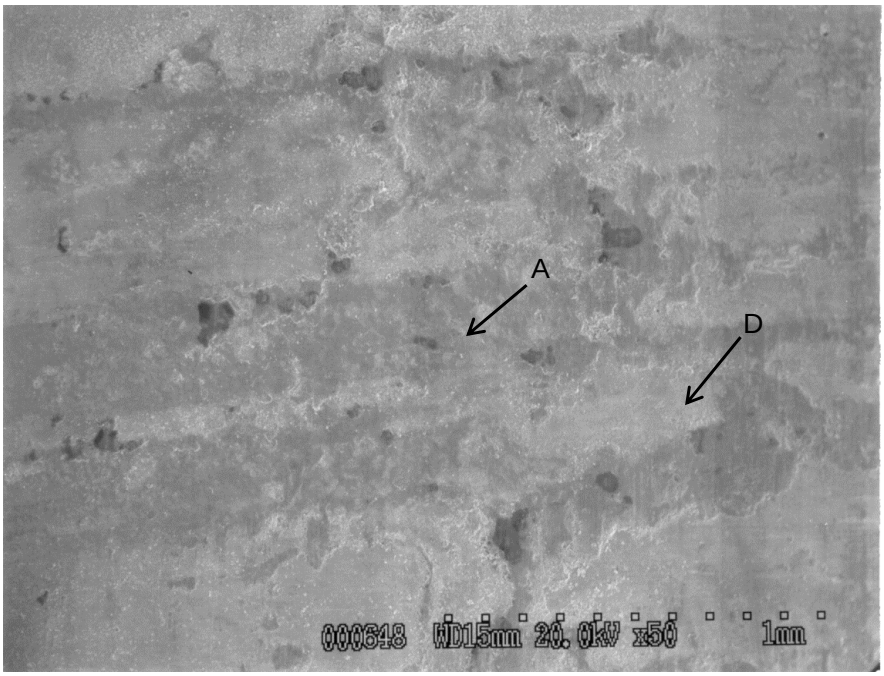

Fig. 299. Scanning electron microscope photograph of surface of blade pin SID 14897 Pc "C" showing areas examined by EDS.

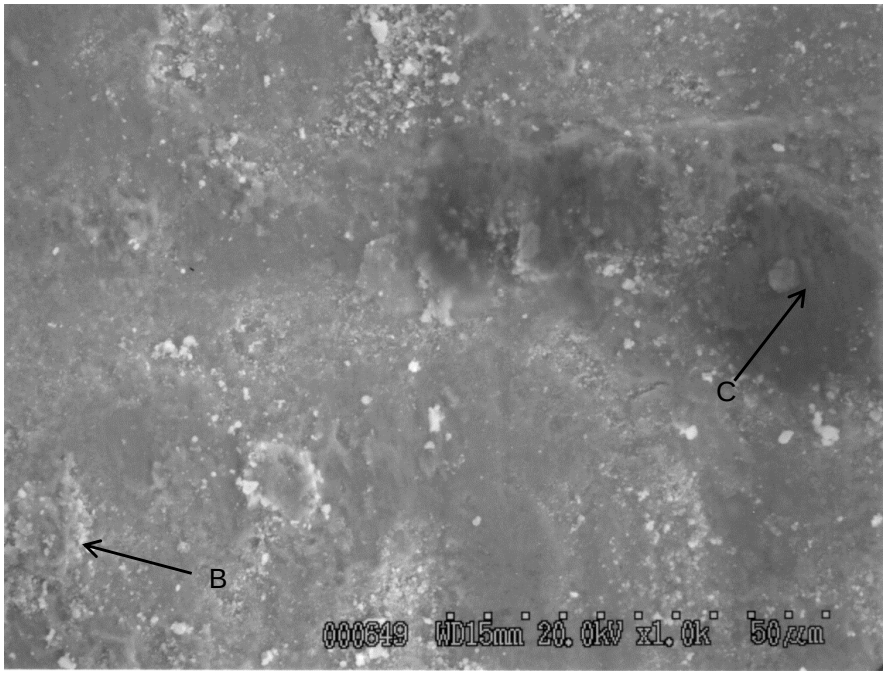

Fig. 300. Scanning electron microscope photograph of surface of blade pin SID 14897 Pc "C" showing areas examined by EDS.

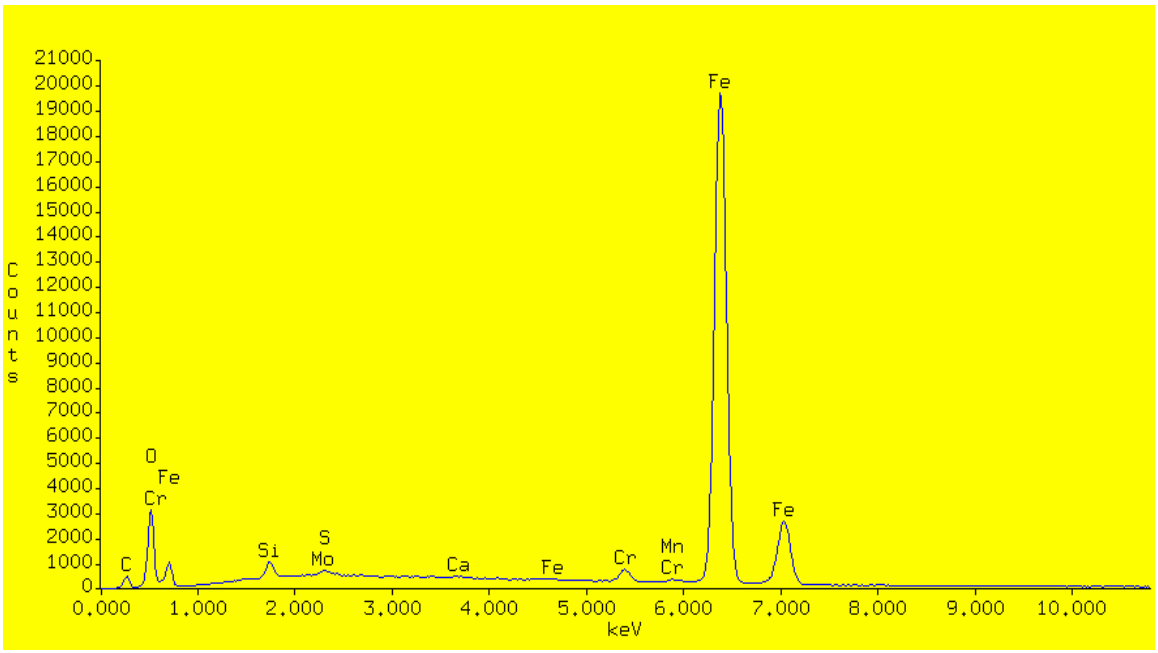

Fig. 301. Energy Dispersive Spectrograph of surface of a blade pin SID 14897 Pc "C" at Area "A" shown in Fig. 299.

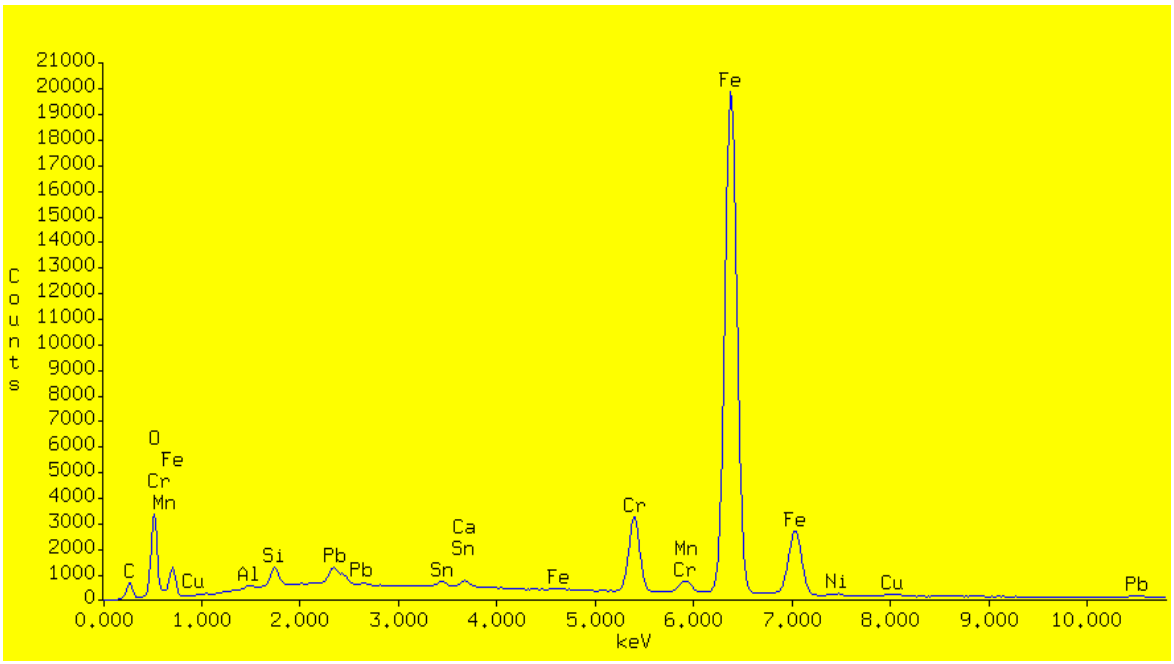

Fig. 302. Energy Dispersive Spectrograph of surface of blade pin SID 14897 Pc "C" at Area "B" shown in Fig. 300.

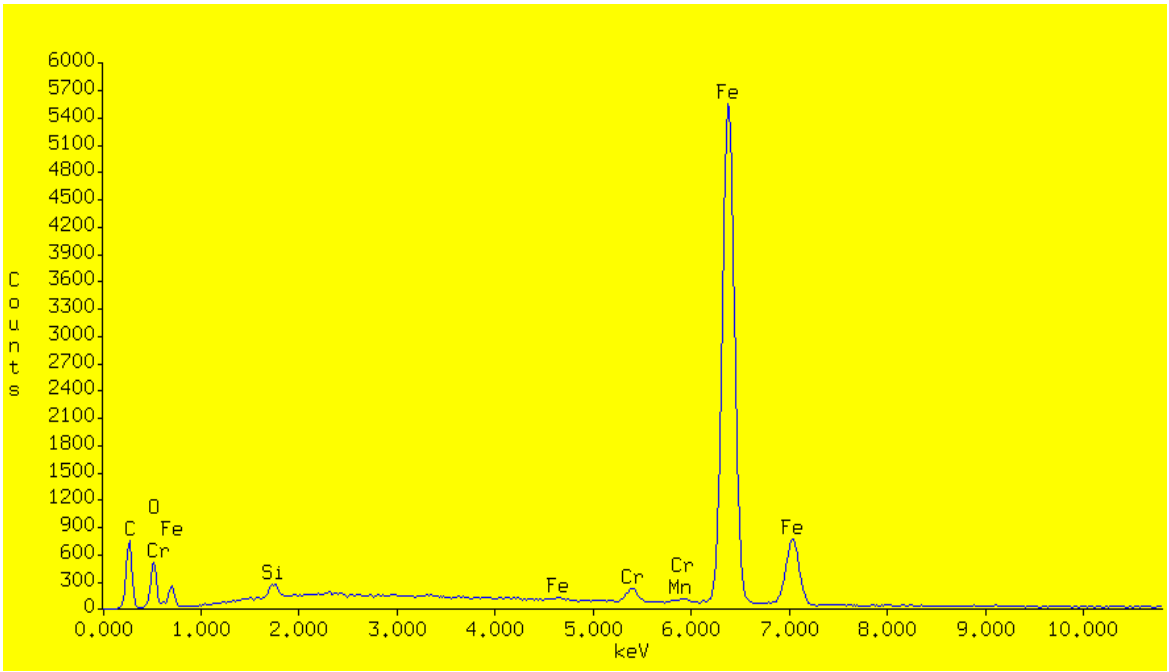

Fig. 303. Energy Dispersive Spectrograph of surface of blade pin SID 14897 Pc "C" at Area "C" shown in Fig. 300.

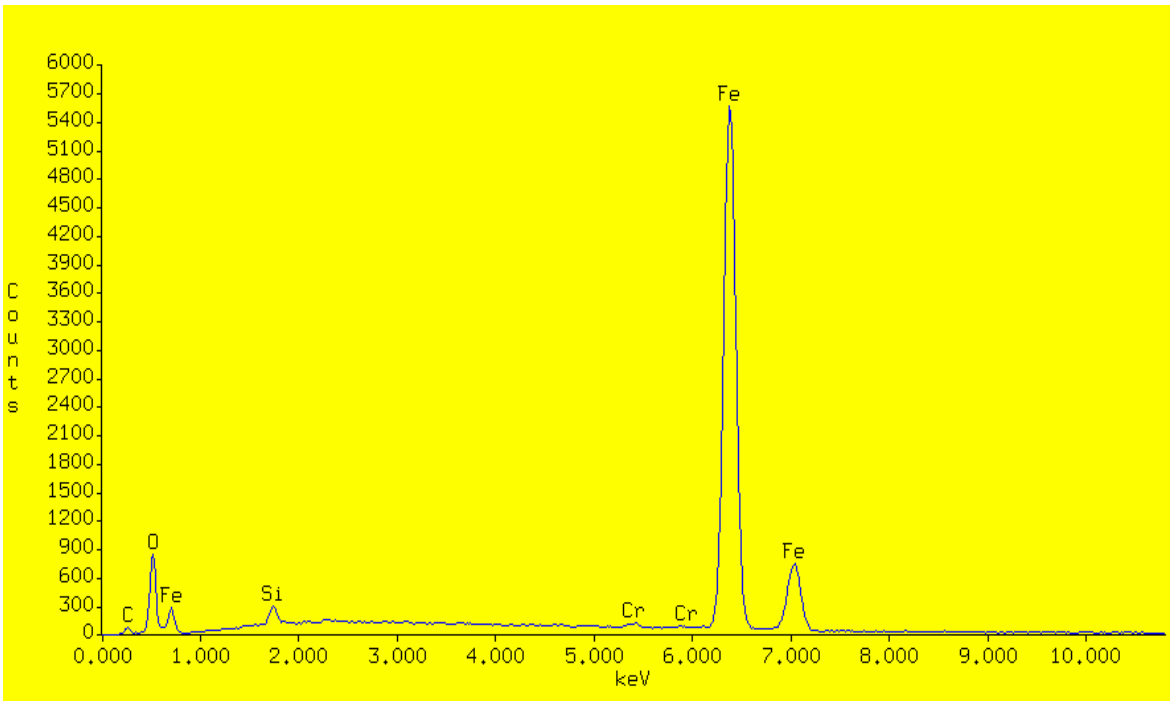

Fig. 304. Energy Dispersive Spectrograph of surface of blade pin SID 14897 Pc "C" at Area "D" shown in Fig. 299.

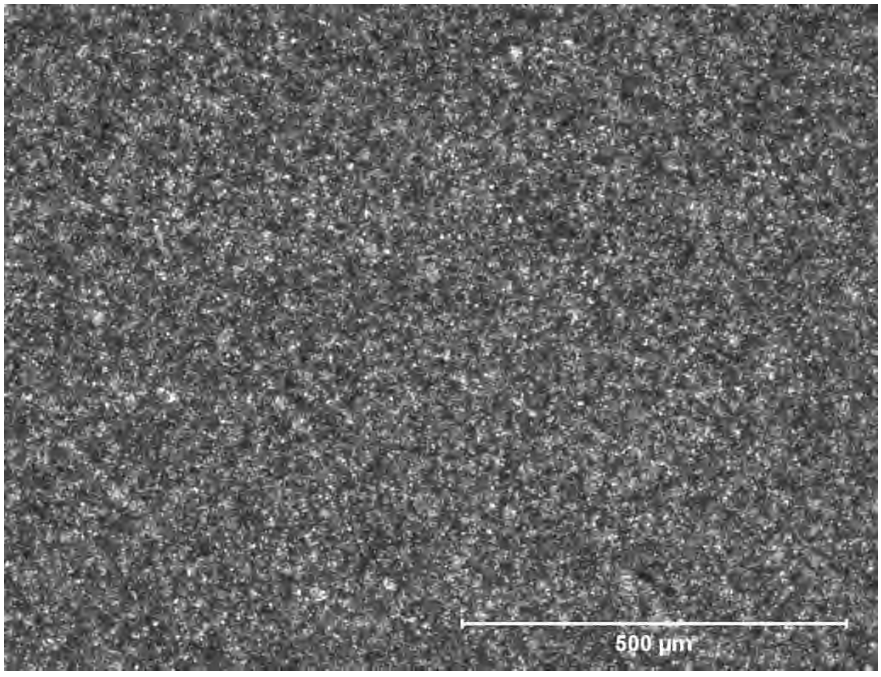

Fig. 305. Photomicrograph of transverse section through blade pin SID 14914 Pc "B".

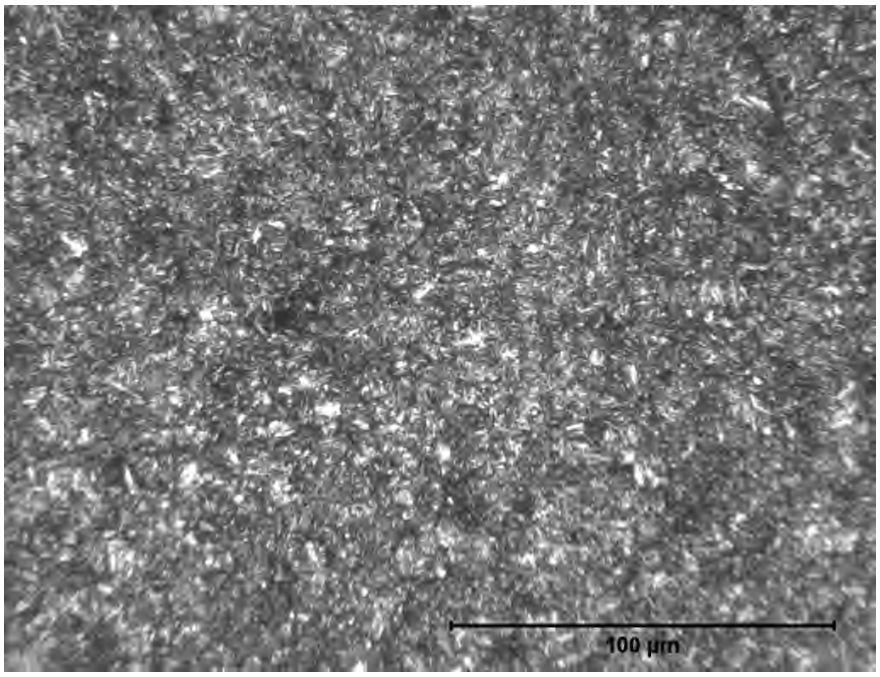

Fig. 306. Photomicrograph of transverse section through blade pin SID 14914 Pc "B".

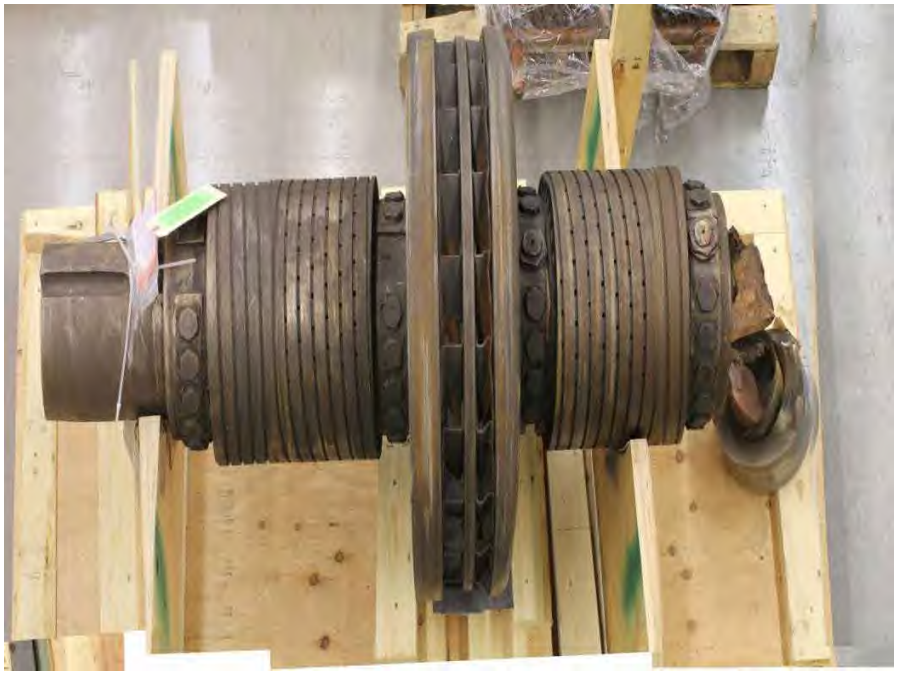

Fig. 307. Aft end of generator shaft which fractured transversely just forward of the generator collector ring.

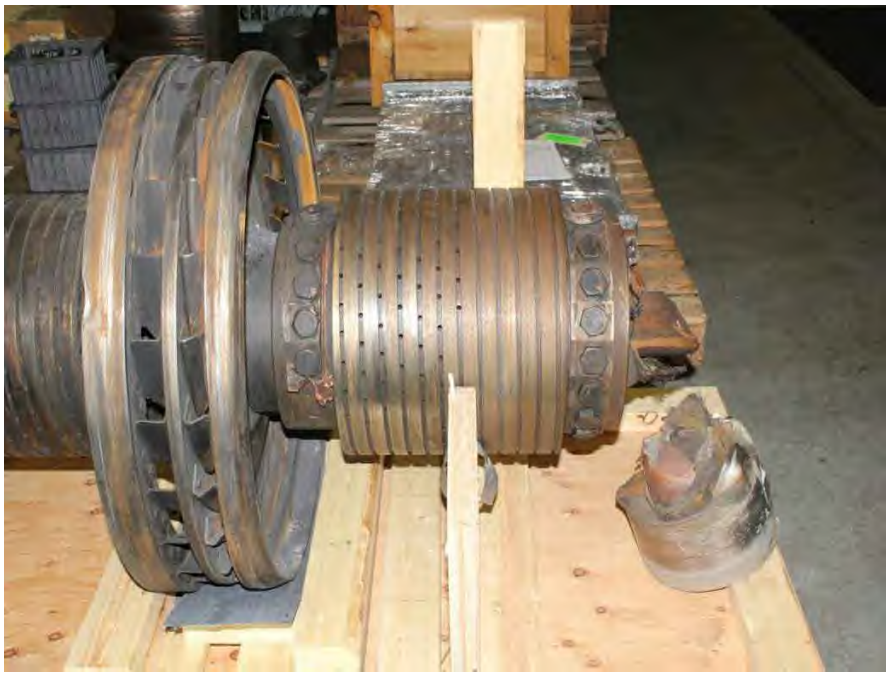

Fig. 308. Forward end of generator shaft shown in Fig. 307 showing both halves of shaft fracture.

Fig. 309. Aft end of generator shaft.

Fig. 310. Aft half of generator shaft fracture.

Fig. 311. Forward half of generator shaft fracture with leads removed.

Fig. 312. Generator shaft coupling half which was liberated from generator shaft during turbine event of Nov. 19, 2011.

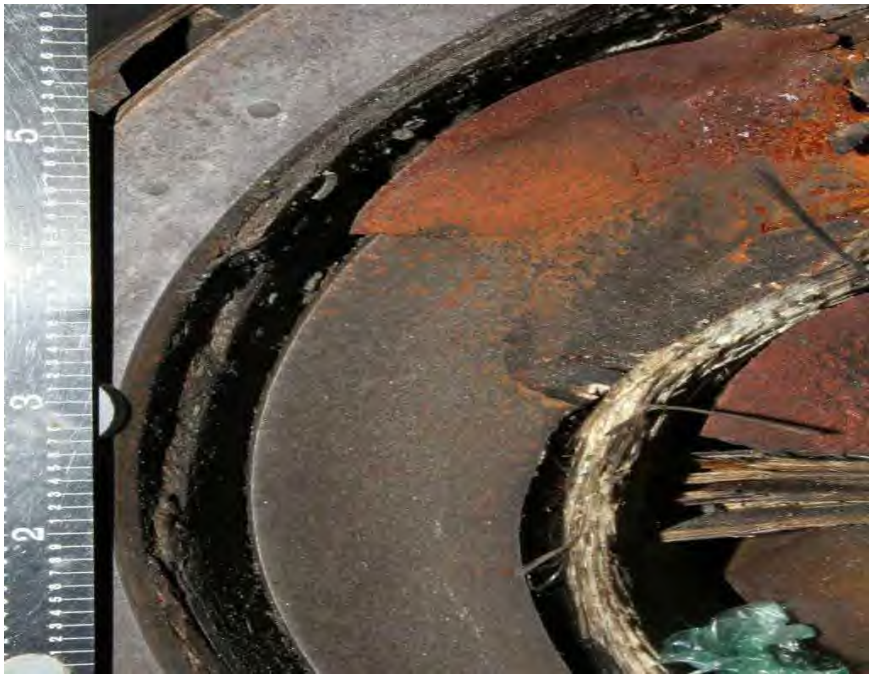

Fig. 313. Close-up photograph of fracture surface of generator shaft aft end fracture half.

Fig. 314. Close-up photograph of fracture surface of generator shaft aft end fracture half.

Fig. 315. Close-up photograph of fracture surface of generator shaft aft end fracture half.

Fig. 316. Close-up photograph of fracture surface of generator shaft forward end fracture half with leads intact.

Fig. 317. Close-up photograph of fracture surface of generator shaft forward end fracture half with leads intact.

Fig. 318. Close-up photograph of fracture surface of generator shaft forward end fracture half with leads intact.

Fig. 319. Close-up photograph of fracture surface of generator shaft forward end fracture half.

Fig. 320. Close-up photograph of fracture surface of generator shaft forward end fracture half.

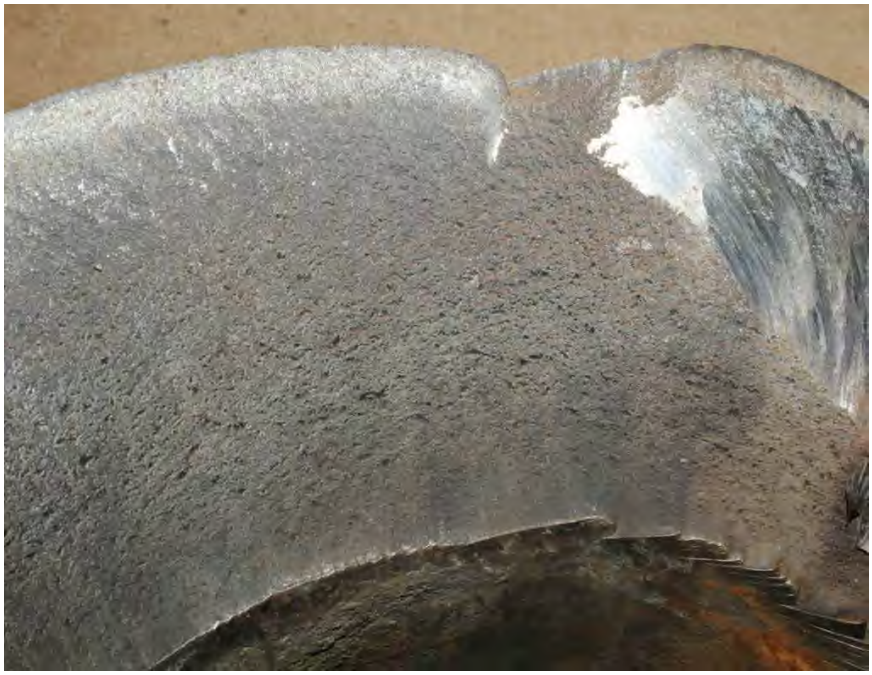

Fig. 321. Close-up photograph of fracture surface of generator shaft forward end fracture half.

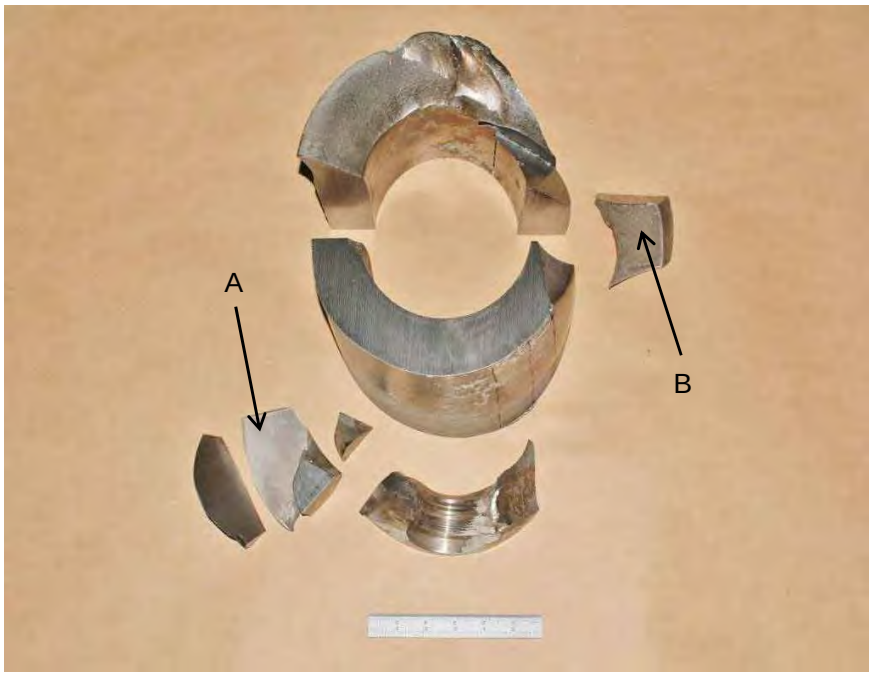

Fig. 322. Close-up photograph of generator shaft forward end fracture half showing two subsegments removed for scanning electron microscope examination.

Fig. 323. Close-up photograph of generator shaft fracture subsegment "A" showing location of scanning electron microscope photograph.

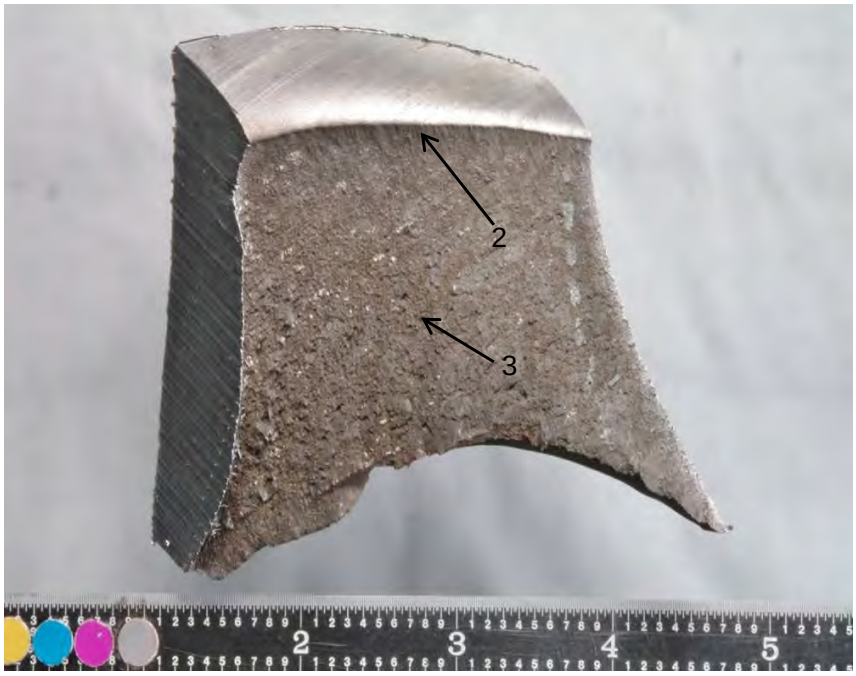

Fig. 324. Close-up photograph of generator shaft fracture subsegment "B" showing locations of scanning electron microscope photograph.

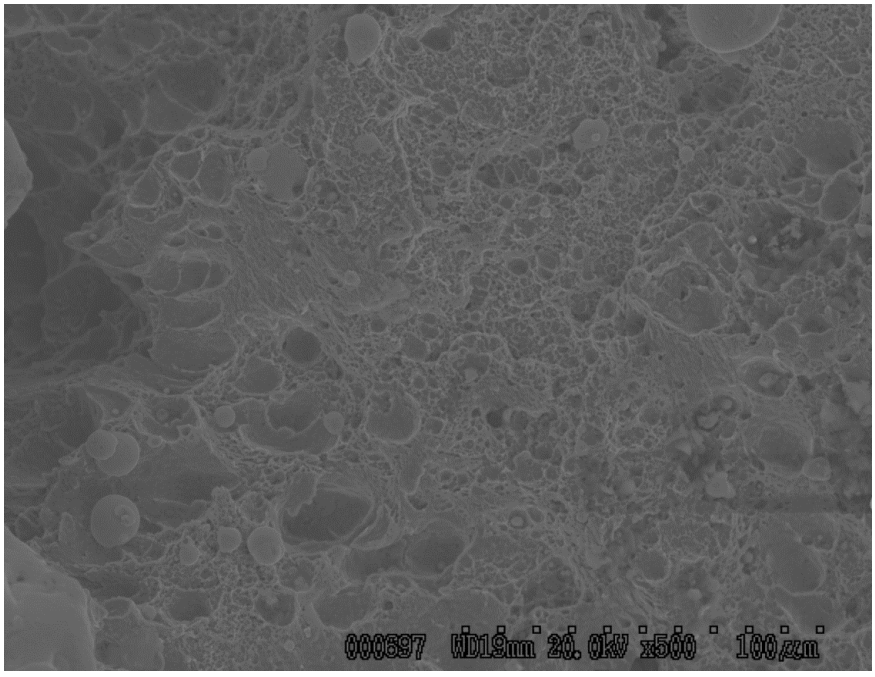

Fig. 325. Scanning electron microscope fractograph of generator shaft fracture subsegment "A", Area 1.

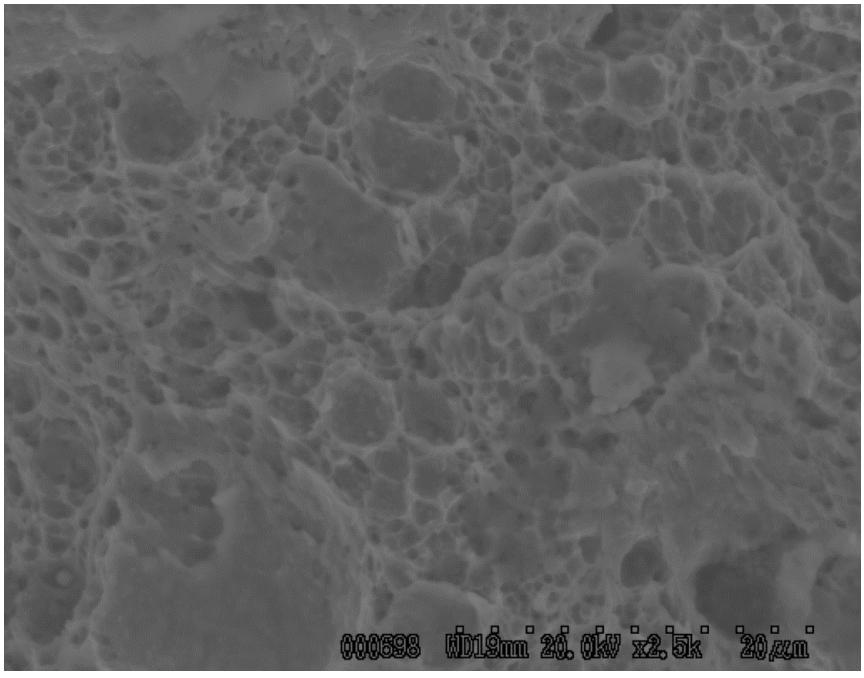

Fig. 326. Scanning electron microscope fractograph of generator shaft fracture subsegment "A", Area 1.

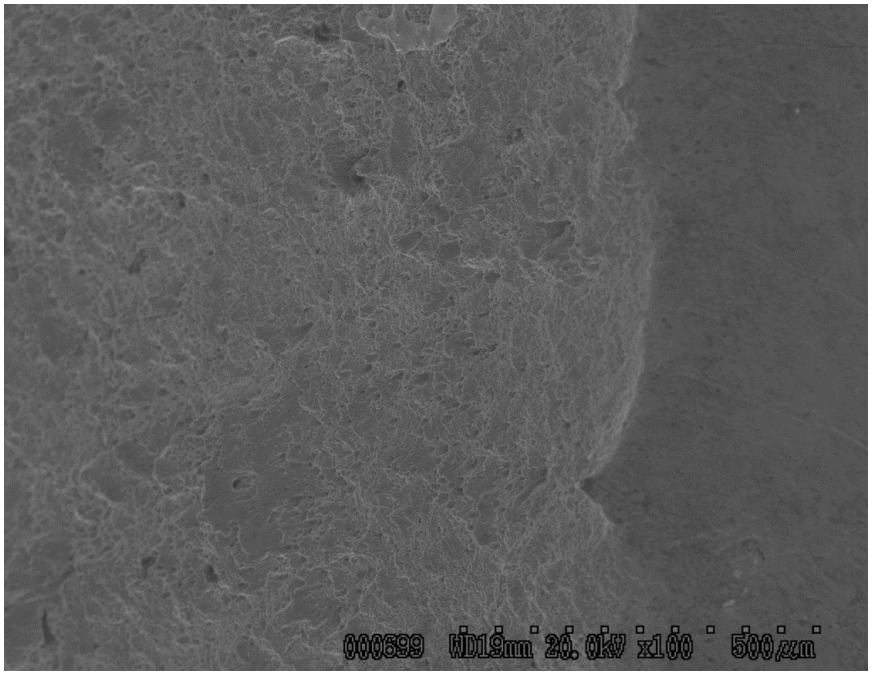

Fig. 327. Scanning electron microscope fractograph of generator shaft fracture subsegment "B", Area 2.

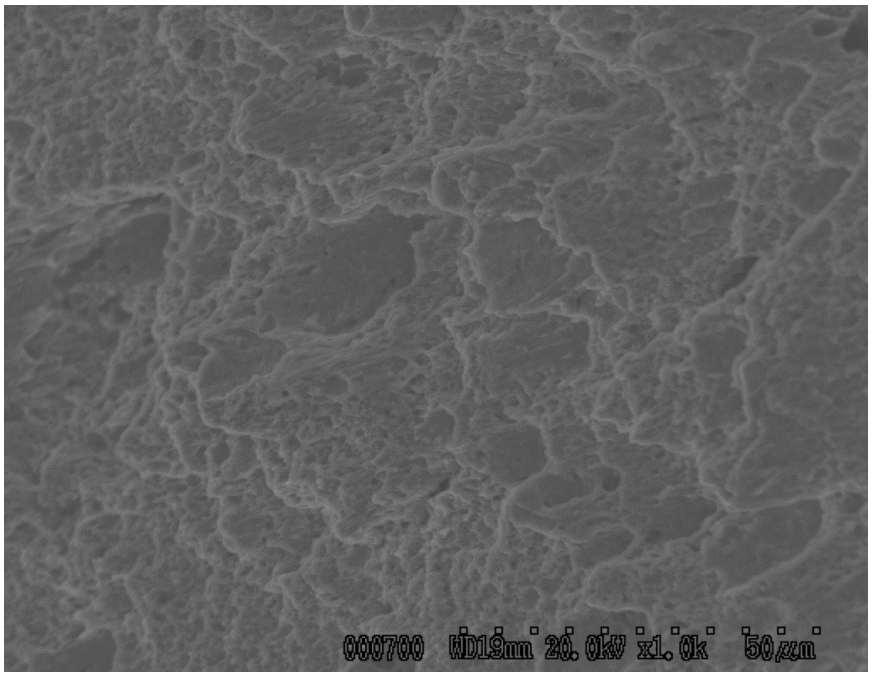

Fig. 328. Scanning electron microscope fractograph of generator shaft fracture subsegment "B", Area 2.